IMMOBILIZED COBALT AFFINITY PURIFICATION FOR HSV-1 BASED GENE THERAPY VECTORS

by

Canping Jiang

B.S. in Chemical Engineering, Zhejiang University, Hangzhou, China, 1998

M.S. in Chemical Engineering, Zhejiang University, Hangzhou, China, 2001

Submitted to the Graduate Faculty of

the School of Engineering in partial fulfillment

of the requirements for the degree of

Doctor of Philosophy

University of Pittsburgh

2006

UNIVERSITY OF PITTSBURGH

SCHOOL OF ENGINEERING

This dissertation was presented by

by

Canping Jiang

It was defended on

February 28, 2006

and approved by

Joseph C. Glorioso, Ph.D., Professor, Molecular Genetics and Biochemistry

William Federspiel, Ph.D., Professor, Chemical Engineering

Richard Koepsel, Ph.D., Associate Professor, Chemical Engineering

Dissertation Advisor: Mohammad Ataai, Ph.D., Professor, Chemical Engineering

ABSTRACT

IMMOBILIZED COBALT AFFINITY PURIFICATION FOR HSV-1 BASED GENE THERAPY VECTORS

Canping Jiang, PhD

University of Pittsburgh, 2006

Herpes simplex virus type 1 (HSV-1) is a promising vector for gene therapy applications. To be used as therapeutic agents, HSV-1 vectors must meet the stringent criteria of high titer and purity. Thus, development of scalable, efficient HSV-1 vector purification strategies is essential to advance HSV-1 vectors into clinic.

In this dissertation, a novel, efficient HSV-1 vector purification method, based on immobilized metal affinity chromatography (IMAC), was developed.

I first evaluated the feasibility of using various transition metal ions (Cu2+, Zn2+, $Ni2^{+}$, and Co^{2+}) for the purification of HSV-1 vectors. Results show that none of the metals investigated provided a means of separating the virus from impurities. However, of interest is the finding that neither the virus nor the impurities bound to immobilized Co^{2+}, suggesting that this metal could be useful for HSV-1 vector purification if the vector could be endowed with the affinity toward cobalt.

Accordingly, I constructed an HSV-1 recombinant bearing a cobalt affinity tag (HAT) in the heparan sulfate binding domain of the virion envelope glycoprotein B (gB). It was found that the productivity and infectivity of the tagged HSV-1 mutant (KgBHAT) was not adversely affected by the mutation; while the binding and elution of KgBHAT on cobalt charged iminodiacetate (IDA-Co^{2+}) columns confirmed that efficient purification was possible. By reducing cobalt ion leakage and optimizing the loading conditions, flow rate,

and chromatographic substrate, efficient purification of KgBHAT from crude supernatant was achieved with over 70% virus infectivity recovery and over 95% reduction in protein and DNA impurities.

Finally, I found that purification of KgBHAT on IDA-Co^{2+} columns using crude supernatant as starting material resulted in significant loss in virus infectivity. Electron spinning resonance revealed that the virus inactivation was caused by hydroxyl free radicals generated from the interaction between cobalt ions and components in crude virus supernatant. Appropriate amounts of free radical scavenger, a free radical scavenger, or imidazole in the loading material was able to protect HSV-1 from inactivation, and led to high virus infectivity recovery from IMAC purification. This finding is the first report of free radical mediated biological inactivation in an actual IMAC purification.

DESCRIPTORS

Ascorbate	Cobalt
Free Radical	Gene Therapy
HSV-1	IMAC
Purification	Tag

TABLE OF CONTENTS

LIST OF TABLES

LIST OF FIGURES

Figure No. Page

ACKNOWLEDGEMENTS

I would like to thank my advisor Dr. Mohammad Ataai, for his guidance, encouragement, support, and friendship. I appreciate all the time and effort he put forth towards helping me better my scientific thinking, writing, and presentation skills.

I would like to express my sincere appreciation to my co-advisor Dr. Joseph Glorioso, who led me into the field of biomedical science, and provided me tremendous resources, without which this work would not have been done.

I would like to thank my other committee members, Dr. William Federspiel and Dr. Richard Keopsel, for their valuable time and comments on this work.

I am deeply indebted to James Wechuck, Ali Ozuer, Bill Goins, David Krisky, and Darren Wolfe, for their technical help during the initial phase of my research, and for the numerous discussions that were an inspiring source of ideas for my research.

I am very thankful to my colleagues, Shaohua Huang, Rahul Srinivasan, April Sunyog, Kyle Grant, Han Li, and Ying Jiang, for their friendship and support throughout my graduate study.

Finally, I would like to express my deepest gratitude to my parents and my sister, without whose understanding and support, I would have never made it thus far. And to them, I dedicate this thesis.

1.0 BACKGROUND

1.1 GENE THERAPY AND GENE THERAPY VECTORS

1.1.1 Gene Therapy

The completion of the human genome project and progress in life science and medicine have resulted in an abundance of information about the molecular and cellular basis of human diseases, which enables the exploration of new therapeutic approaches based on engineered genes and cells.

Gene therapy is a new therapeutic modality that aims at correcting genetic defects or expressing proteins that are therapeutically useful. In most applications, gene therapy can be defined as the transfer of genetic materials (DNA or RNA) to cells of a patient which results in a therapeutic effect[1-3]. Gene therapy has several advantages over existing therapeutic approaches based on small molecules and proteins. These include: (i) correction of the genetic cause of a disease, (ii) *in situ* production of drugs in affected cells or tissues, and (iii) potentially long-term therapeutic effect after single application. As a result, gene therapy provides the potential for the treatment of many acquired and inherited human diseases where conventional clinical procedures are less effective. These diseases include monogenic disorders such as cystic fibrosis[4, 5], but also more complex disorders, such as cardiovascular diseases[6, 7], diseases of nervous system[8, 9], autoimmune diseases[10], and cancers[11, 12].

Although the theoretical advantages of gene therapy are obvious, so far gene therapy has not met its promised goals: the existing clinical experience indicates insufficient therapeutic efficacy, while concerns were raised regarding the safety of gene therapy.

One of the most formidable obstacles of gene therapy exists in gene delivery. In order to achieve the desired therapeutic effect, the therapeutic gene has to be delivered into a specific cell population in a target tissue; and the gene has to be expressed in a safe and regulated manner for an appropriate period of time. Thus, success of gene therapy requires not only the identification of suitable therapeutic genes, but also the development of gene delivery systems of sufficient targeting ability, transfection efficiency, and safety, as well as an appropriate gene regulation system to control the level and timing of therapeutic gene expression. In addition, efficient manufacturing and analytical processes have to be developed to provide well-defined gene therapy products for clinical investigation. Over the past decade, significant progress was made and many technical handles in the field of gene therapy have been overcome. The efficiency and safety profile of delivery systems have been significantly improved; manufacturing processes for gene therapy products have been developed and optimized. These technical advances together with the increasing knowledge and experience in the field will undoubtedly lead to the realization of the full potential of gene therapy in the future.

1.1.2 Gene Therapy Vectors

The process of gene delivery and expression is known as transduction. In order to improve the efficiency of transduction in gene therapy, therapeutic genes are usually carried by delivery vehicles called gene therapy vectors[13-15]. A gene therapy vector serves several functions to the transgene, including (i) enabling delivery of genes into the nucleus of the target cells, (ii) providing protection from gene degradation, and (iii) ensuring gene transcription in the cell. An ideal gene therapy vector should not only be targeted and safe, but also protected from sequestration or immune clearance *in vivo*. In addition, it should be easily produced and purified in large amounts and at high concentrations. Given the diversity

of disease and tissue targets in gene therapy applications, it has become clear that there can be no single vector that is suitable for all applications. Many types of gene therapy vectors have been developed, each with their characteristic advantages, drawbacks, and applications to which they are best suited. These vectors fall into two broad categories: nonviral and viral vectors.

The nonviral vectors consist of naked DNA delivered by injection, liposomes, polyplexes, nanoparticles, and other means[16]. Although nonviral vectors can be produced in relatively large amounts and are likely to present minimal toxic or immunological problems, presently they suffer from inefficient gene transfer. In addition, expression of the foreign gene tends to be transient, precluding their application to many disease states in which sustained and high-level expression of the transgene is required. However, as we continue to unravel and understand the biological mechanisms that underlie gene delivery, such as cell binding and entry, escape from endosomes, and nuclear import, we will be able to apply this knowledge to the development of more efficient nonviral vectors that may ultimately rival the virus-based systems.

Viruses are naturally evolved biological machines that efficiently deliver their genetic materials into host cells and exploit the cellular machinery to facilitate their replication[15]. The basic concept of viral vector is to harness the virus infection pathway, but avoid the expression of viral genes that leads to replication and toxicity. Gene therapy viral vectors are being developed by genetic modification of retrovirus, adenovirus, adeno-associated virus, herpes simplex virus, and others[17]. Table 1.1 provides a summary of the main viral vectors, highlighting their individual properties.

Unlike the wild type viruses, gene therapy viral vectors are engineered by deleting all, or some of essential viral genes that are required for the virus replication, assembling, and transmission, but leaving intact the *cis*-acting sequences that provide the viral origin of

replication and the signal of encapsulation. These deleted genes thus provide space in the vector genome for the insertion of transgene expression cassette. Such vectors lose their abilities to replicate in normal cells but can be produced in a complementary cell line, which supplies the deleted viral functions *in trans*.

Table 1.1 The main groups of viral vectors

Vector	Genetic material	Packaging capacity	Tropism	Vector genome form	Main limitations	Main advantages
Retrovirus	RNA	8 kb	Dividing cells	Integrated	Only transduce dividing cells; integration might induce oncogenesis in some applications	Persistent gene expression in dividing cells
Lentivirus	RNA	8 kb	Broad	Integrated	Integration might induce oncogenesis in some applications	Persistent gene expression in most tissues
adenovirus	dsDNA	8 kb	Neurotropic	Episomal	Capsid mediates a potential inflammatory response	Extremely efficient transduction of most tissues
AAV	ssDNA	< 5 kb	Broad	Episomal (>90%) Integrated (<10%)	Small packaging capacity	Non-inflammatory; non-pathogenic
HSV-1	dsDNA	40 kb	Broad	Episomal	Transient transgene expression other than neurons	Large transgene capacity; strong tropism for neurons

1.1.2.1 Retroviruses Retroviruses, particularly the murine leukemia virus (MLV), were among the first constructed human gene therapy vectors[18]. Replication-defective MLV vectors are generated by replacing all viral protein encoding sequences (*gag, pol, env*) with the exogenous promoter-driven transgene of interest. In addition to the packaging signal, the vectors retain the viral LTRs and adjacent sequences, which are essential for reverse transcription and integration. Retroviral vectors are propagated in the packaging cells which provide the structural proteins *in trans*. The first generation packaging cell lines expressed *gag*, *pol*, and *env* from a complete proviral DNA, lacking only the packaging signal. In order to reduce the risk of generating replication competent virus, newly developed packaging cells have the *gag/pol* and *env* located in separate constructs[19, 20].

Retroviruses have the ability to randomly integrate their genome into the host cell and therefore sustain transgene expression for extended time periods. This can present an advantage in the treatment of inherited and chronic diseases, but also a risk of insertional mutagenesis. The host range of MLV based retroviral vectors has been expanded by pseudotyping the viral envelope with the G glycoprotein from vesicular stomatitis virus (VSV). This modification also stabilizes the vector particles, allowing the vector stocks to be concentrated into high titers[21]. The major disadvantage of MLV based retroviral vectors is the inability to infect non-dividing cells, which restricts their potential applications. Other retroviral vectors have been developed based on lentiviruses[22, 23]. Lentiviruses, which are a special group of retroviruses including the human immunodeficiency virus (HIV), have the ability to infect both proliferating and quiescent cells. The transduction efficiency of lentiviral vectors is significantly higher than the conventional retroviral vectors. However, lentiviral vectors derived from HIV present obvious safety concerns.

1.1.2.2 Adenoviruses Adenoviruses are non-enveloped, double stranded DNA viruses with a diameter of 70 nm, and a genome size of about 36 kb encoding 50 viral polypeptides. More than 50 different serotypes of adenoviruses are known, but the most frequently utilized for gene therapy are type 2 and type 5. Adenoviruses infect both dividing and nondiving cells with high efficiency. The key features that have made adenoviruses popular gene therapy vectors have been the ability to generate high-titer virus stocks and the high-level heterologous gene expression.

First generation adenovirus vectors were obtained by deleting one or two viral early genes (E1 and E3). Cells that were transduced with these vectors expressed other adenoviral genes at low levels, inducing strong cytotoxic T-cell responses that rapidly eliminated transgene expression. Second and third generation vectors that contain additional deletions in other early genes (E2 and/or E4) have shown reduced toxicity in animal models[24-26]. The development of helper-dependent adenoviruses (HD-Ads) that are deleted for all viral genes has been the most important advance to decrease immunogenicity, prolong transgene expression and improve the prospects of adenovirus vectors for long-term gene therapy[27].

1.1.2.3 Adeno-associated virus Adeno-associated virus (AAV) belongs to the parvoviruses. It is a single-stranded, non-enveloped DNA virus of 4.5 kb size. Most AAV vectors have been derived from AAV2, but, so far, a total of eight distinct AAV serotypes have been identified that infect different cell types with different efficiencies[28-30]. Wild-type AAV 2 is non-pathogenic and capable of integrating into the long arm of chromosome 19 after infection of human cells[31]. Recombinant AAV 2 vectors are generated by insertion of a therapeutic gene between two inverted terminal repeats (ITRs), replacing all coding sequences except ITRs[32]. The vector genome can be rescued by supplying *rep* and *cap* proteins *in trans* from a packaging plasmid, together with a helper virus (usually adenovirus or herpes simplex virus) infection[33].

Adeno-associated viral vectors have been shown to transduce a broad range of cells through both episomal transgene expression and by random chromosomal integration. The integration property of AAV vector enables it be used for long-term transgene expression in non-dividing cells. However, there are some disadvantages associated with the application of AAV. The packaging capacity is relatively restricted and the large scale production inefficient. In addition, the integration into the host genome is random, which can lead to unexpected activation or inhibition of endogenous gene expression.

1.1.2.4 Herpes simplex virus type 1 HSV-1 is the largest and most complex of all the viruses described here. One important feature of this vector is its capacity to carry large fragments of foreign DNA. Replication-defective HSV-1 vectors can carry up to 40 kb of foreign DNA, facilitating the delivery of several separate expression cassettes, or large single genes. Wild type HSV-1 is a neurotropic virus that can establish lifelong persistence in sensory neurons. This natural tropism has made neuropathological disorders one of the most promising applications of replication-defective HSV-1 vectors. The next session summaries the basic biology of HSV-1, the construction of HSV-1 vectors, and the use of HSV-1 vectors for the treatment of neurological diseases in animal models.

1.2 HERPES SIMPLEX VIRUS TYPE 1 VECTOR

1.2.1 Basic Biology of HSV-1

Herpes simplex virus type 1 (HSV-1) is an enveloped double-stranded DNA virus of about 200 nm in diameter. Mature HSV-1 virion consists of a 150Kb DNA genome encased in an icosahedral capsid. A lipid envelope, obtained from the infected host cell, surrounds the virus particle. This envelope is studded with at least 10 different types of viral glycoproteins (gB-gE, gG-gJ, gL, and gM) that serve principally to mediate virus entry into host cell.

Between the capsid and the envelope, there is an amorphous layer called the tegument, which contains a number of proteins that are responsible for the induction of viral gene expression and shutoff of host protein synthesis (reviewed in 34).

Entry of HSV-1 into the host cell is mediated by glycoproteins embedded in the viral envelope. Two different steps of this process can be identified: attachment to the cell surface and fusion of the viral and cellular membrane resulting in viral entry. The virus is also capable of infecting neighboring cells by moving transcellularly across cell membranes, a process referred to as lateral spread. HSV-1 infection is initiated with adsorption of virion on permissive cell surface via binding to cell surface glucosaminoglycan (GAGs), primary heparan sulfate (HS) but also dermatan sulfate mediated by exposed domain of gC and gB[35-37]. Together this binding activity represents about 85% of the binding activity to Vero cells with gC contributing the majority[35]. The rest of the binding activity is thought to be contributed by other glycoproteins binding to other receptors. Following the initial adsorption event, a secondary binding event occurs between gD and cellular receptors. Three classes of gD receptors have been identified. They include HveM or HveA, a member of the tumor necrosis factor receptor family[38]; nectin-2 (HveB) and nectin-1 (HveC), two members of the immunoglobulin superfamily[39]; and 3-O-sulfated HS[40]. Binding of gD to its cognate receptors not only secures the adsorption of the virus on cell surface, but also initiates the fusion of the virus envelope with the cellular membrane and subsequent virus entry. The detailed mechanism of the membrane fusion and entry is obscure. However, it is known that gB, gD, and gH/gL complex are necessary in this event. One hypothesis of the entry mechanism is that the binding of gD to one of its receptors results in a conformational change in gD, enabling its interaction with gB or gH/gL and activation of membrane fusion. gB, gD, gH, and gL are thus essential for viral infection[41].

Following cell entry, HSV-1 genes are expressed in a tightly regulated, interdependent temporal cascade[42]. Transcription of the five immediate-early (IE) genes, ICP0, ICP4, ICP22, ICP27 and ICP47, commences on viral genome entry to the cell nucleus. Expression of IE genes proceeds in the absence of *de novo* viral protein synthesis, and is regulated by promoters that are responsive to a viral tegument protein VP16[43, 44]. Expression of IE genes initiates a cascade of viral gene expression, beginning with the transcription of early (E) genes, which primarily encode enzymes involved in DNA replication. In the presence of IE gene products and viral DNA synthesis, the late (L) genes are expressed. The late genes mainly encode structural components of the virion. Following translation of the late gene products, viral genomes are packaged into the newly assembled capsids. Tegument proteins then accumulate around the capsids. Finally, lipid membrane envelopes containing viral-encoded glycoproteins are acquired during the immature virus budding through the cellular membrane system and mature HSV-1 virions are released (reviewed in 34).

Primary infection of wild type HSV-1 on epithelial cells of skin or mucous membrane usually results in a lytic viral replication cycle as described above. Viruses released at the site of the primary infection may enter local sensory nerve terminals. The virus is then transported through the axon in a retrograde way to the neuronal cell body in the peripheral sensory ganglion[45]. In the neuron, HSV-1 may enter into another lytic replication cycle, which will result in neuronal cell death and egress of infectious particles. Alternatively, the viral DNA may enter into a latent state in which the viral genome persists as stable episomal element, sometimes for the lifetime of the host[46]. During latency, the cascade expression of IE, E and L genes is silenced. However, a set of nontranslated RNA species designated as latency-associated transcripts (LATs) is produced[47, 48]. No viral particles or any detectable viral proteins are found in latently infected ganglia *in vivo*. The latent HSV-1 genome can be

reactivated when the host-virus balance is disturbed[49]. The virus reactivation results in lytic virus replication and recrudescence of the disease in the same dermatomal distribution as the original infection.

1.2.2 The Construction of HSV-1 Vectors

Based on different approaches to eliminate the viral toxicity, three types of HSV-1 vectors have been constructed.

1.2.2.1 Amplicon vectors The HSV-1 amplicon is a plasmid DNA that contains a transgene cassette and two viral sequences, the HSV-1 packaging sequence, and an HSV-1 origin of replication, the ori_s sequence[50-52]. Thus, the toxicity of HSV-1 amplicon is maximally reduced by the deletion of essentially all virus-coding genes. HSV-1 amplicon vectors can be generated by cotransfection of eukaryotic cells with the amplicon plasmid and bacterial artificial chromosome (BAC) containing an HSV-1 genome, but devoid of the packaging signals and the origin of replication[53, 54]. HSV-1 structural proteins expressed from the BAC in cells form building blocks that package the concatermeric amplicon plasmids. Thus, the mature amplicon particles possess the same protein structure as the wild type HSV-1 viruses. The HSV-1 BAC is a recent advance on the prior amplicon generation methods using a set of HSV-1 cosmids or a helper virus. Although HSV-1 amplicons could be used to express genes in a variety of eukaryotic cells including neuron, their use as gene therapy vectors is limited by the fact that the production of high titer amplicon stock free of replicating helper virus is extremely difficult.

1.2.2.2 Conditionally replicating vectors This type of HSV-1 vectors are created by the deletion of some non-essential viral genes so that the mutants retain the ability to replicate in vitro but are comprised *in vivo*, in a context-dependent manner[55]. For example, HSV-1 mutants lack of the genes encoding thymidine kinase (TK) or ribonucleatide reductase (RR)

are replication defective in neurons, in which the virus needs to synthesize its own DNA precursors[56, 57]. However, this mutant retains the ability to undergo lytic replication in rapidly dividing cells, such as cancer cells. *In vivo*, viruses that are null of ICP34.5, either alone or in combination with RR, have been shown to replicate selectively in rapidly dividing malignant cells and have been developed as oncolytic agents[57, 58]. The ICP34.5 mutants have been studied in phase I clinic trial for the treatment of brain cancer[57]. Although the conditionally replicating vectors appear non-toxic at present, it is not yet clear whether these therapeutic agents are efficacious.

1.2.2.3 Replication defective vectors Replication defective HSV-1 vectors have been developed by the deletion of the essential immediate early genes (ICP4 and ICP27) [59-62]. Deletion of these genes prevents progression of viral gene expression from the immediate early to the early phase, thus blocking the lytic viral replication cycle. Infection of this type of vectors *in vivo* results in a state this is very similar to latency[63]. The genomes may persist for long period in neuronal or non-neuronal cells. The replication defective vectors can be efficiently produced in complementing cell lines that provide the deleted viral function *in trans*. Vectors deleted of ICP4 and ICP27 may be still toxic, due to the expression of other IE gene products. HSV-1 vectors of less toxicity can be created by the deletion of more IE genes or other essential viral genes[62]. These replication defective genomic vectors may be the best currently attainable compromise between minimizing toxicity and maximizing production.

1.2.3 Applications of HSV-1 Vectors to Diseases of the Nervous System

Many diseases of the nervous system are chronic. Effective gene therapy for these diseases will depend on delivery of appropriate therapeutic genes to a relevant population of neurons or glia, followed by long-term transgene expression. Replication defective HSV-1 vectors are extremely attractive for the treatment of neurological diseases because of their

natural neurotropism and the propensity of the virus to remain latent for the duration of the host lifetime. Direct inoculation of these vectors into neural parenchyma is effective in rodent models of brain tumor, Parkinson disease, spinal cord injury, and spinal root trauma. Subcutaneous inoculation of the HSV-1 vectors can be used to transduce neurons of the dorsal root ganglion to provide a therapeutic effect in models of polyneuropathy and chronic regional pain. The preclinical applications of HSV-1 vectors in animal models of neurological diseases have been reviewed by Glorioso[64, 65] and Burton[8, 66, 67]. In human trials, direct injection of replication-competent HSV-1 into brain tumors has proven safe[57]. Human trials of replication defective HSV-1 vectors by direct inoculation for treatment of glioblastoma and HSV-1 gene transfer by subcutaneous inoculation for the treatment of chronic intractable pain should commence soon.

1.3 VIRAL VECTOR MANUFACTURING

1.3.1 Viral Vector Production from Cell Culture

The clinical implementation of gene therapy requires large scale production of viral vector stocks derived from packaging cell lines. In general, the efficiency of vector production depends on the vector itself, the complementary cell line, and the cell culture conditions.

As mentioned earlier, some genes that are essential for virus replication in host cells are deleted in viral vectors. The deleted genes are stably transfected into packing cell lines to support vector growth. However, the productivity of these crippled viruses in packing cell lines is usually significantly lower than that of wild type viruses, and it depends heavily on how well the packaging cell lines complementarily provide the deleted viral gene products *in*

trans. Therefore, packaging cell lines for vector production should be strategically developed to optimize the expression kinetics of the viral genes so as to achieve high level of viral vector production.

In addition, cell culture parameters, such as temperature, multiplicity of infection, passage number, medium components and serum concentration, level of inhibitory metabolic by-products, and culture confluency at time of infection, will also affect the vector yield. It is expected that the advances in cell culture engineering, cell metabolism, bioreactor design and operation, will all positively impact the efficient production of viral vectors. Recent advances include the removal of serum from the culture medium, the implementation of suspension culture (either by the development of anchorage-independent cell line or through the use of micro-carriers), and the development of more efficient bioreators or cell culture operation models.

1.3.2 Viral Vector Purification

Viral vectors produced from packaging cell lines are invariably contaminated with host cell proteins and DNA, as well as other substances introduced in the manufacturing process. Elimination of these contaminants from viral vector preparations is helpful to improve the transduction efficiency. Further, the high purity specifications are strictly required by the regulatory agencies for the clinical application of viral vectors. In this sense, efficient and scaleable purification processes of high yield are essential for the advancement of gene therapy into clinic.

1.3.2.1 Harvesting, clarification, and concentration At end of viral vector propagation in packaging cell lines, the vectors will be either located intracellularly or extracellularly (through active release or lysis). This feature of viral vectors determines the method to be used to for their harvesting, clarification and concentration.

Retrovirus (including lentivirus) vectors are actively secreted into the culture medium without causing cell lysis. Therefore there is no need to intentionally break up the packaging cells to release the vectors during harvesting. Adenovirus and AAV are lytic viruses, yet the majority of vector particles will remain within the cells after the completion of vector growth. Physical methods such as freezing-and-thawing and sonication are usually employed to further break up the cells and release the intracellular vectors. For HSV-1, vector particles that remain within the cells are unlikely to have reached a sufficiently mature state for harvesting. Among the extracellular HSV-1 particles, a large fraction remains closely associated with the outer membrane of the host cells. Buffers containing high concentration of salt can be introduced into the harvest to release the cell-associated HSV-1 vectors into the culture medium.

After harvesting, the first processing operation in a viral vector purification train will be a solid-liquid separation step that is aimed at recovery of cells enriched with intracellular products (adenovirus and AAV vector), or to eliminate cells and debris from the supernatant that is enriched in extracellular products (retrovirus and HSV-1 vector). In laboratory scale, such clarification step is usually achieved by centrifugation, due to its ease of implementation. However, centrifugation process is hard to scale up and the centrifuges used for large scale operation are usually very expensive. Membrane filtration in dead-end or cross-flow modes provides a more efficient way for solid-liquid separation and it is easy to scale up. We have developed a tangential flow filtration process to clarify cell debris from HSV-1 vector preparations[68]. Over 90% of HSV-1 vectors in the supernatant can be recovered after clarification through a cartridge of hollow fiber membranes of 0.8 μm pore diameter. Membrane filtration processes for the clarification of retrovirus and lentivirus preparations have also been reported[69, 70].

Following the clarification, a concentration step is typically employed to diminish the necessary scale of subsequent operations and to increase the kinetic driving force for the subsequent purification. The concentration of conventional viral vaccines by precipitating or centrifuging the viral particles into solid pellets is commonly undertaken, but some loss of infectivity of the vectors during the phase change appear to have restricted application of these methodologies for gene therapy vectors. In contrast, tangential flow filtration involves no phase change. This process concentrates the viral vectors in retentate and pemeates water and low molecular weight impurities. Kuiper et al. used a 0.3 m^2, 100 kDa molecular weight cut-off Sartocon ultrafiltration module to concentrate moloney murine leukemia viral vector[69]. The process was conducted in a diafiltration mode to wash out protein and DNA impurities. About 160 fold concentration was achieved with an average of 77±14% infectious virus recovery. The concentration of lentivirus vectors by tangential flow ultrafiltration (TFF) was studied by Geraerts et al[70]. TFF allowed a 66-fold concentration of the vectors with complete vector recovery.

1.3.2.2 Purification Impurities in the clarified and concentrated viral vector preparations will be extensively removed in the subsequent purification steps. Traditionally, viral vectors have been purified by CsCl gradient centrifugation, which is both time and labor intensive, and is not amenable to scale up. In addition, in order to achieve a high degree of purity, it was necessary to perform double or multiple rounds of CsCl centrifugation. The lengthy exposure of viral vector to high salt concentration may result in gradual inactivation of the vector. For example, Auricchio et al. documented that the infectivity of AAV vector decreased by a factor of 2 every 24 hr the virus was incubated in CsCl[71]. Moreover, gradient centrifugation may not remove particular contaminants that have size and density properties very close to those of

the viral particles. Replacing the gradient centrifugation in viral vector purification with a more efficient and scaleable purification method such as column chromatography will provide more efficient and cost-effective vector purification.

Chromatography procedures based on ion exchange, affinity, and size exclusive interactions have been used for viral vector purification. The choice of chromatography mode in a particular case depends on the biochemical properties of the viral vector and the stage of purification. If necessary, a sequential combination of chromatography steps based on different interaction modes will be implemented to achieve the required purity.

Ion exchange chromatography separates molecules based on the differences of overall charges of the molecules. For viral vector purification, ion exchange chromatography can be carried out in either retention or flow-through mode. In the retention mode, the viral vectors will bind to the ion exchange column and the impurities will pass through the column. In the flow-through mode, the viral vectors will pass through the column with the retention of impurities. The advantages of ion exchange include its versatility and flexibility. However, the specificity of ion exchange may not be high enough to allow sufficient purification in a single chromatography step.

Ion exchange chromatography has been used for AAV vector purification. Zolotukhin et al. used Q-Sepharose anion exchange chromatography to purify AAV serotype 1, 2, and 5 preparations that were previously partially purified by iodixanol gradient centrifugation[72]. The purified vector stocks after ion exchange are 99% pure with titers of $1*10^{12}$ to $1*10^{13}$ vector genomes/ml. Smith et al. developed a process combining anion-exchange and size exclusion chromatography (SEC) to purify AAV 5 particles to near homogeneity[30]. (SEC or gel filtration chromatography separates biomolecules on the basis of differences in molecular size. Large molecules are excluded from pores and are eluted prior to smaller ones.) In the process developed by Smith et al., AAV particles were directly captured on a Mono-Q anion

exchanger from cellular extracts at pH 6. The AAV particles eluted from the anion exchange column were further purified on a Superdex 200 gel filtration column, which has an exclusion limit for globular proteins of approximately $1.3*10^6$ Da[30]. Kaludov et al. described a process involving the capture of AAV 5 followed by additional purification and concentration using a centrifugal filtration device[73]. Davidoff et al. utilized cation exchanger to capture impurities from the AAV 8 preparation[74]. The AAV8 particles that passed through the cation exchanger were then captured on an anion exchanger. Elution of the bound AAV 8 from the anion exchanger using high salt concentration resulted in an AAV preparation that has greater than 90% purity.

The adenovirus particle has an acidic pI. As such anion exchange resins have been shown to selectively bind adenovirus particles from contaminating cellular components and free viral proteins/DNA. Anion exchange as the sole chromatographic step usually fails to produce adenovirus with purity to or better than 2 X CsCl gradient centrifugation. Therefore, a polishing step is necessary. The studies by Huyghe et al. present data on the use of anion exchange as a capture step and immobilized metal affinity chromatography (IMAC) as a polishing step[75]. Blanche et al. demonstrated the utility of anion exchange to produce high-quality adenovirus[21]. Kamen used Fractogel EMD DEAE-650 anion exchanger to capture adenovirus vectors and utilized a gel filtration step to finish the polishing step[76]. As an alternative polishing step, Green et al. proposed use of a PolyFlo flow-through chromatographic method to remove additional host and viral proteins not removed in the first anion-exchange step[77].

Ceramic hydroxyapatite comprises functional groups of positively charged pairs of calcium ions and clusters of negatively charged phosphate groups. Therefore, it combines

both cation exchange and anion exchange in one column. Hydroxyapatite adsorptive chromatography was found to purify wild-type inactive MoMLV[30] as well as recombinant retroviral vectors[69], with moderate recovery of infectious particles (18–31%).

Affinity chromatography is a technique enabling purification of a biomolecule with respect to individual chemical structure. The substance to be purified is specifically and reversibly adsorbed to a ligand, which is immobilized by a covalent bond to a chromatographic matrix. In comparison to ion exchange, affinity chromatography usually has a higher selectively and efficiency. Sometimes, one-step purification can be achieved from affinity purification.

Heparin and the structurally related heparan sulfate belong to the family of glycosaminoglycans (GAGs) which are linear anionic polymers made up of repeating disaccharides units of glucosamine and uronic acid. The ubiquitously distributed cell surface heparan sulfate serves as receptor for several viruses, such as AAV2 and HSV, to bind to and gain access to susceptible cells. Heparin affinity chromatography proved to be a powerful tool for the purification of AAV2. Zolotukhin demonstrated the use of heparin affinity chromatography to purify AAV2 stock from iodixanol gradient centrifugation[78]. Harnessing the high selectivity of heparin chromatography, Auricchio developed single-step gravity-flow heparin affinity purification for AAV2[71]. The purity of AAV2 prepared from gravity-flow heparin affinity chromatography was higher than that from 2X CsCl gradient centrifugation, yet the latter technique required much more time and labor. O'Keeffe et al. investigated different heparin functionalized matrixes for the purification of herpes simplex virus 2 vaccine. They found that HSV2 vaccine exhibited substantial adsorption on heparin HP matrix[79]. The adsorbed vaccine particles could be completely recovered from the matrix with 1.5 M NaCl buffer to provide a purified preparation containing only 0.05 pg protein/pfu and 1.2×10^{-4} pg DNA/pfu. Segura et al. demonstrated the use of heparin chromatography for the

purification of VSV-G pseudo-typed moloney murine leukemia virus[80]. Intact, infective retroviral particles were recovered by elution with low salt concentrations (350 mM NaCl). A purification factor of 63 with a recovery of 61% of functional retrovirus particles was achieved using this single step.

Another example of receptor affinity purification for viral vectors was demonstrated by Auricchio et al., who isolated AAV5 vectors by a single-step chromatography through a mucin affinity column[81]. The rationale for developing this method was based on the observation that 2,3-linked sialic acid is required for AAV5 entry[82].

Although simple and effective, receptor affinity purification relies on the specific interaction of a particular viral vector with its cell surface receptor. Because of the specificity, the affinity ligand used for purifying one viral vector may not be applicable to others. For example, heparin affinity chromatography is not an effective purification method for AAV serotypes 1, 5, and 8, which do not use heparan sulfate as receptors. Moreover, for many viruses, their entry receptors are either unknown or too expensive to be used as ligands for purification. Thus, inexpensive generic affinity ligands that bind to different types of viral vectors will be promising for viral vector purification.

1.4 IMMOBILIZED METAL AFFINITY CHROMATOGRAPHY

Transition metal ions used in immobilized metal affinity chromatography (IMAC) are classified as generic affinity ligands since specific biological binding sites of proteins are not necessary involved. In contrast, coordination interactions between transition metal ions and protein surface electron donating groups form the basis of IMAC separation[83]. Typically, the metal ions, such as Cu^{2+}, Zn^{2+}, Ni^{2+}, Co^{2+}, or Fe^{3+}, are immobilized on a chromatographic support through coordination with chelating molecules such as iminodiacetate (IDA) or nitrilotriacetate (NTA), which are covalently attached to the support. Amino acids histidine,

tryptophan, and cysteine which contain electron donating imidazole and thiol groups are primarily responsible for the binding of proteins to immobilized metal ions[83]. Factors such as the accessibility, micro-environment of the binding residue, co-operation between neighboring amino acid side groups, and local conformations play important roles in the strength of binding and thus protein retention[84]. Elution of the bound proteins is accomplished by passing solution containing increasing concentration of hydrogen ions or imidazole. Hydrogen ions compete with the immobilized metal ions for the binding site on the protein while imidazole competes with proteins for the immobilized metal ions. After gradient elution, the metal ions and strongly bound proteins can be stripped from the column by passing a solution of ethylene diamine tetraacetic acid (EDTA), which is a strong chelating agent. Low cost of operation, ease of regeneration of the matrix and relatively high specificity of protein-metal interaction are among the key advantages of IMAC.

Since its introduction by Porath in 1975[85], IMAC has been used for the purification of a wide variety of proteins displaying favorable metal binding characteristics[86, 87]. When a protein lacks the prerequisites for retention on IMAC columns, genetic modifications that fuse the protein to a metal binding peptide (referred to as affinity tag) may endow the protein with increased metal binding affinity. One commonly used affinity tag is the sequence comprised of six adjacent histindine residues (His_6)[88, 89]. Literature reports also describe the purification of fusion proteins using other affinity tags that display different levels of metal affinity[90-92]. The level of affinity a desired protein should have for a chelated metal ion should be dictated by the relative affinity of the cellular proteins of the host cell used for expression of that protein[93]. An affinity tag of appropriate affinity is the one that will direct the elution of

the fusion protein to the region of the elution profile where the elution of DNA and host cell proteins are minimal and the expression and activity of the fusion product are not compromised.

Recently, the application of IMAC has been extended to the purification of gene therapy viral vectors. This study describes the development of immobilized cobalt affinity chromatography for the selective purification of HSV-1 vectors engineered with cobalt affinity tags. During the progress of this project, IMAC purifications for AAV[94], adenovirus[75], retrovirus[95], have been reported.

1.5 REACTIVE OXYGEN FREE RADICALS AND METAL CATALYZED OXIDATION

Free radicals are defined as chemical species capable of independent existence that contains one or more unpaired electrons. Dioxygen (O_2) in its ground state, $^3\sum_g$-, is a biradical since it has two unpaired electrons each located in a different π^* antibonding orbital. These unpaired electrons spin in the same direction ("triplet" ground state), rendering dioxygen rather unreactive toward other molecules existing in "singlet" ground state with paired electrons. Thus, the chemistry of dioxygen, except for the excited singlet state $^1\Delta_g$ and $^1\sum_{g+}$, is favored by free radical reactions with the sequential acceptance of electron one at a time.

In the sequential electron-transfer process where O_2 undergoes reduction, several reactive intermediates are formed, such as superoxide ($O_2^{\bullet -}$), hydrogen peroxide (H_2O_2), and the extremely reactive hydroxyl radical (•OH): collectively termed as the reactive oxygen species (ROS)[96-99]. The process can be presented as:

$$\mathbf{O_2} \xrightarrow{e^-} \mathbf{O_2^{\bullet -}} \xrightarrow{e^-} \mathbf{H_2O_2} \xrightarrow{e^-} \mathbf{\cdot OH} \xrightarrow{e^-} \mathbf{H_2O}.$$

1.5.1 Generation of reactive oxygen free radicals

Oxidative free radicals are generated during normal cellular metabolism[100]. During oxidative phosphorylation, the mitochondrial cytochrome oxidase enzyme system links production of ATP to controlled tetravalent reduction of dioxygen to water. In this process, the ROS intermediates are tightly bound to the active sites of the enzymes. Numerous cytosolic enzymes can produce ROS outside the mitochondrial membranes. Those unbound ROS can disrupt normal functioning of the cell in disease states where the cellular antioxidant systems are impaired. Enzymes that catalyze univalent reduction of dioxygen to superoxide anion radical include xanthine oxidase, aldehyde oxidase, dihydrorotic dehydrogenase, flavin dehydrogenases, and peroxidases. A major source of hydrogen peroxide in cell is the dismutation of superoxide anion radical by the superoxide dismutase enzymes (SOD). Hydroxyl radicals are formed in the Fenton reaction whenever hydrogen peroxide comes into contact with transition metal ions[101]. In addition, the respiratory burst during phagocytic activity generates all forms of ROS essential for the host defense against invading microbes[102].

Outside the living systems, transition metal catalyzed oxidation is an important pathway that leads to the ROS generation[103-105]. Many transition metals such as Co, Cu, Fe, and Ni, which exist in several spin states, can function as catalysts to sequentially transfer electrons from electron donors to dioxygen. Normally, transition metals in their oxidized states (i.e., Co^{3+}, Cu^{2+}, Fe^{3+}, Ni^{3+}) do not react readily with dioxygen to generate a more reactive oxygen species. An electron donor or reducing agent is needed to reduce the transition metal ion[106]. This reduced form may then interact with dioxygen to generate ROS[107]. Typically, as illustrated in Eqs.1 & 2, the reduced form of transition metal ion, complexed by appropriate ligands, may donate an electron to reduce dioxygen to form superoxide anion radical. In these equations, C_x represents a complex that may include chelating molecules, solvent, reducing

agent, etc. Superoxide anion radical may acquire another electron from the reduced form of transition metal ion to form hydrogen peroxide (Eqs. 3). It is also possible that hydrogen peroxide is generated directly without the superoxide intermediate.

$$O_2 + C_xM^{n+} \rightarrow C_xM^{n+}\text{-}O\text{-}O\bullet \rightarrow C_xM^{(n+1)+}\text{-}O\text{-}O^- \quad (1)$$

$$C_xM^{(n+1)+}\text{-}O\text{-}O^- \rightarrow C_xM^{(n+1)+} + O_2\bullet^- \quad (2)$$

$$C_xM^{n+} + O_2\bullet^- + 2H^+ \rightarrow C_xM^{(n+1)+} + H_2O_2 \quad (3)$$

The reactivity of either superxide anion radical or hydrogen peroxide by itself to other molecule is rather low. However, in the presence of transition metal ions, they are converted to highly reactive hydroxyl radical via Fenton (Eqs. 4) or Haber-Weiss reaction (Eqs. 6)

$$C_xM^{n+} + H_2O_2 \rightarrow C_xM^{(n+1)+} + OH^- + \bullet OH \quad (4)$$

$$C_xM^{(n+1)+} + O_2\bullet^- \rightarrow C_xM^{(n)+} + O_2 \quad (5)$$

$$H_2O_2 + O_2\bullet^- \rightarrow O_2 + OH^- + \bullet OH \quad (6)$$

It is of note that Eqs. 6 is the combination of Eqs. 4 and Eqs. 5. Eqs. 3 and Eqs. 6 indicate that, depending on the reaction conditions, $O_2\bullet^-$ may serve as either the reductant or oxidant of the metal ion.

The ligand with which the transition metal ion is complexed has a profound effect on the oxidative activity of transition metal ions. It may either enhance or inhibit the dioxygen activation. For example, activity of Fe^{2+} is enhanced by EDTA or nitrilotriacetic acid (NTA), but inhibited by *o*-phenanthroline and deferoxamine[108]. Unchelated Ni^{2+} reacts with H_2O_2 only very slowly. However, its reactivity toward H_2O_2 and other oxygen species may be greatly accelerated by oligopeptides or proteins[109, 110]. Likewise, Co^{2+}, stable under air, becomes sensitive to oxidation with atmospheric O_2 in the presence of organic ligands[111, 112].

1.5.2 Oxygen free radical mediated damage to biomolecules

The highly reactive free radical intermediates can cause irreversible oxidative damages to proteins [113, 114], nucleic acids [115, 116], and lipids [117, 118] in the cell, resulting in deleterious biological consequences such as aging [118], carcinogenesis [116] and other disease states [119, 120]. In addition, metal catalyzed free radical generation *in vitro* is an important pathway that leads to the inactivation, modification, or degradation of biological products during bioprocessing, transport, and storage [121].

ROS from metal catalyzed oxidation cause protein damage such as fragmentation, carbonyl formation, and oxidative modification of amino acid residues[114]. It is important to note that the oxidative free radical intermediates react immediately with the amino acids at the metal-binding site before diffusion into bulk solution. This feature makes metal catalyzed oxidation a site-specific process[104]. The amino acid residues most susceptible to metal catalyzed oxidation are Cys, His, Arg, Lys, and Pro. The sulfhydryls of Cys are commonly oxidized to disulfides, but they may be turned into sulfino- sulfeno-, and solfono- derivatives as well. The His imidazole may be oxidized to aspartic acid, asparagines, or 2'-OH-His. Arg is converted to γ-glutamic-semialdehyde; Lys, to 2-amino-adipic-semialdehyde; and Pro is turned into glutamic acid, pryoglutamic acid, γ-aminobutyric acid, and γ-glutamic-semialdehyde. Glutamic and aminoadipic semialdehydes are the main carbonyl products of metal catalyzed oxidation of proteins. The oxidative free radicals could also cause intra- or inter-protein cross-linking. Because of this, proteins also may become cross-linked with DNA.

Although loss of activity of protein is a sensitive and vital indicator of protein damage, it does not necessarily reflect all forms of damage, nor does it elucidate the nature of the damage. SDS-PAGE is a common method for measuring fragmented or cross-linked proteins,

while amino acid analysis or peptide mapping can used to measure chemical modification. Another important indication of protein damage is an increased sensitivity to digestion by proteolytic enzymes such as chemotrypsin or trypsin. A damaged protein with increased proteolytic susceptibility but retained biological activity might have a decreased half-live *in vivo* [122].

ROS can also cause oxidative damage to DNA: both nuclear and mitochondrial. The nature of such damage includes mainly base modification, deoxyribose oxidation, strand breakage, and DNA-protein cross-links. Among the various ROS, •OH generates various products from the DNA bases which mainly include C-8-hydroxylation of guanine to form 8-oxo-7, 8 dehydro-2'-deoxyguanosine, a ring-opened product; 2, 6-diamino-4-hydroxy-5-formamimodipyrimidine, 8-OH-adenine, 2-OH-adenine, thymine glycol, cytosine glycol, etc[123]. ROS-induced DNA damages include various mutagenic alterations as well. For example, mutation arising from selective modification of G:C sites specially indicates oxidative attack on DNA by ROS[124].

Oxidative free radicals catalyze the oxidative modification of lipids. While lipid peroxidation is not initiated by $O_2^{\bullet -}$ and H_2O_2, the generation of •OH in the presence of transition metals results in the initiation of lipid peroxidation[125]. This can lead to a propagation process since peroxy radicals are both the products of lipid peroxidation as well as reaction initiators. Lipid peroxy radicals react with other lipids, proteins, and nucleic acids. Cell membranes, which are structurally made up of large amounts of polyunsaturated fatty acid, are highly susceptible to oxidative attack. As a consequence, changes in membrane fluidity, permeability, and cellular metabolic functions may result.

During IMAC purification, immobilized transition metal ions contact a wide variety of compounds in the mobile phase, which may include dissolved oxygen and reducing agents from cell culture. Thus, there are possibilities that the metal ions could trigger free radical

generation and cause damage to the biological product upon purification on IMAC. However, in contrast to the large body of literatures that address metal catalyzed oxidation in solution, the metal catalyzed oxidation of biological products in IMAC has not been well recognized. This study describes the inactivation of HSV-1 vector by •OH radicals when it is purified on immobilized cobalt affinity column. The virus inactivation could be substantially reduced by the inclusion of free radical scavenger such as ascorbate in the chromatographic mobile phase. This finding is the first demonstration of oxygen free radical mediated biological inactivation in an actual IMAC purification and an effective method to prevent it.

2.0 MATERIALS AND METHODS

2.1 VIRUSES AND CELLS

All viruses were derived from KOS strain of HSV-1. Vector QOZHG[126] (derived from d106[63, 127]) was used as the untagged virus in the initial IMAC study. The d106 vector (kindly provided by Neal DeLuca, Univeristy of Pittsburgh) has deletions of the essential immediate early (IE) genes ICP4 and ICP27. Two other IE genes, ICP22 and ICP47 have mutations in their promoters such that they are expressed as early genes. The ICP27 deletion was replaced with a human cytomegalovirus (HCMV) IE gene promoter driving a green fluorescence protein (GFP) reporter gene cassette. The UL41 gene was disrupted in d106 by the insertion of HSV-1 ICP0 IE promoter driving a *lacZ* expression cassette to produce the QOZHG. The QOZHG vector was propagated in 7B cells[61, 128], a Vero cell line stably transfected with ICP4 and ICP27. HSV-1 mutant K082[129] (gift from Dr. Stan Person, Johns Hopkins University) was used as backbone virus to construct the gB tagged virus KgBHAT. The gB gene of K082 harbors an *Hpa*I linker insertion that introduces a chain terminator codon at gB amino acid residue 43. K082 virus produces no gB-specific polypeptide and can only grow in the gB expressing Vero cell line, D6 (also a gift from Dr. Stan Person). Once constructed, KgBHAT was propagated in Vero cells. The KgBpK$^-$ control virus[35], in which the heparan sulfate binding of gB was deleted, was propagated on Vero cells. All cell lines were maintained at 37^{o}C in Dulbecco's modified essential medium (DMEM: Life Technologies Inc. Gaithersburg, MD) supplemented with 10% fetal bovine serum, 2 mM L-glutamine, and 100 U/ml penicillin/streptomycin (all media supplements were supplied from Life Technologies Inc).

2.2 CONSTRUCTION OF gB MUTANT PLASMID

Plasmid pgBHAT was constructed by inserting in frame the sequence encoding the cobalt affinity peptide tag (HAT) [90] within a plasmid (pTZ18UgBpK$^-$) encoding a mutant form HSV-1 gB (UL27). Plasmid pTZ18UgBpK$^-$ was previously constructed by us[35], in which the 27 nucleotides encoding the heparan sulfate binding domain of gB (amino acid 68-76 [KPKKNKKPK]) was replaced by an in-frame *BamH*I site for future cloning. The synthesized oligonucleotides encoding HAT (HAT amino acid sequence: KDHLIHNVHKEEHAHAHNK[90]) were designed (sense:5'GATCTGAAGGATC ATCTCATCCACAATGTCCACAAAGAGGAGCACGCTCATGCCCA CAACAAA-3' and anti-sense: 3'-ACTTCCTAGTAGAGTAGGTGTTACAGGTGTTTCTCCTCGTGCGA GTACGGGTGTTGTTTCTAG-5') to be flanked by *Bgl*II sticky ends (Fig. 5). The oligonucleotides (10 pM) were mixed in PBS, denatured at 100^{o}C for 10 min and then annealed for 1 h. *BamH*I digested plasmid pTZ18UgBpK$^-$ DNA was dephosphorylated, gel purified, and then ligated with the annealed HAT coding oligonucleotide mixture and then the ligation mixture was transformed into DH5α competent cells (Invitrogen, Carlsbad, CA). Single colonies from the transformation were cultured and plasmid DNA extracted using the Qiagen Quick Plasmid Kit (Qiagen, Valencia, CA). Clones containing HAT inserts were screened for the lack of a *BamH*I site and the orientation of HAT coding sequence was confirmed by DNA sequencing analysis (forward primer: 5'-CTCTTGGGGTTGACGCT GGGGG-3', reverse primer 5'-GTTTGCATCGGTGTTCTCC GCC-3') in University of Pittsburgh Molecular Medicine Institute DNA sequencing core facility.

2.3 CONSTRUCTION AND ISOLATION OF gB TAGGED HSV-1 MUTANT

To construct the gB tagged virus KgBHAT, plasmid pgBHAT was co-transfected with K082 viral DNA on Vero cells using LipofectAmine (Invitrogen Corporation, Carslbad, CA). Single recombinant virus plaques formed on Vero cells were purified three times by limiting dilution[130]. On each round of plaque purification, DNA from single plaque isolates in 96-well were screened by Southern hybridization with a gB probe that hybridized to the gB coding sequence. The positive plaques were then subjected to the next round plaque purification. The viral DNA was extracted from positive plaques after the third round isolation and subjected to polymerase chain reaction (PCR) using primers that flank the locus of the HAT insertion (forward 5'-CTCTTGGGGTTGACGCTGGGGG-3', reverse 5'-GTTTGCATCGGTGTTC TCCGCC-3'). The PCR product was further subjected to DNA sequencing analysis to verify the incorporation HAT coding sequence in KgBHAT genome.

2.4 SOUTHERN BLOT HYBRIDIZATION

Southern blot analysis was performed to confirm that KgBHAT genome carries the HAT coding sequence. Viral DNA of KgBHAT and control virus K082 were digested with *BamH*I or *Hpa*I, separated on an agarose gel, and transferred to a nitrocellulose membrane for analysis. A biotin-labeled gB probe was synthesized from a 1.3kb *Sph*I and *Sal*I digested pTZ18UgBpK$^-$ fragment using North2South biotin random prime kit (Pierce Biotechnology, Rockford, IL). The hybridization and detection procedures were followed according to North2South chemiluminescent nucleic acid hybridization and detection kit (Pierce Biotechnology).

2.5 WESTERN BLOT HYBRIDIZATION

Western blot analysis was performed to verify the presence of HAT peptide on HSV-1 gB molecule. Vero cells were infected with KgBHAT or control virus KgBpK$^-$ respectively. 48 hour after infection, cells were harvested, pelleted, washed with PBS, and lysed in RIPA buffer (150 mM NaCl, 10 mM Tris, 0.1% SDS, 1% Triton X-100, 1% Deoxycholate, 5 mM EDTA, 1 mM phenylmethylsulfonyl fluoride, and 10 mM benzamidine). After clarification by centrifugation, an appropriate amount of supernatant was mixed with 4X NuPAGE LDS Sample Buffer (Invitrogen, Carlsbad, CA) and heated at 70^{o}C for 10 minutes. Each protein sample was loaded into duplicated wells on NuPAGE Novex Tris-Acetate gel (Invitrogen, Carlsbad, CA) and electrophoresed. The gel proteins were then transferred onto Immobilon-P PVDF membrane (Millipore, Billerica, MA). The membrane was cut into halves with each half containing proteins from both KgBHAT and KgBpK$^-$ samples. The membranes were probed separately either with a rabbit polyclonal antibody (Clontech, Palo Alto, CA) against HAT peptide, or with a HSV gB monoclonal antibody (Virusys, Sykesville, MD) overnight at 4^{o}C in PBS containing 2% dry milk. The membranes were then washed with PBS containing 0.05% tween-20, incubated with either anti-rabbit or anti-mouse horseradish peroxidase conjugated antibodies (Sigma, St. Louis, MO) in 2%Milk/PBS for 1 h at 25^{o}C. After additional washes, the membranes were juxtaposed together and the signals were developed into one X-film according to the standard protocol using the Amersham ECL kit (Amersham Pharmacia Biotech, Piscataway, NJ).

2.6 VIRUS ADSORPTION ASSAY

Monolayers of confluent Vero cells in 6-well plates were incubated at 4^{o}C with 250 pfu/well of KOS, KgBpK$^-$, or KgBHAT viruses suspended in 1ml/well serum medium (DMEM containing 10% FBS) for 10 to 110 min, after which the unbound viruses were

removed and the cell monolayer was washed three times with cold serum medium. The cell monolayer was subsequently overlaid with 2 ml serum medium containing 0.5% methylcellulose, shifted to 37^{o}C, and incubated for 2 days to allow plaques to form. In control wells, the cells were incubated with the viruses for 2 h at 4^{o}C, the plates shifted to 37^{o}C for additional 1 h incubation, and the previous medium replaced with 2 ml methylcellulose medium. The plaques formed in each well were counted and normalized to control wells. The increase in normalized plaque number with the increase of adsorption time was taken as a measure of mutant virus adsorption rate.

2.7 VIRUS PNENETRATION ASSAY

The penetration rate of the gB mutants was assayed by determining the rate at which penetrated virus became resistant to inactivation by treatment of infected monolayer with low-pH glycine buffer. Confluent Vero cells in 6-well plates were incubated with 250 pfu/well of KOS, KgBpK^{-}, or KgBHAT in 1 ml/well serum medium for 2 h at 4^{o}C. Following adsorption, the cells were rinsed three times, overlaid with serum medium, and shifted to 37^{o}C to allow virus penetration. At selected times after shifting, cells will be treated with 1 ml/well 0.1 M glycine (pH 3.0) for 1 min to inactivate virus that had not penetrated the cells. The control monolayer was treated with 1 ml PBS for 1 minute. The cells will be washed 3 times with complete medium, overlaid with methylcellulose medium, and incubated in 37^{o}C for 2 days. Plaques were visualized and counted as described above.

2.8 VIRUS PROPAGATION

QOZHG virus was propagated in 7B cells at 37^{o}C in roller bottles containing 100ml D-MEM supplemented with 10% FBS, while KgBHAT virus and its counterpart KgBpK^{-} virus were propagated in Vero cells using UltraMDCK serum free medium (Cambrex

Bioscience Inc., Baltimore, MD) by the same procedure. Upon cell confluence in a 150 cm^2 vented cap polystyrene tissue culture flask (Becton Dickinson, San Diego, CA), the original cell culture medium was removed, and 2 ml cell culture medium (10% FBS in DMEM for QOZHG, UltraMDCK for KgBHAT) containing $2x10^6$ pfu (plaque forming unit) QOZHG or KgBHAT viruses was added into the flask. This resulted in a multiplicity of infection (MOI) of 0.1 pfu/cell. After 1 hour infection at 37^oC, 18 ml of fresh cell culture medium (10% FBS in DMEM for QOZHG, UltraMDCK for KgBHAT) was added over the infected cell monolayer and incubated at 37^oC for 3 days for the virus replication.

2.9 VIRUS HARVEST AND PROCESSING

The infected cells typically detach from the surface at about 72h post-infection. At that time, the culture was harvested and mixed with 2 M NaCl in PBS (pH 6.5) to the final salt concentration of 0.5 M in order to release cell-associated viruses. Cell debris was removed by centrifugation at 2,000g for 10 minutes. The virus supernatant was further clarified by filtering through a 1.2μm Acrodisc syringe filter (Pall Life Science). The clarified supernatant, designated as crude supernatant, was used as loading sample for the subsequent IMAC step. Alternatively, the crude supernatant was centrifuged at 20,000g for 1 h to pellet the viruses. The virus pellet was resuspended in PBS, 0.5 M NaCl, pH6.5. The virus suspension, designated as partially purified virus preparation or pellet suspension, was also used as a loading sample for the IMAC.

2.10 IMMOBILIZED METAL AFFINITY CHROMATOGRAPHY

Chromatography was performed with a 1 ml HiTrap IDA metal-chelating column. An LKB P-1 pump was used to load samples and buffers (both the column and the pump were from GE Healthcare, Piscataway, NJ). The column was washed with 5 column volumes (CV) of distilled water and then loaded with 5 CV of selected metal $CuSO_4$, $ZnCl_2$, $NiSO_4$, and $CoCl_2$ in water. The column was subsequently washed with 7 CV of distilled water followed with 7 CV of PBS, 0.5 M NaCl, pH4.0 buffer. This step was used to remove any nonspecifically bound metal ions. The column was then equilibrated with 7 CV of equilibrium buffer (PBS, 0.5M NaCl, pH6.5) or equilibrium buffer containing various concentrations of ascorbate or imidazole as noted for each experiment. Virus samples which were harvested and processed, as noted earlier, were directly loaded on the column with or without ascorbate or imidazole. After loading the sample, the column was washed with 4 CV of the equilibrium buffer. Bound viruses were eluted with 4 CV of a low pH buffer (PBS, 0.5 M NaCl, pH5.5) or the same buffer containing various concentrations of ascorbate. Alternatively, the column was eluted with an imidazole containing buffer (PBS, 0.5M NaCl, 140 mM imidazole, pH6.5). Finally, an EDTA containing buffer (PBS, 0.5 M NaCl, 50 mM EDTA, pH6.5) was used to strip the metal ions and any residual bound materials from the column. The loading virus suspension and all of the elution fractions were assayed for virus, total protein, and DNA concentrations.

2.11 PLAQUE ASSAY

The quantification of infectious viral particles was accomplished by a standard plaque assay. Serial dilutions of virus were added to 8 $x10^5$ Vero cells in a 1.7 ml Eppendorf tube and rocked on a Nutator rocker (Becton Dickinson, San Diego, CA) at 37°C. After a 1 h adsorption period, the cells were plated in six-well plates. After 12 h, the inoculum was

replaced with complete medium containing 0.8% (wt/vol) methylcellulose (Aldrich, Milwaukee, WI.) and incubated for an additional 2 days. The plates were then stained with 1% (wt/vol) crystal violet (Aldrich, Milwaukee, WI.) in 50% methanol–50% H_2O (vol/vol), and the numbers of plaques were counted. Titers were calculated as PFU per milliliter of virus suspension.

2.12 PROTEIN AND DNA ASSAYS

Total protein concentrations in loading samples and elution fractions were measured with a Bio-Rad (Hercules, CA) protein assay kit. Bovine serum albumin was used as the standard protein for calibration. A Picogreen double-stranded DNA quantitation kit (Molecular Probes, Inc., Eugene, OR) was used to measure the DNA concentrations in all of the samples, with lambda DNA used as a calibration control. All assays were performed in triplicate under the conditions specified by the manufacturers.

2.13 TAQMAN REAL-TIME QUANTITATIVE PCR

Primer and probe specific to HSV-1 ICP47 gene sequence were used for the quantification of viral genomes. Q-PCR assays were conducted in 50 μl PCR volume containing 2 μl of DNA samples or standards, 400 nM of each primer, 200 nM Probe, and 1xTaqMan Universal PCR Master Mix (PE Applied Biosystems, Foster City, CA). Primer sequences for ICP47 (sense- CACGACATGCTTTTCCCGA, and antisense-TTCCCGCAGGAGGAACG) were designed using the Primer Express program (PE Applied Biosystem). The TaqMan probes for detection of ICP47 (CGCCGGTCGCCTCGACGA) were labeled with fluorescent reporter dye 6-FAM at the 5’ end and the quencher dye TAMRA at the 3’ end (PE Applied Biosystem). All PCR reactions were set up in a MicroAmp Optical 96-well Reaction Plate (PE Applied Biosystem).

Amplification conditions were 2 min at 50°C and 10 min at 95°C for the first cycle, followed by 40 or 50 cycles of 95°C for 15 sec and 60°C for 1 min. Standard curves for viral genes ICP47 were generated using 10-fold serial dilutions of plasmids known to contain the respective target sequences. The emission data was collected in real-time from an ABI PRIME 7000 Sequence Detector and analyzed by Sequence Detection program.

2.14 ELECTRON SPIN RESONANCE

Samples for ESR measurement were prepared as followed. 10 □l of 5,5-dimethylpyrroline-N-oxide (DMPO, Aldrich, Milwaukee, WI) solution (1M in buffer A) was added in 90 □l of one of the following samples: KgBHAT crude supernatant, KgBHAT pellet suspension in pH6.5 buffer (PBS, 0.5M NaCl, pH6.5), or the crude supernatant containing 20 mM ascorbate. The resultant mixture was added to 100 µl of IDA-Co^{2+} beads. The beads were obtained from a HiTrap IDA metal-chelating column charged with cobalt ions as described in the Immobilized Metal Affinity Chromatography section. 10 µl of the bead slurry was transferred into a capillary tube and subjected to ESR measurement.

EPR spectra were recorded at room temperature using a Bruker Elexsys E580 spectrometer (Bruker BioSpin GmbH, Rheinstetten, Germany) operating at 904 GHz with a 100-kHz modulation frequency. A microwave power of 20 mW and modulation amplitude of 1 G was employed. Spectra were simultaneously recorded on an IBM computer interfaced to the spectrometer.

3.0 DEVELOPMENT OF IMMOBILIZED COBALT AFFINITY CHROMATOGRAPHY FOR HSV-1 VECTOR PURIFICATION

Herpes simplex virus type 1 (HSV-1) is a promising vector for gene therapy applications particularly to peripheral nerves, the natural site of virus latency. Many gene vectors require large particle numbers for even early phase clinical trials emphasizing the need for high yield, scalable manufacturing processes that result in virus preparation nearly free of cellular DNA and protein contaminants. HSV-1 is an enveloped virus that requires the development of gentle purification methods. Ideally, such methods should avoid centrifugation and may employ selective purification processes that rely on the recognition of unique envelope surface chemistry. Here we describe a novel method that fulfills these criteria. An immobilized metal affinity chromatography (IMAC) method is described for the selective purification of vectors engineered to display a high affinity binding peptide. Feasibility studies involving various transition metal ions (Cu^{2+}, Zn^{2+}, Ni^{2+}, and Co^{2+}) showed that cobalt had the most desirable features which include low interaction with either normal virus envelope or contaminating DNA and proteins. The introduction of a cobalt specific recognition element into the virus envelope may provide a suitable target for cobalt dependent purification. To test this possibility, a peptide with affinity for immobilized cobalt was engineered in-frame in the heparan sulfate (HS) binding domain of HSV-1 glycoprotein B (gB) known to be surface exposed on the virion particle and recombined into the viral genome. By optimizing IMAC loading conditions and reducing cobalt ion leakage, we recovered 78% tagged HSV-1 recombinant virus with greater than 96% reduction in contaminating proteins and DNA.

3.1 INTRODUCTION

Human herpes simplex virus type 1 (HSV-1) is a neurotropic DNA virus that has been engineered for gene transfer applications including human gene therapy. HSV-1 based vectors exhibit the advantages of broad host cell range, large transgene packaging capacity, and potentially lifelong transgene expression in neurons using components of the natural virus latency promoter system[131, 132]. Recent reports describe extensive efforts to improve the quality of replication defective, genomic based, HSV-1 gene vectors, including reducing vector cytotoxicity, exploiting viral persistence in neurons for long term gene therapy, and targeting vector tropism by glycoprotein modification[61-63, 127, 133]. This class of HSV-1 vectors has been exploited for treatment of animal models of pain[50, 134-137], peripheral neuropathy[138, 139], and cancer[57, 77, 140-143]. In addition, characterization of the optimum conditions for replication defective vector growth enabled the efficient production of clinically relevant quantities of this vector[144-147]. However, efficient, validated methods for purification of vector nearly free of contaminating protein and nucleic acid are in development, and are required for advancing HSV-1 based gene therapy for patient applications.

Currently, HSV-1 vector preparations are harvested by clarifying the virus from cell debris using low speed centrifugation followed by a high speed centrifugation step to pellet the virus from soluble protein and DNA molecules[148, 149]. However, cell organelles, proteins, and DNA aggregates co-sediment along with the viral particles during the second centrifugation step. Removal of those impurities in the virus preparation conventionally relies on density gradient centrifugation[149-152], which is both time and labor intensive, and is not easily amenable to scale up. Moreover, gradient centrifugation may not remove particular contaminants that have size and density properties very close to those of the viral particles.

Replacing the gradient centrifugation in HSV-1 vector purification with a more efficient and scaleable purification method such as column chromatography will provide more efficient and cost-effective vector purification.

Column chromatography such as ion exchange or size exclusion has been used in purification of retrovirus[69, 153], adenovirus and adeno-associated virus (AAV) [77]gene therapy vectors as well as HSV vaccines[79]. Although these procedures can be effective, they may prove less efficient than ligand affinity chromatography. Immobilized metal affinity chromatography (IMAC) is a powerful and inexpensive ligand affinity purification method used in purification of a variety of proteins and peptides. IMAC utilizes the affinity interaction between the immobilized transition metal ions, such as Cu^{2+}, Zn^{2+}, Ni^{2+}, or Co^{2+}, and protein surface electron-donating groups, such as histidine, cysteine, and tryptophan residues. In comparison to affinity separation utilizing bio-molecules, such as antibodies or receptors, the chromatography substrate used in IMAC is more stable and inexpensive while providing the same high selectivity. Although IMAC was introduced two decades ago[85], it has been mainly applicable to protein and peptide purification. Recently this technique was reported for purification of adenovirus[75], adeno-associate virus[94], and retrovirus[95].

In this chapter, we report the use of IMAC for purification of recombinant HSV-1 preparations that have been clarified and concentrated by centrifugation or other methods such as filtration. In order to select the proper IMAC column, we first evaluated elution profiles for both HSV-1 vector and contaminants (protein and DNA) on iminodiacetate (IDA) chelating columns charged with different transition metals (Cu^{2+}, Zn^{2+}, Ni^{2+}, and Co^{2+}). Chromatographic analysis showed that neither the virus nor the contaminants bound IDA-Co^{2+}, suggesting that this column could be useful for HSV-1 vector purification if the vector could be endowed with the ability to bind to immobilized cobalt. Accordingly, we constructed an HSV-1 recombinant with a cobalt affinity tag replacing the heparan sulfate

(HS) binding domain of virion envelope glycoprotein B (gB). The binding and elution properties of the recombinant virus on IDA-Co^{2+} columns confirmed that efficient purification was possible. This method may also prove to be broadly applicable to purification of gene transfer vectors derived from different virus backgrounds.

3.2 RESULTS

3.2.1 Immobilized Metal Affinity Chromatography for Untagged HSV-1

The binding selectivity of IMAC can be tailored through the choice of metal ions, buffer conditions or by surface modification of the target product (protein, cell, or virus). The most desirable scenario would be that IMAC, using one of the commonly employed transition metal ions (Cu^{2+}, Zn^{2+}, Ni^{2+}, Co^{2+}), could be used to substantially purify HSV-1 based vectors. Therefore, we first examined the feasibility of using those metal ion columns for the purification of untagged HSV-1.

The HSV-1 based vector QOZHG[126] was used to test the binding and elution properties of untagged HSV-1 in IMAC. QOZHG is a replication defective virus deleted for the essential IE genes and contains expression cassettes for both lacZ and green fluoresscent protein (GFP). The vector was grown on 7B cells that complement *in trans* the missing essential viral genes. QOZHG was harvested from virus-infected cells, clarified by low speed centrifugation and concentrated by high speed centrifugation (see chapter 2 Materials and Methods for details). An aliquot of virus was re-suspended in loading buffer (PBS, 0.5M NaCl, pH7.0) and introduced into IDA columns charged with different metal ions. The columns were washed with loading buffer to remove any non-specifically bound material, eluted with a pH step gradient, and finally stripped with an EDTA containing buffer (PBS, 0.5M NaCl, 50mM EDTA, pH7.0). The eluent samples were collected and assayed for protein and DNA content as well as infectious viral particles. The IDA-Cu^{2+} column (Fig.1) captured most of the loaded untagged virus with only a very small percentage of virus present in the flow through (0.67%) and the pH 7.0 wash fraction (0.29%). Protein and DNA also efficiently bound Cu^{2+} and was only removed by stripping the column with EDTA. Only a small percentage of infectious viruses were recovered by this method, suggesting that

exposure to the copper column resulted in virus inactivation. The Zn^{2+} (Fig.2), Ni^{2+} (Fig.3), and Co^{2+} (Fig.4) columns displayed decreasing protein, DNA, and virus binding, respectively. The protein, DNA, and virus elution profiles from the each of these four columns did not provide a means of separating virus from contaminants. However of interest was the finding that the Co^{2+} column bound minimal amounts of protein, DNA, and virus; in certain fractions (pH5.5 and pH5.0); negligible amounts of contaminant proteins and DNA were eluted from the column, thus creating a low background region. These results suggested that immobilized cobalt affinity chromatography might be useful for separating virus from contaminants if the virus particles could be tagged with a cobalt specific ligand to enhance virus binding to cobalt under loading conditions and subsequently eluted in the low background region identified.

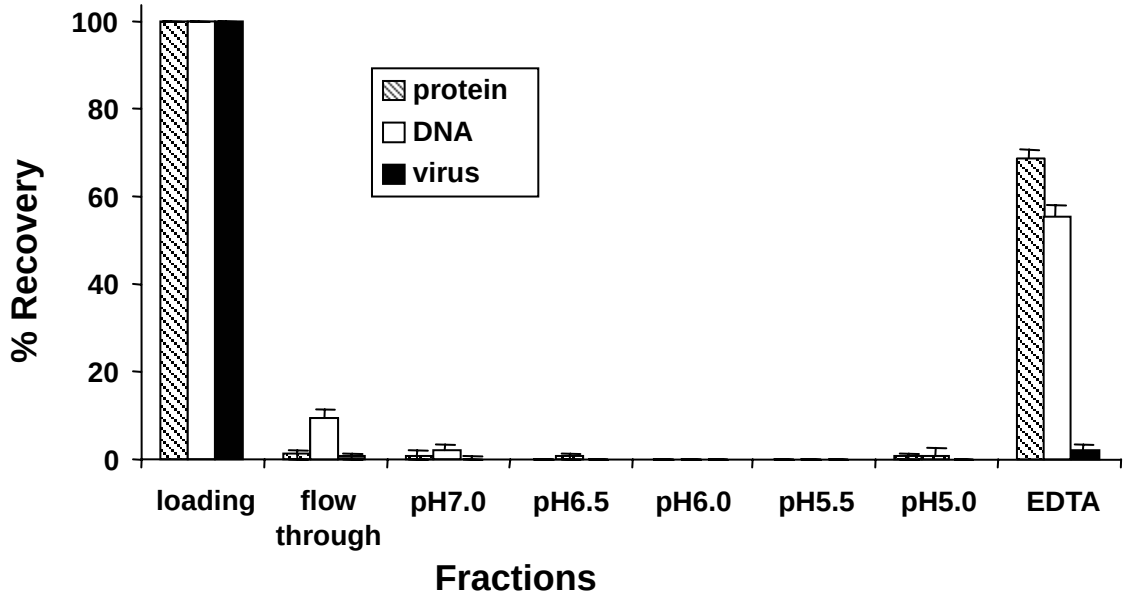

Figure 1. Elution Profiles of Virus, Total Protein and DNA on IDA-Cu^{2+} Column.

QOZHG virus after centrifugation was re-suspended in 10 ml loading buffer (PBS/0.5 M NaCl/pH 7.0) and applied on the columns. After washing with 5 column volumes (CV) of loading buffer, the columns were eluted with a pH step gradient (PBS/0.5 M NaCl, pH 6.5, pH 6.0, pH 5.5, and pH 5.0) using 5 CV per step and 5 CV of an EDTA solution (50 mM EDTA/PBS/0.5 M NaCl/pH 7.0) at a flow rate of 0.5 ml/min. The percentages of virus, protein, and DNA in wash and step gradient elution factions are added and the summations represented by bars at the right side of each plots. The total amount of virus, protein, and DNA loaded on each of the columns was $2.4x10^7$ pfu, 1.2 mg and 15.8 μg respectively.

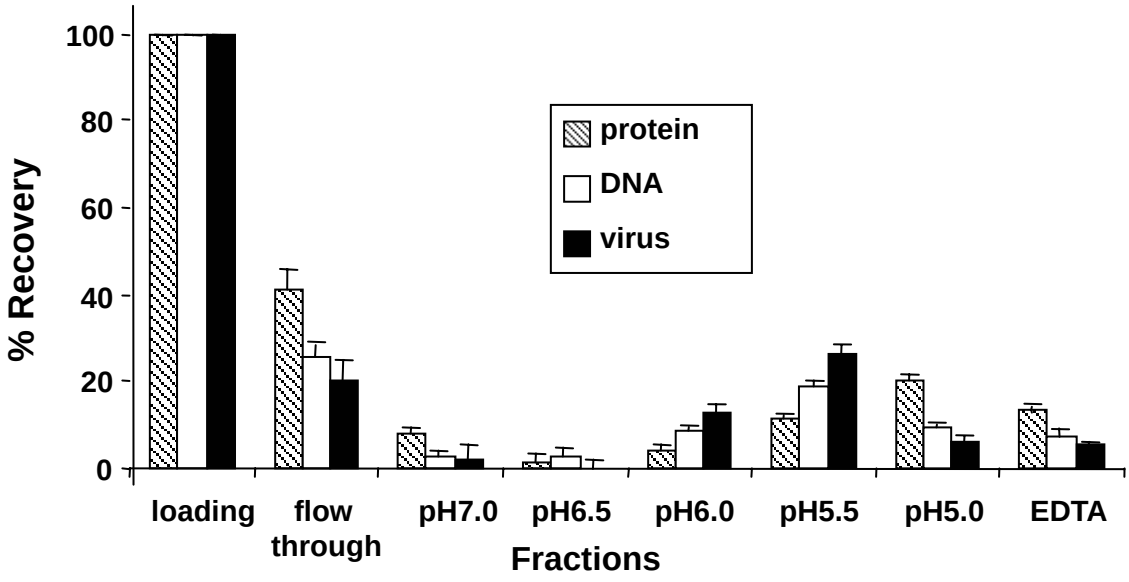

Figure 2. Elution Profiles of Virus, Total Protein and DNA on IDA-Zn^{2+} Column.

QOZHG virus after centrifugation was re-suspended in 10 ml loading buffer (PBS/0.5 M NaCl/pH 7.0) and applied on the columns. After washing with 5 column volumes (CV) of loading buffer, the columns were eluted with a pH step gradient (PBS/0.5 M NaCl, pH 6.5, pH 6.0, pH 5.5, and pH 5.0) using 5 CV per step and 5 CV of an EDTA solution (50 mM EDTA/PBS/0.5 M NaCl/pH 7.0) at a flow rate of 0.5 ml/min. The percentages of virus, protein, and DNA in wash and step gradient elution factions are added and the summations represented by bars at the right side of each plots. The total amount of virus, protein, and DNA loaded on each of the columns was $2.4x10^7$ pfu, 1.2 mg and 15.8 µg respectively.

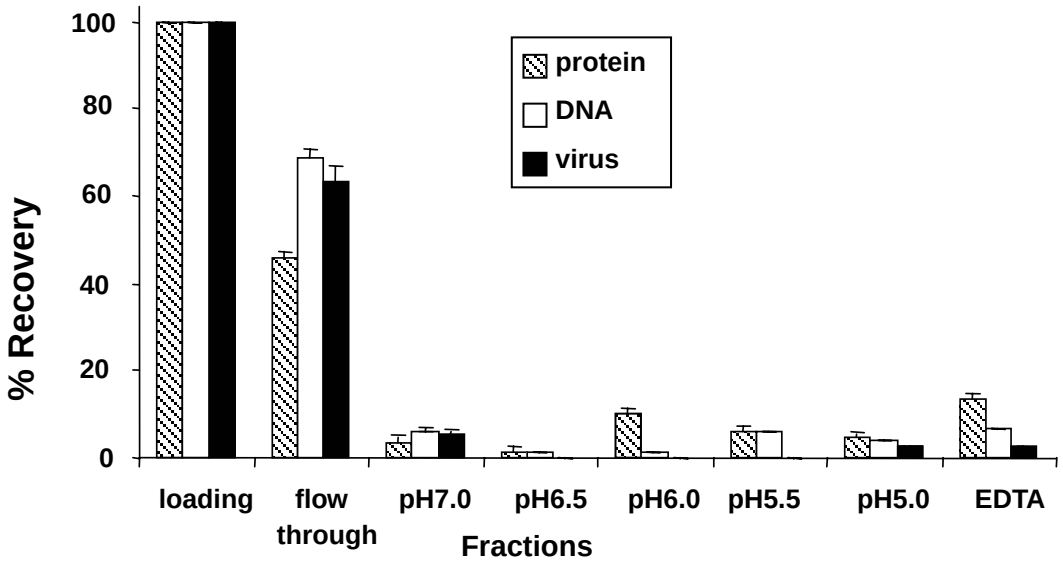

Figure 3. Elution Profiles of Virus, Total Protein and DNA on IDA-Ni^{2+} Column.

QOZHG virus after centrifugation was re-suspended in 10 ml loading buffer (PBS/0.5 M NaCl/pH 7.0) and applied on the columns. After washing with 5 column volumes (CV) of loading buffer, the columns were eluted with a pH step gradient (PBS/0.5 M NaCl, pH 6.5, pH 6.0, pH 5.5, and pH 5.0) using 5 CV per step and 5 CV of an EDTA solution (50 mM EDTA/PBS/0.5 M NaCl/pH 7.0) at a flow rate of 0.5 ml/min. The percentages of virus, protein, and DNA in wash and step gradient elution factions are added and the summations represented by bars at the right side of each plots. The total amount of virus, protein, and DNA loaded on each of the columns was $2.4x10^7$ pfu, 1.2 mg and 15.8 μg respectively.

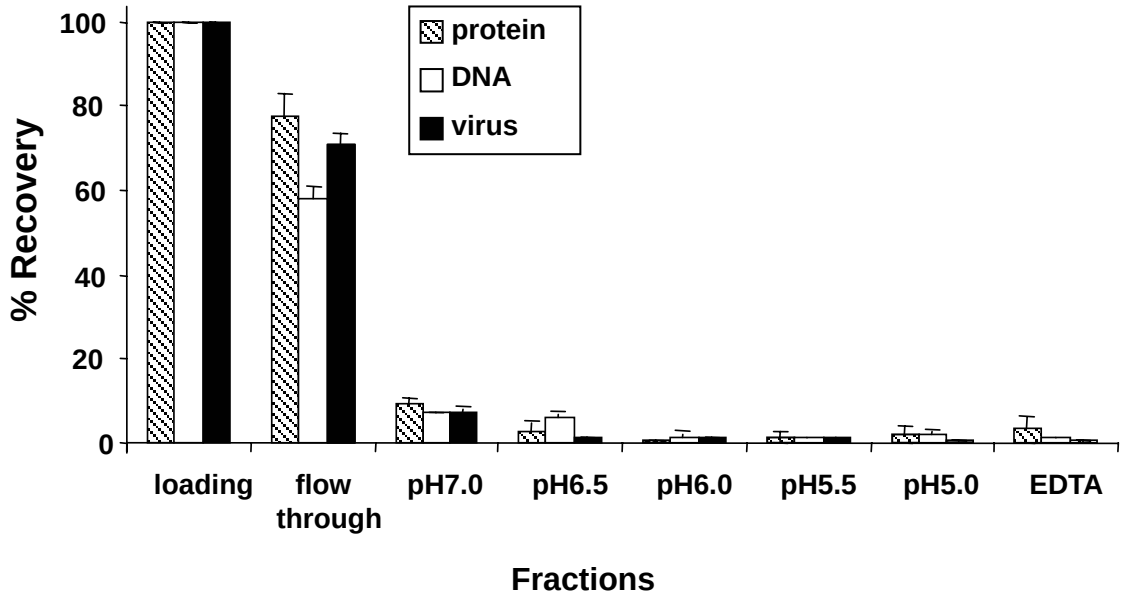

Figure 4. Elution Profiles of Virus, Total Protein and DNA on IDA-Co^{2+} Column.

QOZHG virus after centrifugation was re-suspended in 10 ml loading buffer (PBS/0.5 M NaCl/pH 7.0) and applied on the columns. After washing with 5 column volumes (CV) of loading buffer, the columns were eluted with a pH step gradient (PBS/0.5 M NaCl, pH 6.5, pH 6.0, pH 5.5, and pH 5.0) using 5 CV per step and 5 CV of an EDTA solution (50 mM EDTA/PBS/0.5 M NaCl/pH 7.0) at a flow rate of 0.5 ml/min. The percentages of virus, protein, and DNA in wash and step gradient elution factions are added and the summations represented by bars at the right side of each plots. The total amount of virus, protein, and DNA loaded on each of the columns was $2.4x10^7$ pfu, 1.2 mg and 15.8 μg respectively.

3.2.2 Construction of Cobalt Affinity Peptide Tagged HSV-1 Virus: KgBHAT

Based on the above elution profiles (Fig.1-4), we postulated that the fusion of a short cobalt binding peptide to an HSV-1 virion surface protein might endow the virus with sufficient affinity for immobilized cobalt. This enhanced binding under loading conditions could also direct its elution to the low background region of the elution profile identified in Fig.4. For the peptide to be effective it must be exposed on the virus envelope and accessible for binding to the immobilized cobalt. Moreover, the peptide-bearing virus should be minimally adversely affected in its ability to efficiently bind to the normal HSV-1 cell surface receptors and enter into the target host cells.

A 19-mer polyhistidine affinity tag (HAT), KDHLIHNVHKEEHAHAHNK[90], that naturally exists in the N-terminus of chicken lactate dehydrogenase, has high affinity to cobalt ions and can be eluted in conditions milder than those for the His_6 tag. Therefore, we selected HAT as a cobalt affinity peptide for incorporation into the HSV-1 virion. A replication competent HSV-1 viral recombinant carrying the HAT peptide in the HS binding site of glycoprotein B was constructed to evaluate the binding and elution properties of tagged HSV-1 on IDA-Co^{2+} column. A plasmid (pgBHAT) encoding HAT tagged gB (Fig.5B), was constructed with annealed oligonucleotides encoding the HAT peptide inserted into the deleted HS binding site in (Fig.5A), which encodes an HS binding deficient form of gB[35]. The HAT tagged gB construct was recombined into the HSV-1 genome by marker rescue of a gB nonsense mutant virus K082 (Fig.5C)[129]. The recombinant viruses were selected on non-complementing Vero cells, which cannot support the replication of the K082 parental virus, which was deficient for the essential viral gene gB.

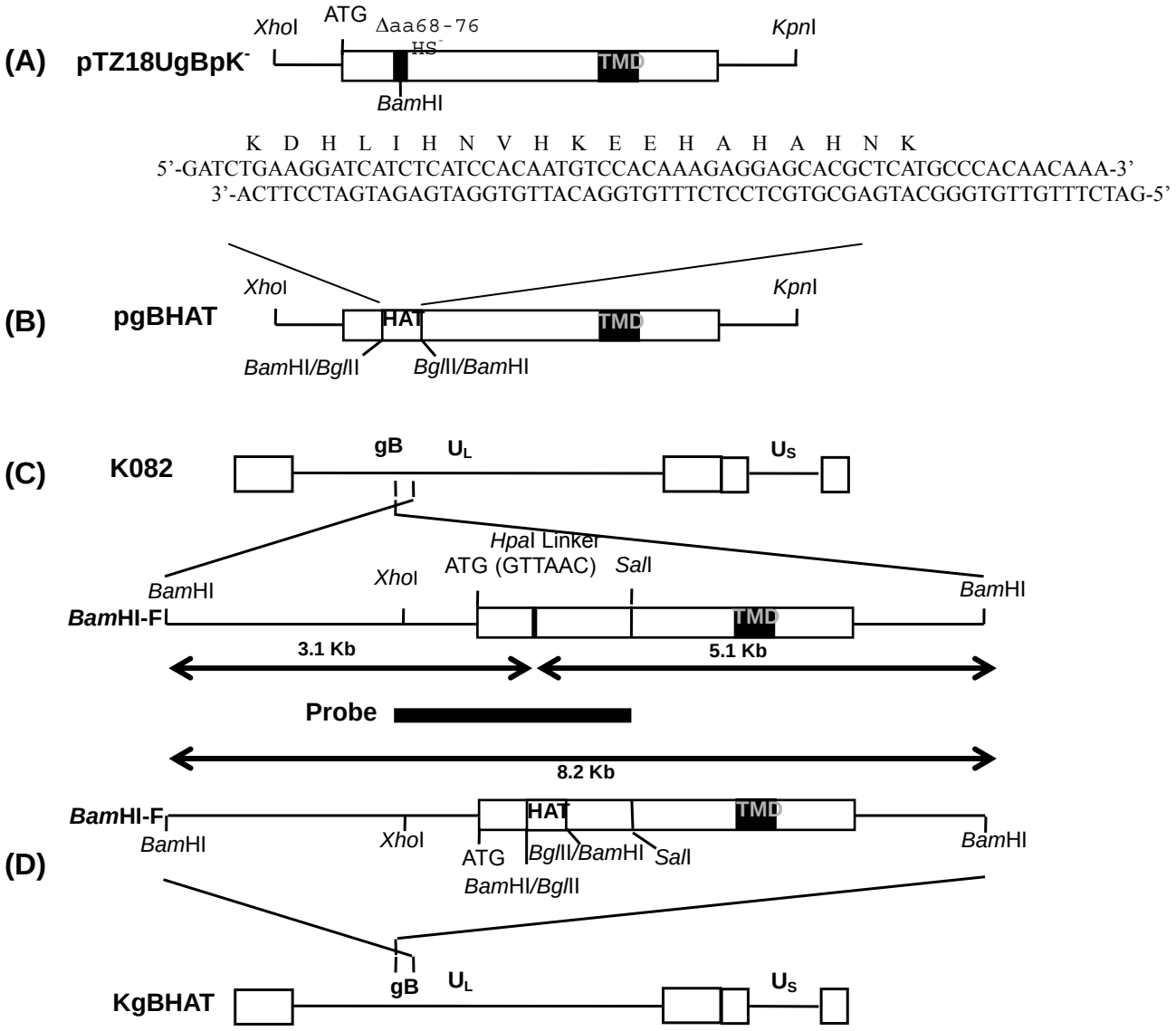

Figure 5. Construction of Recombinant HSV Virus Expressing HAT Tag in gB.

The HAT coding oligonucleotides containing *Bgl*II sticky ends were introduced into the *Bam*HI site of the **(A)** plasmid pTZ18UgBpK$^-$, in which the sequence encoding the HS binding domain of gB was replaced by a *BamH*I site, to create the plasmid **(B)** pgBHAT. The pgBHAT plasmid was used to rescue the gB defective mutant virus **(C)** K082, to create the recombinant **(D)** KgBHAT. (Abbrevations: UL=long unique segment; US=short unique segment; TMD=transmembrane domain; HS=heparan sulfate).

Southern blot analysis was performed to confirm the presence of HAT coding sequence in the recombinant virus genome. Viral DNA from K082 and 2 recombinant isolates were extracted from virus infected cells, digested with *Bam*HI and *Hpa*I, subjected to electrophoresis, transferred to a Nytran membrane then hybridized with a biotin labeled gB probe (Fig.5C). The gB probe hybridized to two fragments (3.1 Kb and 5.1Kb) in the parental K082 virus genome (Fig.6, lane 1) because of the existence of the *Hpa*I site in the gB locus[129]. This *Hpa*I site incorporates the stop codon in the parental virus and is a marker for the null gB phenotype. The gB probe hybridized to a single 8.2 Kb fragment in the putative HAT bearing isolates KgBHAT (Fig.6, lanes 2 and 3), demonstrating that this region in K082 genome has been replaced with the sequences from pgBHAT by homologous recombination, or that the isolates were revertants that had rescued the gB nonsense mutation during passage on complementing cell lines. To verify the insertion of the HAT sequence within the gB locus of the recombinant viruses, candidate recombinant viruses were subjected to PCR with two primers flanking the locus of HAT insertion. The ~250bp PCR products were analyzed by DNA sequencing and the results verified that the HAT encoding sequences were inserted in those recombinant viral genomes in-frame in the proper orientation.

To verify the expression of the HAT epitope, proteins were extracted from control virus KgBpK$^-$ and KgBHAT virus infected Vero cells and subjected to Western blot analysis using an anti-gB monoclonal antibody or an anti-HAT polyclonal antibody for detection. As shown in Figure 7, the gB antibody detected the HS binding deficient form of gB in KgBpK$^-$ (Fig.7, lane 1) and the HAT tagged gB in KgBHAT (Fig.7, lane 2) infected Vero cell samples. The HAT tagged gB is 28 amino acid residues longer than its HS binding deficient counterpart, resulting in 3.3 kDa molecular weight difference. This size difference is readily seen in Fig.7, as the tagged gB migrated slightly slower on the NuPAGE tris-acetate gel. The HAT antibody detected a protein with a molecular weight equivalent to the tagged gB in KgBHAT infected

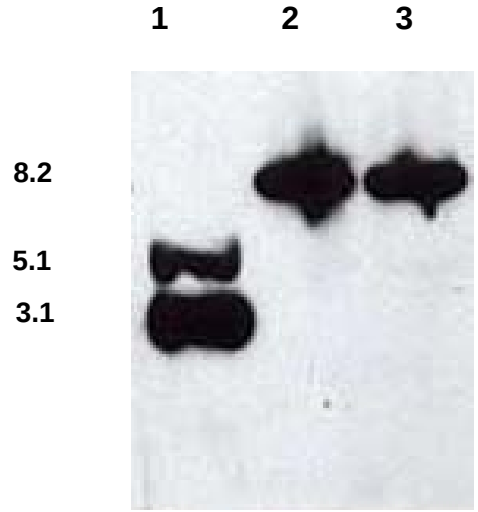

Figure 6. Southern Blot Analysis

Two rescued virus isolates **(lanes 2-3)** were digested with *Bam*HI and *Hpa*I and probed with the *sph*I-*Sal*I fragment (Fig.5 D) of *Bam*HI-F compared to the parental K082 **(lane 1)** virus.

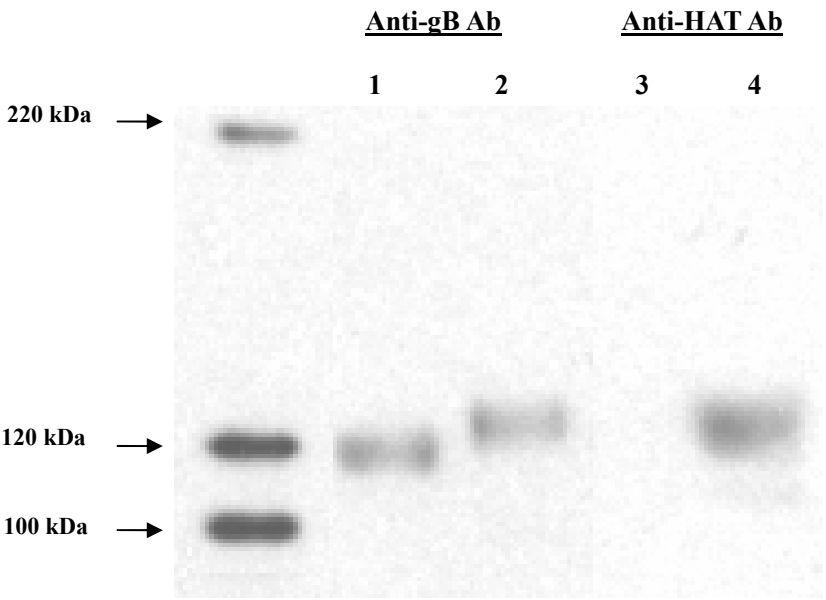

Figure 7. Western Blot Analysis Detection of HAT-Tagged gB.

Protein lysates from Vero cells infected with KgBHAT **(lanes 2 and 4)** and the control virus KgBpK$^-$ **(lanes 1 and 3)** were separated using the NuPAGE system and transferred to a PVDF membrane. The membrane was then cut in half and each was probed separately either with a monoclonal antibody against HSV-1 gB **(lanes 1 and 2)** or with a polyclonal antibody against HAT peptide **(lanes 3 and 4),** followed by detection using HRP-conjugated anti-mouse or anti-rabbit antibody respectively.

Vero cell sample (Fig.7, lane 4), confirming that the HAT peptide was successfully incorporated into gB. As expected, no HAT epitope was detected in the untagged KgBpK$^-$ infected control sample (Fig.7, lane 3). These experiments verify the insertion of the HAT sequences within the HS binding region of gB and the expression of the HAT peptide during productive infection.

3.2.3 Infectivity and Productivity of KgBHAT

Glycoprotein B is believed to be involved in both the adsorption and penetration steps during HSV-1 infection. Replacement of the HS binding region with the cobalt affinity peptide HAT within this glycoprotein may alter its function and affect infectivity or productivity of the recombinant virus.

The infectivity of KgBHAT was compared to that of KOS and KgBpK$^-$ by measuring the adsorption and penetration kinetics on Vero cells. The adsorption studies were done at 4^{o}C to avoid the complication of viral entry. As shown in Fig.8A, the adsorption rate of the three types of HSV-1 viruses was essentially the same within the 2 h incubation period on Vero cells. The rate of virus entry into host cells was determined as the rate at which penetrated viruses become resistant to low-pH glycine buffer treatment, compared with the untreated virus control. The results presented in Fig.8B show that the KgBpK$^-$ displayed an approximately 20% reduction in penetration rate compared to wild type virus KOS, which is consistent with published results[35]; while the penetration rate of the tagged virus KgBHAT was slightly lower than the KgBpK$^-$. The data indicated that although virus binding was not affected by the gBHAT construction, virus entry was less efficient than wild type virus but not substantially different from the gB mutant lacking the HS binding element.

The productivity of KgBHAT on Vero cells was determined and compared with that of wild type virus KOS. Vero cells were infected with either KgBHAT or KOS at the same MOI

of 0.01 and incubated at 37^{o}C for virus propagation. At different time point post infection, samples from culture supernatant were taken and the number of viral particles produced was measured by standard plaque assy. Fig.9 shows that KgBHAT has the same productivity as KOS on Vero cells, suggesting that the virus production is not affected by the insertion of HAT tag in gB.

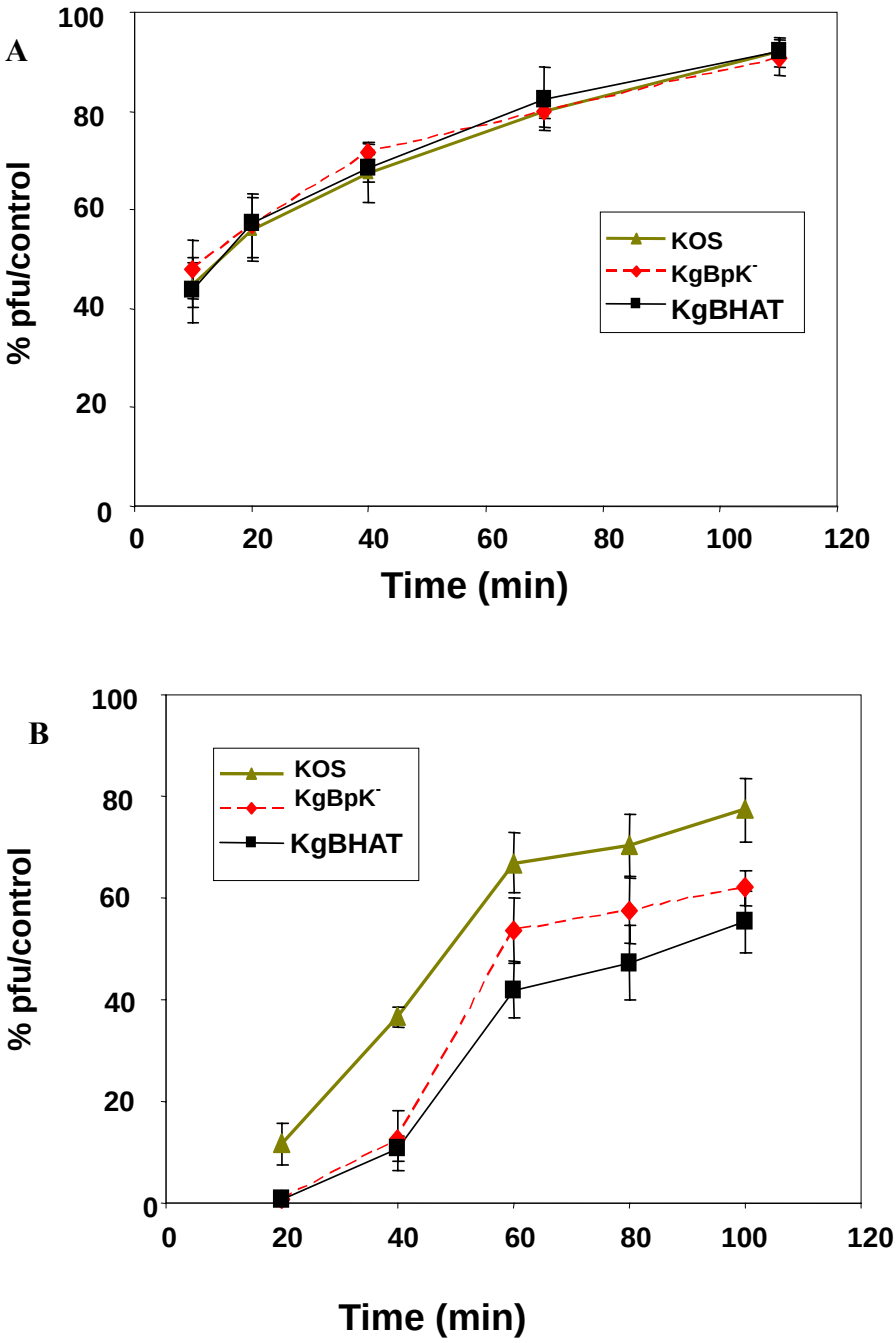

Figure 8. Infectivity of KgBHAT Virus on Vero Cells

The relative infectivity of KgBHAT compared to KOS and KgBpK$^-$ viruses was assessed by measuring the virus adsorption **(A)** and penetration **(B)** kinetics on Vero cells.

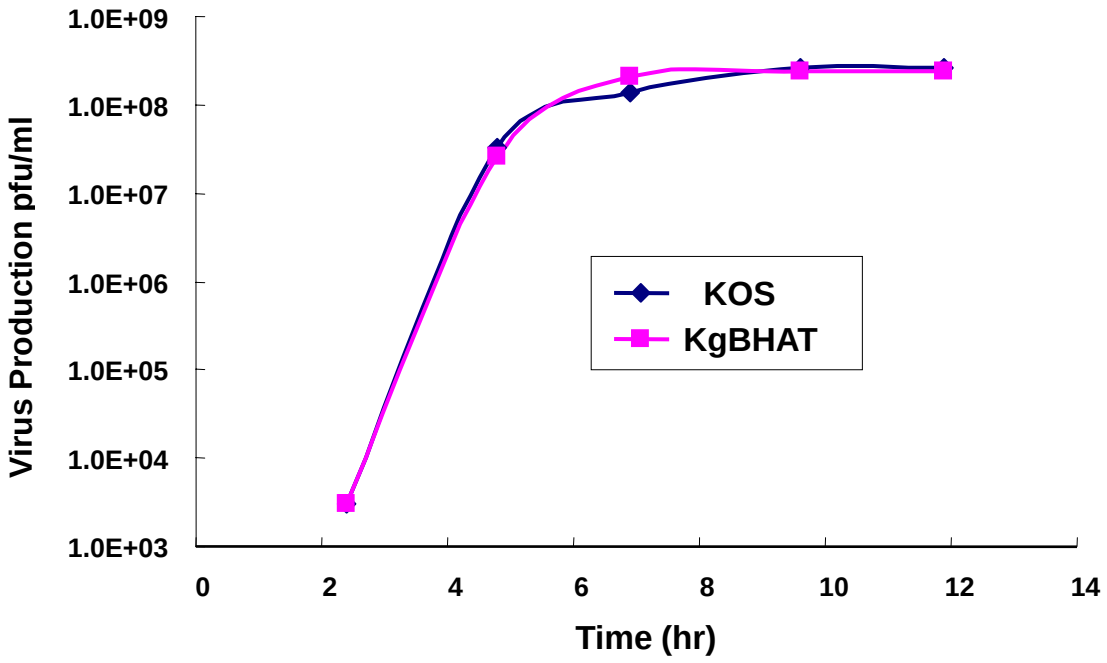

Figure 9. Productivity of KgBHAT Virus on Vero Cells

Vero cells were infected with KOS or KgBHAT at MOI of 0.01, and incubated at 37^{o}C for virus propagation.

3.2.4 Chromatography of KgBHAT on IDA-Co^{2+}

The binding and elution properties of KgBHAT on IDA-Co^{2+} column were investigated using a virus stock harvested from KgBHAT infected Vero cell supernatant. The infections were carried out in serum-free media. After harvesting, the virus stock was processed with two centrifugation steps. The virus containing supernatant was clarified from cell debris at 2,000g, and the viral particles were pelleted from the supernatant at 20,000g. The virus pellet was then resuspended in a loading buffer (PBS, 0.5M NaCl, pH7.0) and loaded on an IDA-Co^{2+} column. The same chromatography procedures were employed for the tagged virus as those for untagged virus in Fig.1-4. The results demonstrated that by tagging gB with the HAT peptide, the elution of the KgBHAT virus was directed into the pH 5.5 elution fraction (Fig.10), a region shown to have insignificant amounts of contaminating proteins and DNA (Fig.4). The amount of KgBHAT virus in the pH 7.0 wash step and in the pH 6.5 elution fraction was negligible, demonstrating that the tagged virus efficiently binds cobalt ions above pH 6.5. Small amounts of bound viruses were eluted at pH6.0 and there was a major elution peak at pH 5.5, suggesting that the pH 5.5 buffer was sufficient to elute the majority of the bound virus from the immobilized cobalt column. Although the elution of the tagged virus from the column was directed to the low background area (Fig. 10), the recovery of virus, as measured by the percentage of recovered infectivity, was relatively low (approximately 20%) for this experiment.

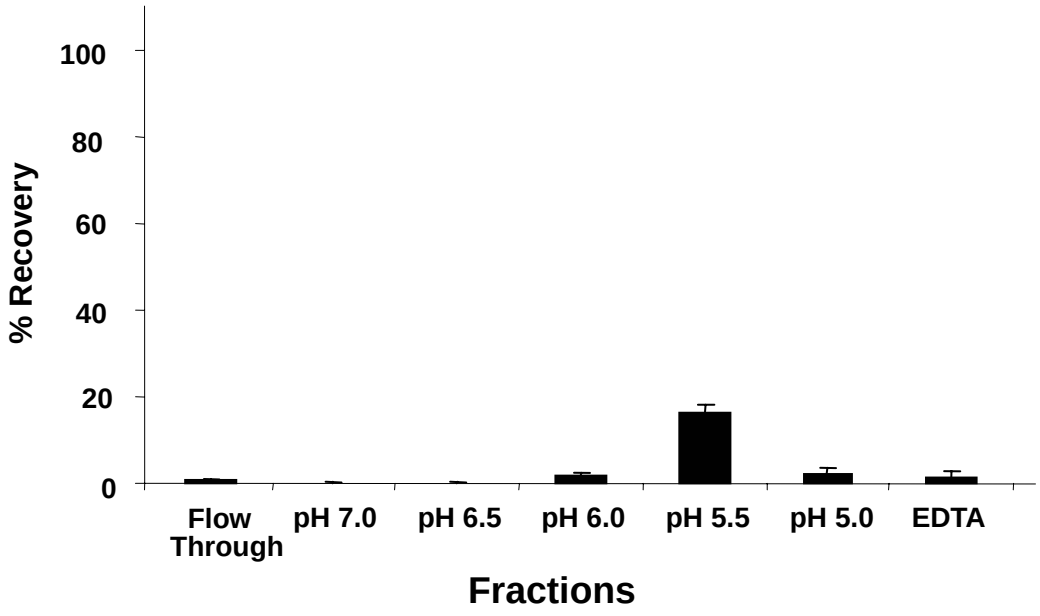

Figure 10. Elution Profile of the Tagged Virus KgBHAT on IDA-Co^{2+} Column.

Approximately $4.0x10^7$ pfu of clarified KgBHAT virus was re-suspended in 10 ml loading buffer (PBS/0.5 M NaCl/pH 7.0) and applied on IDA-Co^{2+} column. After washing with 5 column volumes (CV) of loading buffer, the column was eluted with a pH step gradient as shown in the figures using 5 CV per step and 5 CV of an EDTA solution (50 mM EDTA/PBS/0.5 M NaCl/pH 7.0). The flow rate of the was 0.5 ml/min.

3.2.5 IMAC Parameter Optimization

To be effective, the IMAC purification should provide high infectious HSV-1 yield and high binding capacity for the viral particles. The effect of several IMAC parameters on the recovery and capacity of HSV-1 viruses during purification was investigated. The loading pH, flow rate, and chromatography substrate were optimized to achieve the high yield and high binding capacity of the tagged HSV-1 viruses.

The effect of altering the loading pH on infectious virus recovery was examined for a range of pHs (Fig.11). For these assays, the KgBHAT virus pellets were re-suspended in buffers at pH 7.0, 6.5, 6.0 or 5.5 and loaded on the IDA-Co^{2+} column. The column was washed with loading buffer and eluted at pH 5.5, after which each column was stripped with EDTA to remove any remaining virus. Fig.11 shows that the summation of the viable KgBHAT virus percentage from all fractions increased as loading pH was decreased, although initial virus binding to the column was also reduced as loading pH was reduced. Virus loaded at pH 7.0 showed the highest column binding as demonstrated by the negligible amount of virus found in the flow through. However, the strength of this binding appeared to inactivate the viruses on the column, resulting in low total virus recovery (Fig. 11A). Lowering the loading pH to 6.5 also allowed high affinity to the column as confirmed by the minimal amount of virus collected from the flow through fraction and resulted in increased virus recovery at the pH 5.5 elution step (Fig.11B). A reduction in loading pH to 6.0 resulted in reduced virus binding to the column and increased virus in the flow through fraction (Fig. 11C). This reduction in virus binding resulted in reduced relative recovery in the pH 5.5 elution fraction compared to the pH 6.5 loading. When the samples were loaded at pH 5.5, a condition at which most viruses do not bind, a vast majority of the loaded virus was collected

in the flow through with a small amount recovered from the pH 5.5 elution step thereby suggesting that at the lower pH, virus binding was inefficient and not suitable for purification (Fig. 11D).

These results suggested that loading the virus at higher pH (7.0) results in an avid column binding and lower recovery at pH 5.5 elution, whereas loading at lower pH (6.0) weakened the binding of the virus to the column resulting in overall virus loss due to flow through. The optimal balance of binding and recovery was seen by loading at pH 6.5 which was deemed optimal for purification of a HAT tagged virus on an immobilized cobalt column.

The effect of flow rate on the performance of IMAC was investigated while keeping the loading pH at pH6.5. KgBHAT pellet was suspended in the pH6.5 buffer (PBS, 0.5M NaCl) and loaded on the IDA-Co^{2+} at different flow rates. The column was washed with the pH6.5 buffer, eluted with the pH 5.5 buffer (PBS, 0.5MNaCl) and finally stripped with the EDTA buffer (PBS, 0.5M NaCl, 50 mM EDTA, pH6.5) at the same flow rate as the loading. Fig.12 shows that increasing the flow rate from 0.5 ml/min to 1.0 ml/min gave rise to increased infectious virus recovery in the pH5.5 elution: from 45% (0.5ml/min) to 60% (1.0 ml/min). However, further increasing the flow rate to 1.5 ml/min did not have beneficial effect on the recovery, but resulted in decreased binding capacity, as the percentage of infectious viruses in the flow through was increased. Further more, the summation of the viable KgBHAT percentage from all fractions increased as the flow rate was increased, indicating that the shorter the viruses stay on the column, the less virus inactivation would be. Overall, Fig.12 suggested that 1.0 ml/min was a suitable flow rate for the IMAC purification.

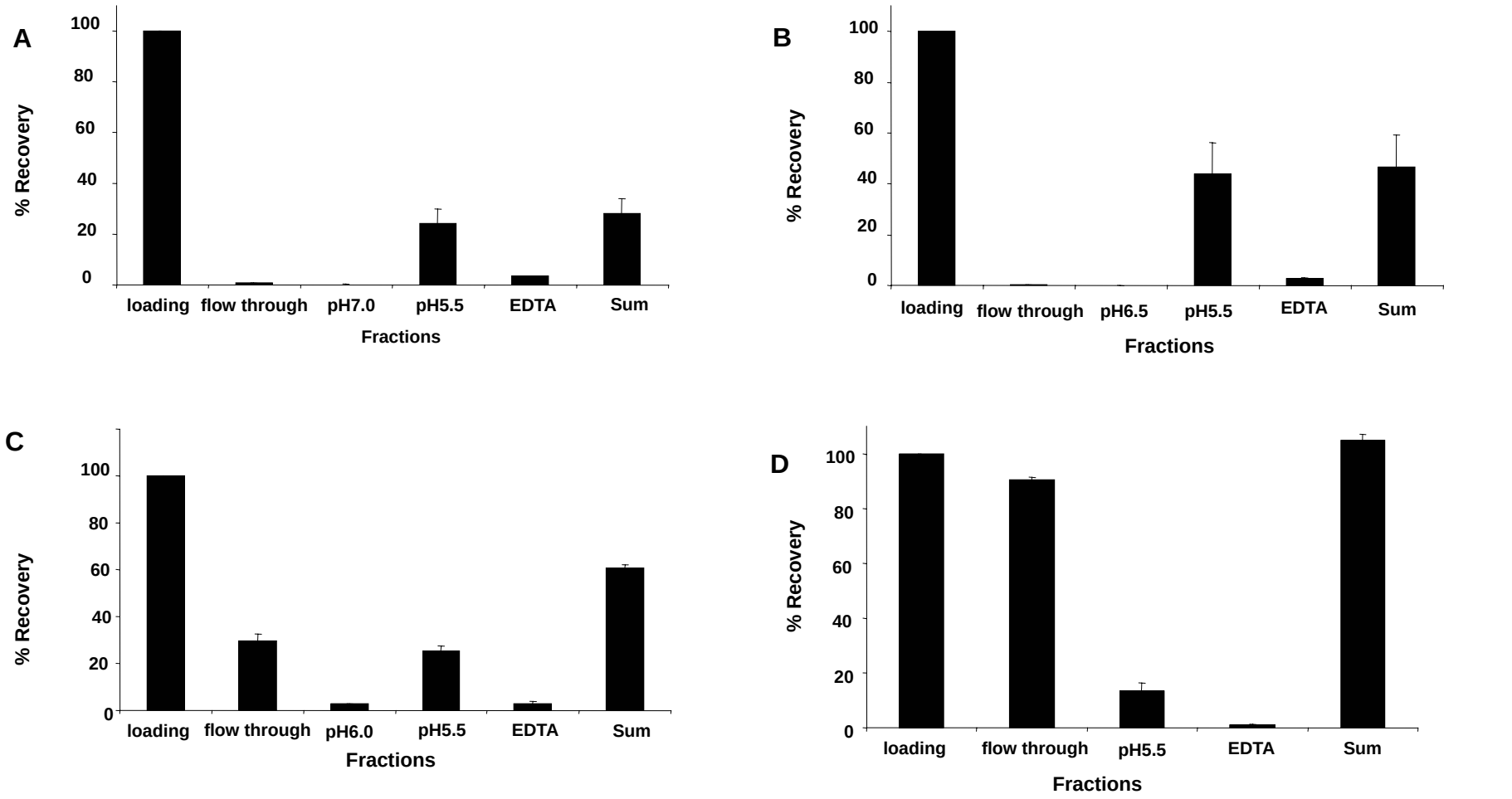

Figure 11. Effect of Loading pH on the Recovery of KgBHAT Virus on IDA-Co^{2+} Column.

Clarified KgBHAT virus ($4.0x10^7$ pfu) was re-suspended in 10 ml of different loading buffers [PBS/0.5 M NaCl, pH 7.0 **(A)**, pH 6.5 **(B)**, pH 6.0 **(C)**, and pH 5.5 **(D)**]. After virus loading (flow rate=0.5 ml/min), the column was washed with 5 CV of the same loading buffer. The column was eluted with 5 CV PBS/0.5 M NaCl/pH 5.5 buffer if loaded in pH 7.0, pH 6.5, or pH 6.0. The columns in all the experiments were finally stripped with 5 CV of 50 mM EDTA/PBS/0.5 M NaCl/pH 7.0.). The percentages of recovered virus in wash and step gradient elution factions were added and the summations represented by bars at the right side of each plot.

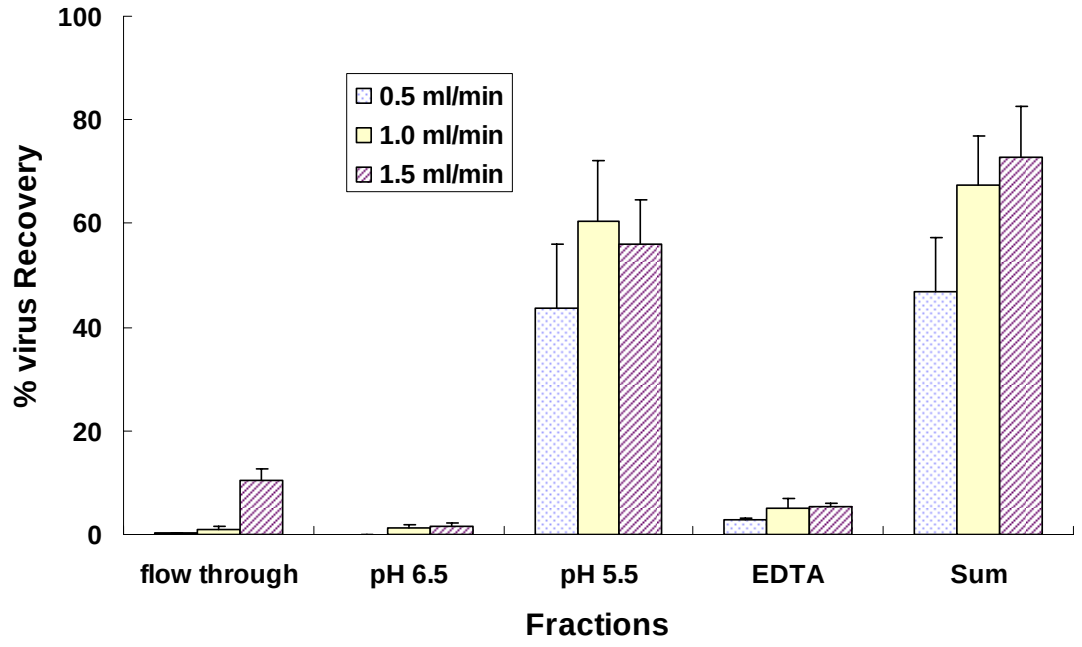

Figure 12. Effect of Flow Rate on the Chromatography of KgBHAT on IDA-Co^{2+} Column.

Clarified KgBHAT virus ($4.0x10^8$ pfu) was re-suspended in 5 ml of loading buffers [PBS/0.5 M NaCl, pH 6.5, and loaded on the IDA-Co^{2+} column at different flow rate **(A)**, 0.5ml/min **(B)**, 1.0 ml/min and **(C)**,1.5 ml/min. Keeping the flow rate the same as loading, the column was washed with 5 CV of the same loading buffer, eluted with 5 CV PBS/0.5 M NaCl/pH 5.5 buffer, and finally stripped with 5 CV of 50 mM EDTA/PBS/0.5 M NaCl/pH 7.0.). The percentages of recovered virus in wash and step gradient elution factions were added and the summations represented by bars at the right side of each plot.

Breakthrough experiments were conducted on columns packed with various commercial IMAC substrates to measure the dynamic binding capacity of KgBHAT at 1 ml/min flow rate. Three commercial substrates were investigated: IDA beads from GE healthcare, NTA beads from Qiagen, and Talon beads from BD science. These chromatographic substrates are all derived from 6% agarose gel but with different bead diameters and functionized with different chelating ligands. The physical properties of the substrates are illustrated in Table 2. These substrates were packed into 50 X 5 mm I.D. glass columns using a downward slurry technique in equilibrium buffer (PBS, 0.5 M NaCl, pH6.5) at a flow rate of 3 ml/min. During the breakthrough experiments, 20 ml of KgBHAT suspension ($1.5*10^8$pfu/ml) in loading buffer (PBS, 0.5 M NaCl, pH6.5) was continuously pumped through the columns packed with different beads at a flow rate of 1 ml/min. The effluent was collected into 1-ml fractions, and the virus titer in each fraction was determined by standard plaque assay. The ratio of virus titer in the breakthrough fractions to that in loading was calculated and plotted against the fraction number in the breakthrough curve. The dynamic capacity was defined as total bound viruses at 10% breakthrough.

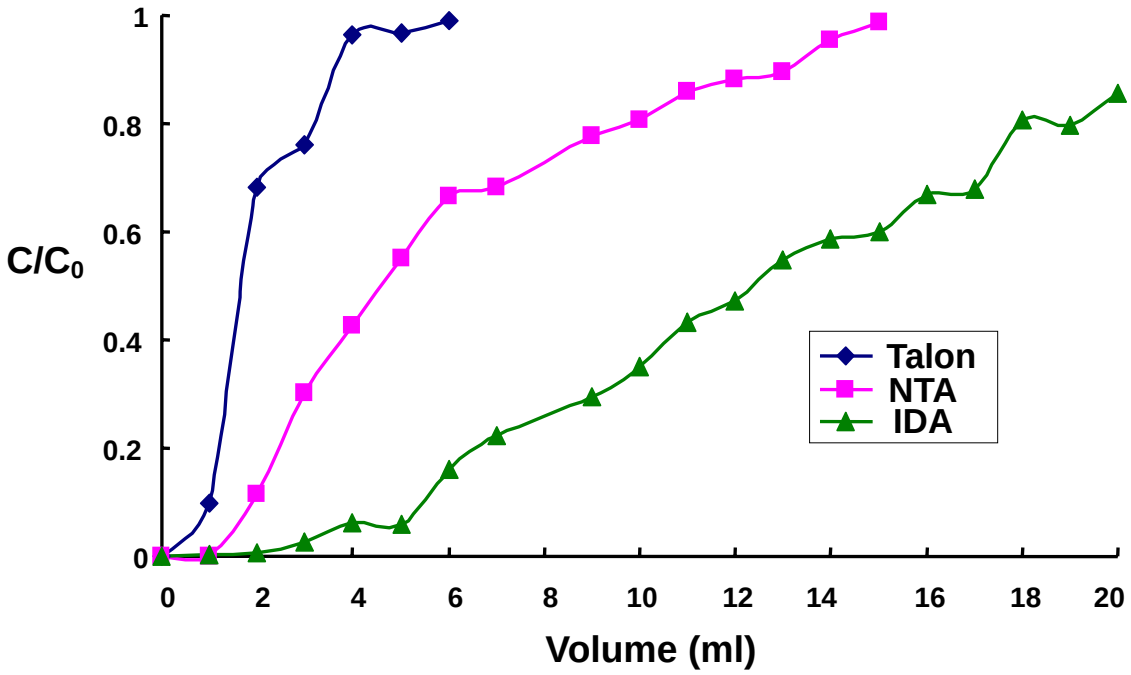

Figure 13. Breakthrough of KgBHAT on different IMAC substrates

Virus concentration in loading: $1.5*10^8$ pfu/ml

Table 2. Characteristics of IMAC substrates investigated.

Substrates	Talon	NTA	IDA
Ligand	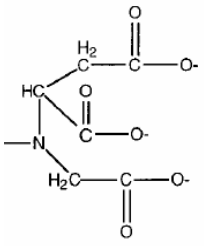	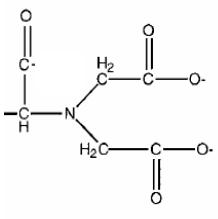	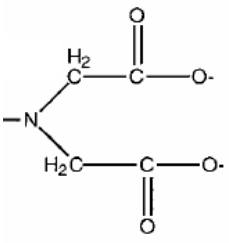
Bead size (distribution)	90 µm (45-165 µm)	90 µm (45-165 µm)	34 µm
Dynamic capacity	$1.5*10^8$ pfu/ml gel	$3.0*10^8$ pfu/ml gel	$8.5*10^8$ pfu/ml gel

As shown in Fig. 13, among the substrates investigated, the IDA beads provide the highest dynamic binding capacity ($8.5*10^8$ pfu/ml gel), and the NTA and talon beads showed decreased dynamic capacity: $3.0*10^8$ and $1.5*10^8$ respectively. Thus the IDA beads appeared to be the suitable substrate for the purification of the tagged HSV-1 vectors on immobilized cobalt affinity chromatography.

Experiments were conducted to test whether there was cobalt leakage from the column because this could be an important consideration in the acceptance of this method for purification of vector for clinical purposes. Atomic absorption analysis indicated that 4-5 parts per million (ppm) of cobalt was present in the eluted samples. To address the problem of residual cobalt, an IDA column which is not charged with any metal ion was placed downstream of the immobilized cobalt column. The aim was to capture any cobalt ions that may leak from the purification column. This simple modification to the protocol indeed reduced the cobalt contamination in the final viral product to undetectable levels as measured by atomic absorption. In addition, we hypothesized that residual cobalt associated with purified virus could reduce infectivity. A second uncharged column should remove cobalt from the virus stock and thereby potentially increase virus infectivity and yield. As expected, the addition of an uncharged IDA column downstream of the cobalt charged column increased the total virus recovery up to 78% of the total loaded virus (Fig. 14) compared to around 60% observed with a single cobalt charged column (Fig. 12). The final protein concentration in the purified virus stock was 54 ng/ml, a reduction of more than 96.8 % from the loaded virus stock. The final DNA contaminant concentration was 3.5 ng/ml for a reduction of more than 96.7%.

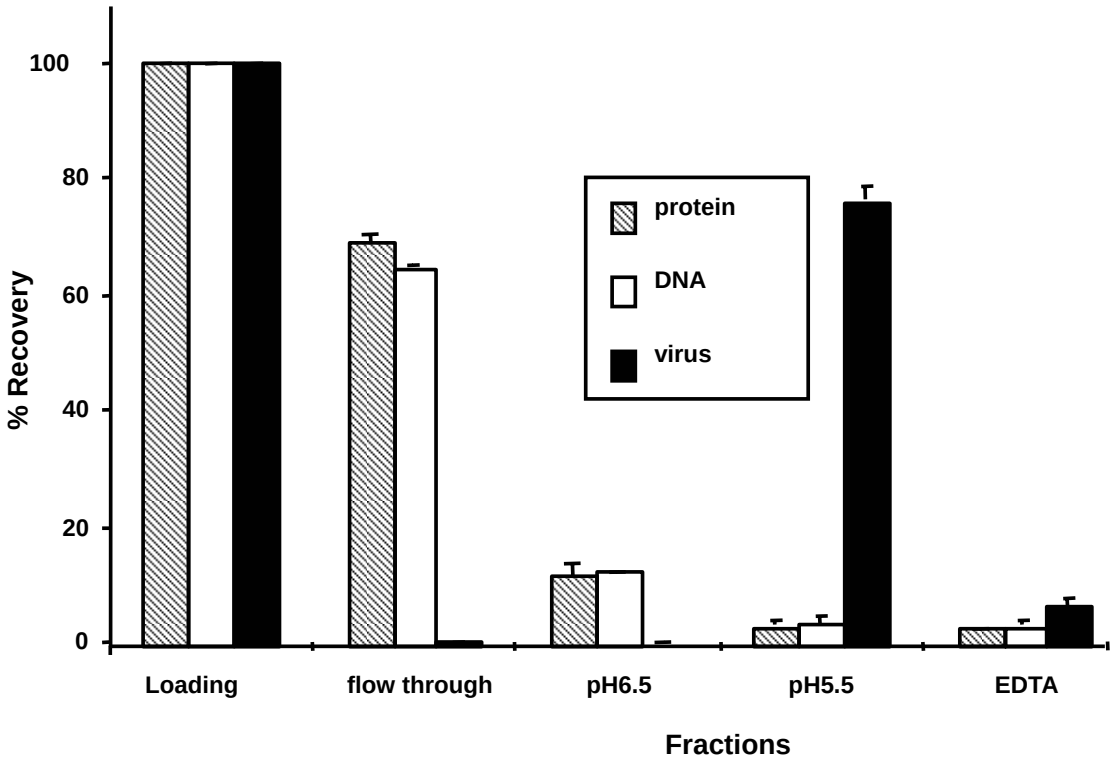

Figure 14. Chromatography of KgBHAT on IDA-Co^{2+} Followed by a Downstream Uncharged IDA Column.

Clarified KgBHAT virus ($4.0x10^7$ pfu) was re-suspended in 10 ml of loading buffer (PBS/0.5M NaCl/pH6.5). After loading (flow rate=1 ml/min.), the column was washed with 5 CV loading buffer. The column was subsequently eluted with 5 CV PBS/0.5M NaCl/pH5.5 buffer, and finally stripped with 5 CV 50mM EDTA/PBS/0.5M NaCl/pH7.0 buffer.

3.3 DISCUSSION

HSV-1 vectors provide a promising platform gene delivery technology especially for applications involving gene delivery to sensory nerves, the natural site of virus latency. Near term clinical applications include the treatment of certain solid tumors and sensory nerve conditions such as chronic pain and peripheral nerve degeneration. For patient applications, a scaleable and efficient purification process is an essential step in providing clinical grade HSV-1 vectors for early phase human trials to assess vector safety and eventual efficacy. The objective of this chapter was to test the feasibility of utilizing IMAC column purification and surface glycoprotein tagged virus to replace the current methods for purification of recombinant HSV-1 virus vectors.

Initial experiments were aimed at determining whether one of the commonly used immobilized metal ion columns was able to separate untagged HSV-1 virus from protein and DNA contaminants. The binding of untagged HSV-1 to transition metal ions infers the existence of metal ion binding sites on the native virion surface. The outermost layer of the HSV-1 virion is a lipid membrane envelope from which at least 10 HSV-encoded glycoproteins (gB-gE, gG-gJ, gL, and gM) project beyond the lipid bilayer[34, 154]. Every glycoprotein contains a variable number of histidine residues and since only a single histidine is required for binding to IDA-Cu^{2+} [83], it is likely that some of these residues are exposed on the surface of the viral glycoprotein moiety producing strong binding between the HSV-1 virion and the IDA-Cu^{2+} column. This interaction was so strong that untagged virus was resistant to elution even at low pH. There are also several polyhistidine clusters present in the amino acid sequences of some HSV-1 glycoproteins that may account for binding to Ni^{2+} and Zn^{2+}.

The affinity of protein and DNA contaminants to each of the above immobilized metal ions followed the same trend as the untagged HSV-1 virus (Fig.1-4). No purification of untagged HSV-1 was achieved by solely selecting one of the above immobilized metal ion columns. However, the selectivity of IMAC can be tailored by surface modification of one or more of the viral glycoproteins. Since the majority of virus or contaminants did not bind to the immobilized cobalt ion (Fig.4), augmentation of the affinity of HSV-1 virus to the cobalt ion could enhance binding and direct the elution of the virus into a fraction low in non-viral contaminants. We tested this possibility through engineering a cobalt affinity peptide into a virus surface glycoprotein.

In order to construct an effective tagged HSV-1 recombinant, the peptide tag and the locus of tag insertion should be appropriately selected so that the tag must be accessible and bind to the cobalt ion. Moreover, the tag insertion must have minimal impairment of virus infectivity. It has been established that HAT is an efficient tag for cobalt ions[90]. Glycoprotein B was selected as the target for tag insertion because gB has the longest amino acid ectodomain among the HSV-1 glycoproteins[155], and because the clustering of gB spikes in protrusions of the virion envelope[156] implies that regions of gB are surface exposed and thus accessible for binding to the immobilized cobalt on the column. It is well known that gB participates in mediating adsorption of HSV-1 virion to susceptible cells by binding to the herapan sulfate (HS) moieties of cell surface proteins[35, 37, 157], and subsequently in contributing to virus penetration into cell through envelope-membrane fusion[158, 159]. The HS binding domain (amino acids 68-76 KPKKNKKPK) of gB was selected to be replaced by the HAT peptide for the following reasons. First, the existence of an HS binding domain and the presence of a neutralizing epitope localized to this region of the molecule suggest that this domain of gB is exposed on the virion surface and can be easily recognized by one of its natural receptors (HS)[35]. Thus replacement of the HS-binding domain with the HAT tag may

also be available for binding cobalt. Second, most of the HS binding function of HSV-1 is contributed by gC while only minor HS binding activity is ascribed to gB[35]. Deletion of the HS binding domain results in a 20% reduction in virus infectivity on Vero cells. Third, it has been predicted by neural network computational analysis that insertional mutagenesis of the secondary loop structure region of gB protein can minimize the outcome of a miss-folded mutant, with the HS domain of gB predicted to be in a loop conformation[160]. The rationale for placement of the HAT tag into gB was supported by the experimental findings using the recombinant virus. The productivity of the tagged virus on Vero cells was not negatively affected by the insertion of the HAT tag in gB. The tagged virus was bound to the immobilized cobalt column and the elution profiles indicated that the virus particles could be directed into a fraction nearly devoid of contaminants.

The effect of replacement of HS binding domain with HAT peptide on virus infectivity was assessed. It was found that, compared with wild type virus, virus mutant with HS binding deficient form of gB showed 20% reduction in binding capacity on mouse L cells after 5 hours incubation [35]. High amounts of radioactive virus particles (over 1000 viruses/cell) were used in the adsorption assay in order to see the capacity difference of different virus mutants. In HSV-1 vector gene transfer applications, the multiplicity of infection applied is normally far from the virus binding capacity on target cells. More interesting to us is the rate of the virus adsorption. In this work, we found that, when low MOI (250pfu/10^6 cells) was used, KgBpK$^-$ or KgBHAT shows essentially the same adsorption rate as KOS on Vero cells (Fig.7A). The rate of penetration of KgBHAT on Vero cells was found slightly lower than its KgBpK$^-$ counterpart (Fig.7B). This minimal loss in tagged virus infectivity is compensated by gains in vector purity and more economical manufacturing.

The recovery of viable virus from IMAC varies with different chromatography conditions and different metal ions used. It appeared that the stronger the virus binding to

metal ions or the longer contacting time of the virus with metal ions, the greater the extent of metal ion induced virus inactivation. For example, the immobilized copper ion appeared to strongly bind to untagged virus, thus the recovery of infectious virus from copper IMAC was significantly lower than for the other columns tested. Sagripanti et al found that HSV-1 can be inactivated in Cu^{2+} solution by free radicals generated from a series of Cu^{2+} catalyzed redox reactions, referred to as Fenton reactions[161]. Similar free radicals could be generated during IMAC purification and cause virus inactivation, which could account for the inactivation of untagged virus in IDA-Cu^{2+} column (Fig.1) and the tagged virus in IDA-Co^{2+} column (The free radical mediated virus inactivation will be systematically investigated in the next chapter). As shown in Fig. 11 and Fig. 12 decreasing the binding strength and reducing the resident time of the virus on the column would minimize virus inactivation.

The effect of chromatographic substrates on the binding capacity of the tagged HSV-1 virus was also investigated. Among three commercial available substrates studied, the IDA beads from GE healthcare provided the highest virus binding capacity. The chelating ligand in the IDA beads, iminodiacetate has three metal binding sites, while the ligands in the talon and NTA beads have four metal binding sites. Consequently, cobalt ions immobilized by the IDA beads have one more orbital for the virus binding, which resulted in higher virus binding affinity. In addition, the IDA beads have a smaller diameter and higher total surface area than the NTA and talon beads. Since the virus could not penetrate inside the beads due to its large diameter, only surface binding occurs during IMAC. The higher binding capacity in the IDA beads could partly be due to the higher total surface area on the IDA beads.

Elution from a single cobalt charged column resulted in loss of infectious virus and the concomitant presence of leeched cobalt in the eluate. Thus, cobalt bound to gB on the viral envelope may interfere with essential function of gB similar to the inhibition seen by adding

Co^{2+} directly to an aliquot of KgBHAT stock (data not shown). We found that Co^{2+} leakage was substantially mitigated simply by connecting a metal-free IDA column downstream to capture the free and/or virus bound Co^{2+}.

By loading the virus in pH 6.5 at 1ml/min, and using the second uncharged column downstream (Fig.14), the recovery of tagged HSV-1 virus from IDA-Co^{2+} was increased to approximately 80%, while protein and DNA contamination was reduced by more than 96.5% for protein and DNA, that is 54 ng/ml and 3.5 ng/ml respectively. Together, these results suggest that introduction of a HAT tag into HSV-1 gB enabled the rapid purification of the recombinant virus using immobilized cobalt columns.

4.0 INACTIVATION OF HSV-1 VECTOR ON IMMOBILIZED COBALT AFFINITY CHROMATOGRAPHY BY HYDROXYL FREE RADICALS

Metal catalyzed oxidation (MCO), which typically involves oxygen free radical generation, is an important pathway that leads to the deterioration of many biological molecules in solution. The occurrence of MCO in immobilized metal affinity chromatography (IMAC) systems and its potential for inactivating biological products has not been well recognized. In this chapter, we report the inactivation of HSV-1 vector on immobilized cobalt affinity chromatography. We observed that purification of KgBHAT on IDA-Co^{2+} columns using crude supernatant as starting material resulted in signification loss in virus infectivity (<5% recovery). Electron spin resonance (ESR) revealed that the virus inactivation was caused by hydroxyl free radicals generated from the interactions between cellular impurities and the metal ions on the column. Inclusion of 20 mM ascorbate, a free radical scavenger, in the chromatography mobile phase effectively scavenged the hydroxyl radicals. Alternatively, the hydroxyl radical formation could be effectively prohibited by inclusion in the chromatographic mobile phase of 20 mM imidazole, a competitive agent usually used to elute bound material from IMAC columns. In both cases, the infectivity recovery was dramatically augmented to 70%. This finding is the first demonstration of oxygen free radical mediated biological inactivation in an actual IMAC purification and an effective method to prevent it.

4.1 INTRODUCTION

Transition metal ions form coordination complexes with a variety of cofactors and proteins in cells where they carry out crucial regulatory and catalytic roles, particularly in electron transfer in many important redox reactions [107, 162]. However, this essential ability of

metal ions to transfer electrons can make them toxic to cells when present in excess. The toxic effects are partly due to their capability of generating oxygen free radicals such as superoxide or hydroxyl radicals [103-105]. These highly reactive free radicals can cause irreversible oxidative damages to proteins [113, 114], nucleic acids [115, 116], and lipids [117, 118], resulting in deleterious biological consequences such as aging [118], carcinogenesis [116] and other disease states [119, 120]. Metal catalyzed oxidation (MCO) is also an important pathway that leads to the inactivation, modification, or degradation of biological products during bioprocessing, transportation, and storage *in vitro* [121]. The nonenzymatic MCO pathway typically starts with the binding and reduction of molecular oxygen to hydrogen peroxide on the reduced state of chelated metal ions (e.g. Fe^{2+}, Cu^{+}, or Co^{2+}) in the presence of an appropriate reducing agent, with or without a superoxide intermediate [103, 121]. The resultant peroxide reacts with the reduced metal ions to generate highly reactive hydroxyl radicals that rapidly oxidize essentially any biological molecules they encounter [163].

During IMAC purification, immobilized transition metal ions contact a wide variety of compounds in the mobile phase, which may include dissolved oxygen and reducing agents from cell culture. Thus, there are possibilities that the metal ions could trigger free radical generation and cause damage to the biological product which is being purified by IMAC. Inactivation of lactate dehydogenase has been reported when exogenous hydrogen peroxide or reducing agents such as ascorbate, glutathione or cysteine were intentionally introduced into IDA-Cu^{2+} column to create the MCO conditions [122, 164]. However, no inactivation of lactate dehydrogenase was observed during the actual IMAC purification in which no exogenous reducing agent was deliberately introduced [122, 164]. Indeed, free radical mediated inactivation of biological products in an actual IMAC purification has not yet been reported.

In this chapter, we demonstrate significant infectivity loss of HSV-1 vectors during chromatography on an IDA-Co^{2+} column, when crude virus supernatant was used as starting

material. Electron spin resonance (ESR) revealed that the virus inactivation was caused by hydroxyl free radicals generated from reaction between soluble impurities from cell culture and the immobilized cobalt ions. Inclusion of 20 mM ascorbate or imidazole in the chromatography mobile phase effectively prohibited hydroxyl radical generation and dramatically reduced virus inactivation. The results are the first demonstration of free radical mediated damage of biological product during an actual IMAC purification and we describe methods to overcome this problem using free radical scavengers.

4.2 RESULTS

4.2.1 Inactivation of KgBHAT on IDA-Co^{2+} Column

In Chapter 3, we developed an immobilized cobalt affinity chromatography for selective purification of HSV-1 vectors engineered to display a cobalt affinity tag (HAT) on viral envelope glycoprotein B (gB), referred to as KgBHAT. KgBHAT was first partially purified from cell debris and soluble protein/DNA impurities using two centrifugation steps. Then, this partially purified preparation was used as starting material for further purification on IDA-Co^{2+} column.

To fully exploit the high specificity of the affinity between immobilized cobalt and the tagged HSV-1, it was desirable to assess the feasibility of IMAC purification of KgBHAT from a crude preparation. The second step centrifugation which was used to pellet the viruses from soluble impurities in Chapter 3 was omitted here. The crude KgBHAT supernatant, obtained after salt-releasing and clarification (see Chapter 2 Materials and Methods), was directly loaded on the IDA-Co^{2+} chromatography column and eluted as summarized in Table 3. The loading volume was 2 ml, which contained the amount of viruses ($5.1*10^8$ pfu/ml) corresponding to a column dynamic capacity of 10% breakthrough for the flow rate of 1 ml/min. This crude supernatant contained substantially higher amounts of soluble impurities than the partially purified sample used in our earlier work. The large amounts of impurities present in the crude sample did not lead to any complication, as most of protein and DNA impurities still did not bind to IDA-Co^{2+} and were removed in the flow through and washing fractions. However, only 4.9% of the loaded virus infectivity was found in pH 5.5 elution. This fraction constituted our purified virus and thus it indicated an effective virus recovery of 4.9%. Table 3 also shows that total infectious viruses found in all output fractions was substantially lower (about 25%) than the number of loaded infectious particles. The output

fractions were distributed as follows: flow through (11.5%), washing (7.1%), pH 5.5 elution (4.9%), and the EDTA striping fractions (2%). The low amounts of infectious virus present in output suggested that the majority of bound viruses were inactivated during the chromatography. In addition, we found that using an uncharged chelating column downstream the IDA-Co^{2+} column did not have significant effect on the infectious virus recovery in this case.

To further understand the virus inactivation, samples from each fraction were subjected to TaqMan real-time quantitative PCR (Q-PCR). Q-PCR with primer pair and probe specifically hybridized to HSV-1 gene ICP47 was used to amplify and quantify HSV-1 genomes (both the infectious and non-infectious ones). The non-infectious genomes consist of naked viral DNA, non-enveloped HSV-1 capsids, and HSV-1 virions with physical or chemical damages [34]. Therefore, if only the viral proteins were damaged, Q-PCR should be able to detect the inactivated viruses. As shown in Table 3, Q-PCR detected extremely low genome number in the output fractions. The amount of Q-PCR detectible genome number from all output fractions is only a very small percentage of the input. This result suggested that the inactivation of KgBHAT on IDA-Co^{2+} happened at the DNA level so that the damaged viral genomes were not able to serve as functional templates for Q-PCR amplification.

Table 3. Chromatography of KgBHAT crude supernatant on IDA-Co^{2+} column.

Fractions	Loading	Flow through	Wash	Elution	EDTA
Protein (μg/ml)	**153.0±9.1**	**36.8±2.9**	**45.9±4.9**	**3.8±1.8 (5.0%)**	**1.8±0.8**
DNA (ng/ml)	**723.6±3.5**	**339.1±15.1**	**199.8±2.3**	**11.7±5.8 (3.2%)**	**3.8±1.3**
Infectivity (10^7pfu/ml)	**68.8±5.3**	**7.4±1.7**	**3.5±1.0**	**1.7±0.5 (4.9%)**	**0.64±0.04**
Genome number (10^9/ml)	**21.2±2.2**	**0.86±0.2**	**0.84±0.3**	**0.086±0.03 (0.8%)**	**0.1±0.02**

2 ml of clarified KgBHAT crude supernatant was loaded on the column. After loading, the column was washed with 4ml of buffer A (PBS, 0.5 M NaCl, pH6.5). The elution of the bound viruses and other materials was achieved by passing 4 ml buffer B (PBS, 0.5 M NaCl, pH 5.5). The column was then washed with an EDTA containing buffer C (PBS, 0.5 M NaCl, 50 mM EDTA, pH6.5) to release the metal ions and remove any remaining viruses or impurities on the column. Flow rate was 1ml/min. The data represents the average of three independent experiments.

4.2.2 Stability of KgBHAT on Suspension

To determine what caused the low recovery, we assessed the stability of KgBHAT in the crude supernatant in room temperature. KgBHAT pellet resuspended in elution buffer (PBS, 0.5 M NaCl, pH5.5) and fresh cell culture medium UltraMDCK was used as control. As shown in Table 4, the virus had no statistically significant decay in 3 hours, a time period longer than the chromatography runs. The stable feature of KgBHAT in various suspensions indicated that Co^{2+} complexes on the column might have played a key role in the virus inactivation during the chromatography.

In our previous experiments, KgBHAT was pelleted from the crude supernatant by centrifugation (20,000Xg, 1hr). The virus pellet was then resuspended in a loading buffer (PBS, 0.5 M NaCl, pH6.5), which had the same salt and pH conditions as the crude supernatant. When the virus pellet suspension was loaded on the column, the infectious virus recovery was significantly improved to about 60% (Fig. 12). This suggested that the soluble impurities removed by high speed centrifugation were responsible for the virus inactivation on IDA-Co^{2+}.

Table 4. Stability of KgBHAT in different suspension conditions.

Incubation time hr	A 10^7 pfu/ml	B 10^7 pfu/ml	C 10^7 pfu/ml
0	47±4	46±6	42±2
1	43±3	43±3	41±2
2	46±4	42±3	42±3
3	41±2	42±4	41±3

Decay rate of KgBHAT in (A) freshly prepared crude supernatant, (B) low pH elution buffer (PBS, 0.5 MNaCl, pH5.5), or (C) fresh UltraMDCK cell culture medium at 25^{o}C was analyzed. The virus suspensions in B and C were prepared by suspending partially purified KgBHAT pellet in the elution buffer and UltraMDCK medium, respectively. Samples were removed over time and analyzed for the presence of infectious virus using standard plaque assay. The data represents the average of three independent experiments.

4.2.3 Effect of Ascorbate on KgBHAT Inactivation

Chelated Co^{2+} ions are known to have the ability to activate dioxygen and catalyze oxygen free radical generation. Based on the stable feature of KgBHAT in suspension (Table. 4) and the virus inactivation on IDA-Co^{2+} (Table. 3), we hypothesized that the infectivity loss might be due to oxidative free radicals generated on cobalt complexes on the column. If this were the case, presence of free radical scavengers in the mobile phase should prevent the loss of infectivity. The effect of ascorbate, a water-soluble free radical scavenger, on preventing virus inactivation on IDA-Co^{2+} was studied. The ascorbate was present in the mobile phase throughout chromatography including the loading, wash, and elution buffers. The pH and the NaCl concentration in the buffers were not changed by the addition of ascorbate. The virus inactivation was defined as:

$$\% \text{ Inactivation} = \frac{L-(F+W+E+S)}{L-(F+W)} * 100$$

where L, F, W, E, and S represent amount of infectious viruses present in loaded sample (L), flow-through (F), wash (W), elution (E), and final EDTA stripping step (S), respectively. The term L – (F + W) represents the viruses that remain bound after washing is complete. The numerator denotes the amount of inactivated viruses.

As shown in Fig. 15, when crude KgBHAT supernatant was used as starting material, the percentage of viruses recovered in elution increased with the increase in ascorbate concentration in the mobile phase. At a concentration of 20 mM, ascorbate almost completely prevented virus inactivation.

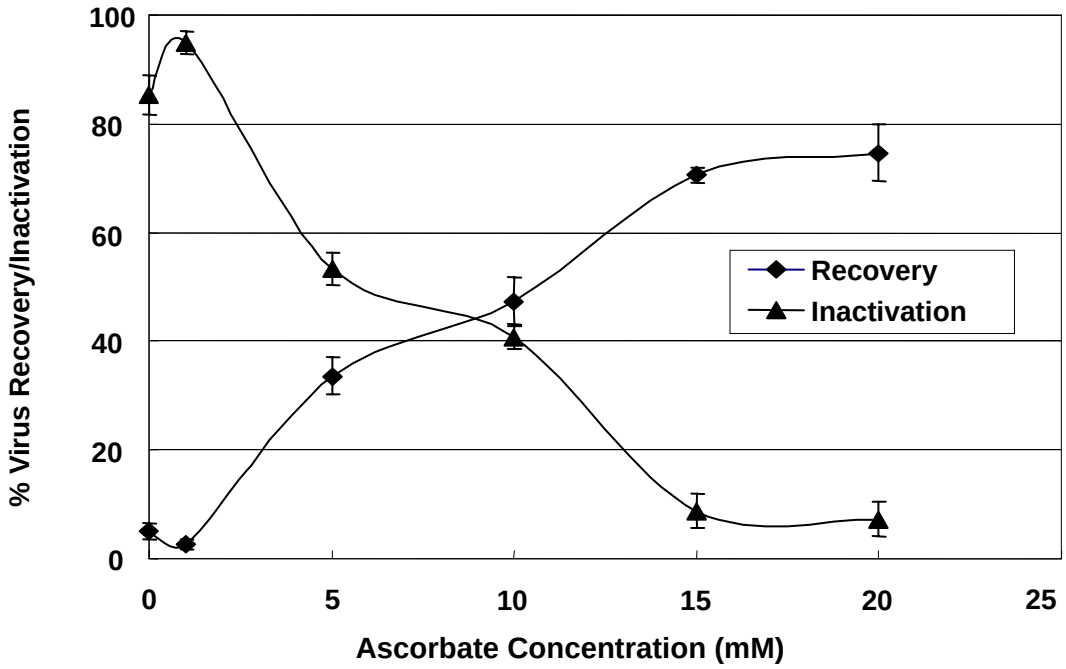

Figure 15. Effect of ascorbate on the virus inactivation when crude KgBHAT supernatant was used as loading material.

Ascorbate buffer (PBS, 0.5 M NaCl, 200 mM ascorbate, pH6.5 or pH5.5) was added to the load (crude KgBHAT supernatant, pH6.5), the wash buffer (buffer A, pH 6.5), and elution buffer (buffer B, pH5.5) to the final ascorbate concentrations as indicated in the figure. The virus recovery and inactivation rates from IMAC runs were plotted against the concentration of ascorbate present in chromatography mobile phase. Flow rate was 1 ml/min. Two milliliters crude supernatant containing $1*10^9$ pfu viruses in were loaded. The data represents the average of three independent experiments.

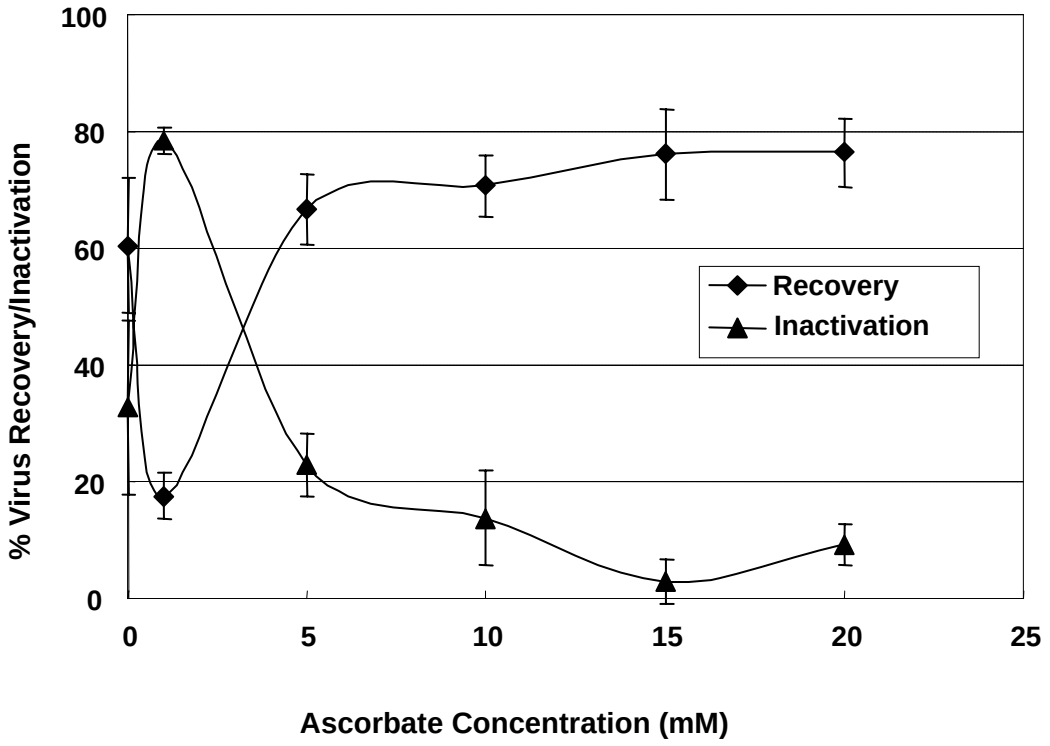

Figure 16. Effect of ascorbate on the virus inactivation when partially purified KgBHAT suspension was used as loading material.

Ascorbate buffer (PBS, 0.5 M NaCl, 200 mM ascorbate, pH6.5 or pH5.5) was added to the load (partially purified KgBHAT suspension, pH6.5), the wash buffer (buffer A, pH 6.5), and elution buffer (buffer B, pH 5.5) to the final ascorbate concentrations as indicated in the figure. The virus recovery and inactivation rates from IMAC runs were plotted against the concentration of ascorbate present in chromatography mobile phase. Flow rate was 1 ml/min. $1*10^9$ pfu viruses in 4 ml loading buffer were loaded. The data represents the average of three independent experiments.

However, at low concentration of 1 mM, ascorbate promoted virus inactivation instead of preventing it. The effect of low ascorbate concentration was more prominent when, instead of a crude virus preparation, a virus preparation that was first partially purified from cell debris and soluble protein/DNA impurities was applied to the column (Fig. 16). Partial purification of the virus preparation was achieved by centrifugation (20,000Xg, 1hr) of the crude supernatant and suspending the virus pellet in the loading buffer (PBS, 0.5 M NaCl, pH6.5), which had the same salt concentration and pH as the crude supernatant. As shown in Fig. 16, the presence of 1 mM ascorbate in partially purified suspension resulted in a 78% loss of infectivity as compared to 35% without ascorbate. Furthermote, comparison of Fig.15 and 16 at zero concentration of ascorbate reveals that the removal of soluble impurities leads to a much lower inactivation rate.

These experiments established that 20 mM ascorbate in mobile phase was able to effectively protect KgBHAT viruses from inactivation during the purification of crude supernatant on IDA-Co^{2+}. Fig. 17 demonstrated the distribution of protein, DNA, and infectious viruses found in flow through, wash, elution, and EDTA fractions. The infectious virus recovered in elution was significantly increased from 4.9% in the absence of ascorbate (Table 3) to 72% in the presence of 20mM ascorbate in loading, wash, and elution buffers (Fig. 17). In contrast, the ascorbate had no effect on the elution profiles of protein and DNA impurities as most of the protein and DNA impurities were released in the flow through and wash steps, with less than 5% distributed in elution (Fig.17).

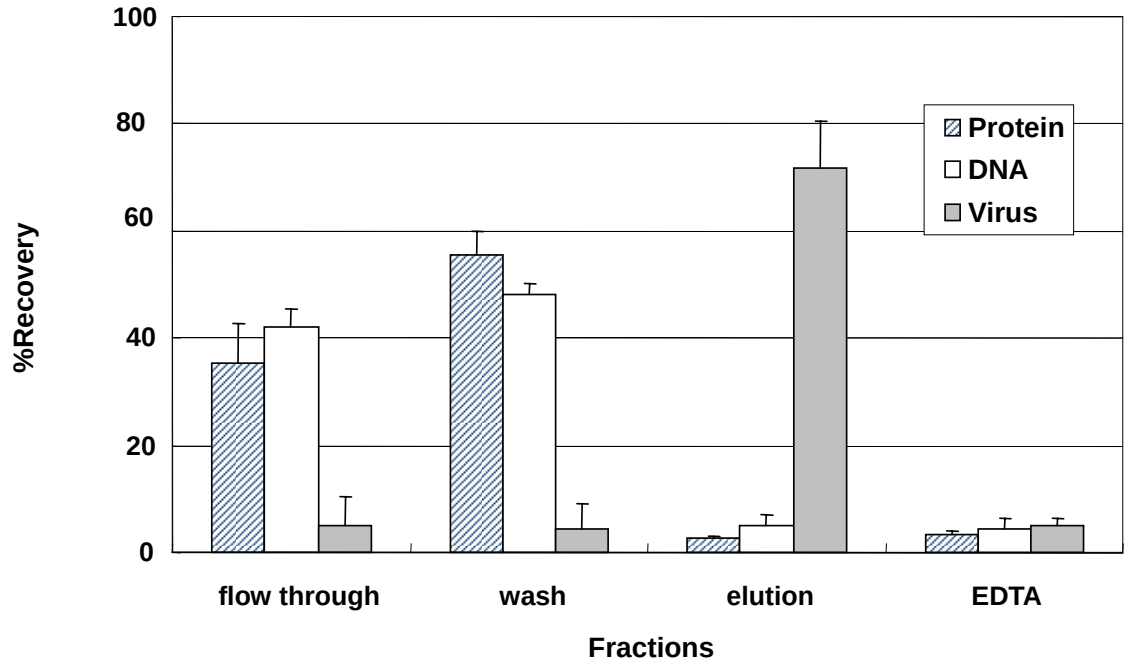

Figure 17. Inclusion of 20 mM ascorbate in mobile phase protected KgBHAT from inactivation.

2 ml KgBHAT crude supernatant ($5.1*10^9$ pfu/ml) containing 20 mM ascorbate was loaded on an IDA-Co^{2+} column. After loading, the column was washed with 4 ml pH 6.5 buffer (PBS, 0.5M NaCl, pH6.5) containing 20 mM ascorbate. The bound viruses were eluted with 4 ml pH5.5 buffer (PBS, 0.5M NaCl, pH5.5) containing 20 mM ascorbate. Finally, 4 ml EDTA buffer (PBS, 0.5M NaCl, 50mM EDTA, pH6.5) was used to strip the column. Flow rate was 1ml/min. The distribution of virus, protein, and DNA in flow-through, wash, elution, and EDTA strip fractions are shown in the Figure. The data represents the average of three independent experiments.

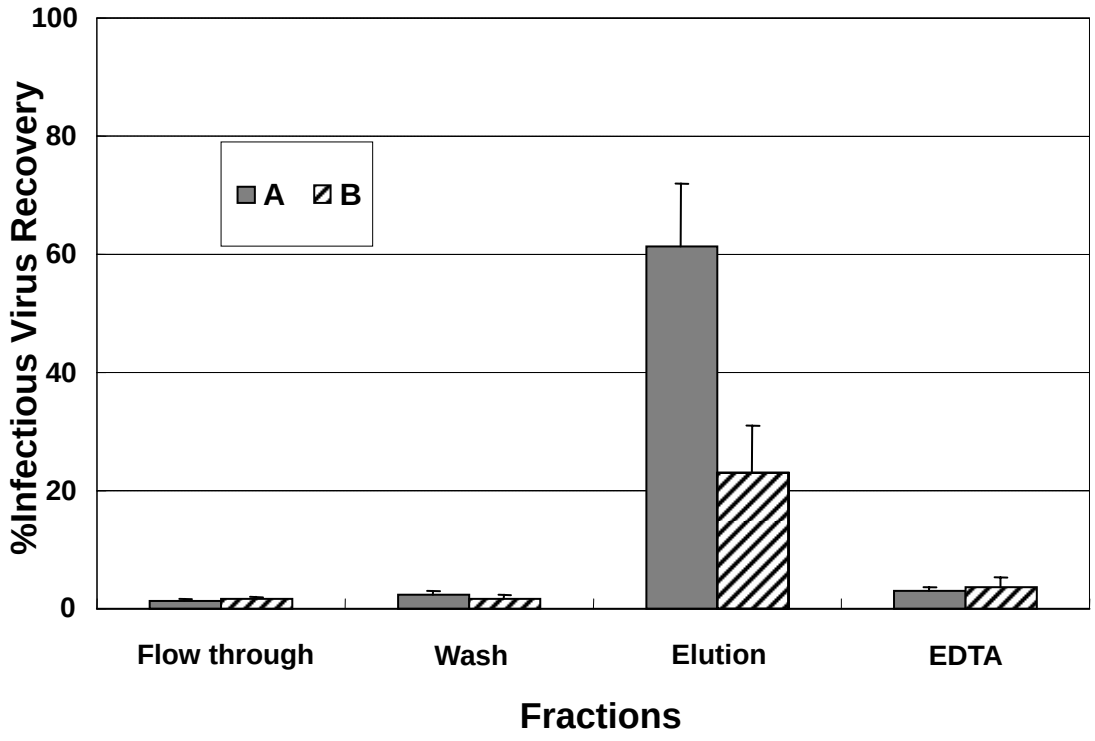

Figure 18. Effect of ascorbate presence only in loading and wash (A) or only in wash and elution (B) on the recovery of KgBHAT.

(A) 2ml KgBHAT crude supernatant ($5.1*10^9$ pfu/ml) containing 20 mM ascorbate was loaded on an IDA-Co^{2+} column. After loading, the column was washed with 4 ml pH6.5 buffer (PBS, 0.5M NaCl, pH6.5) containing 20 mM ascorbate. The column was eluted with pH 5.5 buffer (PBS, 0.5M NaCl, pH5.5) without ascorbte. (B) 2ml KgBHAT crude supernatant ($5.1*10^9$ pfu/ml) without ascorbate was loaded on an IDA-Co^{2+} column. After loading, the column was washed with 4 ml of the same pH6.5 buffer containing 20 mM ascorbate. The column was eluted with the pH5.5 buffer containing 20mM ascorbte. Flow rate was 1ml/min. The data represents the average of three independent experiments.

Finally, we found that ascorbate had to be present in the loading suspension of the virus preparation to impart significant protection. As shown in Fig. 18, incorporation of 20 mM ascorbate in the washing and elution buffers increased the infectious virus recovery to 20% (Fig.18B); whereas adding the same amount of ascorbate in the loading and washing improved the recovery to 60% (Fig. 18A). As noted earlier, the infectious virus recovered in elution was 72% in the presence of 20mM ascorbate in loading, wash, and elution buffers (Fig. 17). Thus, virus inactivation occurs to a large extent during the loading of virus preparations on the chromatography column.

4.2.4 Effect of Imidazole on KgBHAT Inactivation

In practice, during IMAC purification, the retained product is usually eluted from the column with a buffer gradient either with decreasing pH or increasing concentration of imidazole. The imidazole competes with proteins for the binding to the chelated metal ion while the proton competes with the immobilized metal for the protein.

It is of interest to examine if there is any improvement on the virus recovery by eluting the column with imidazole containing buffers. In Fig.19, same amount of KgBHAT crude supernatant was loaded on the IDA-Co^{2+} column as in Table 3. After loading, the column was eluted instead with an imidazole step gradient: 20mM imidazole (PBS, 0.5M NaCl, pH6.5) followed by 140mM imidazole (PBS, 0.5M NaCl, pH6.5). As shown in Fig.19, this imidazole elution strategy gave rise to a similar distribution of infectious viruses in the elution fractions as in Table 3: 10% in 20mM imidazole, 5% in 140mM imidazole, and 1.5% in the EDTA fraction. There was no improvement on virus infectivity recovery in any of the elution fractions.

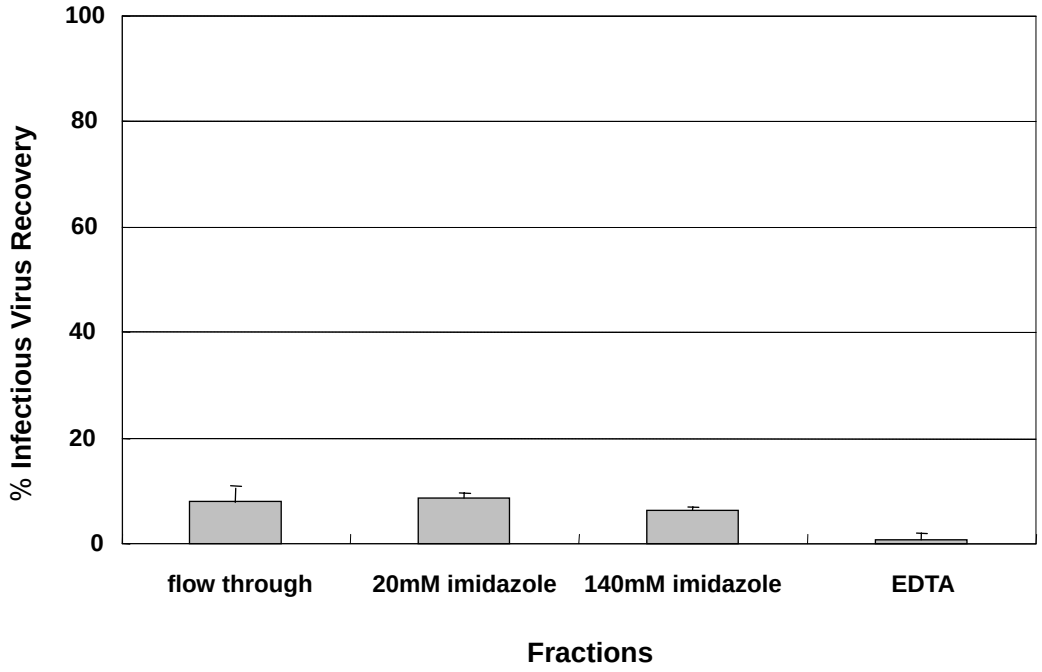

Figure 19. Chromatography of KgBHAT crude supernatant on IDA-Co^{2+} column: eluting with imidazole gradient

2 ml of clarified KgBHAT crude supernatant ($5.3*10^9$ pfu/ml) was loaded on the column. After loading, the column was eluted with 4ml of 20mM imidazole buffer (PBS-0.5 M NaCl, pH6.5), followed by 4ml of 140mM imidazole buffer (PBS-0.5M NaCl, pH6.5). Finally, the column was passed through with an EDTA containing buffer (PBS-0.5 M NaCl, 50 mM EDTA, pH6.5) to release the metal ions and remove any remaining viruses or impurities on the column. Flow rate was 1ml/min. The data represents the average of three independent experiments.

Interestingly enough, if imidazole was also added in the loading material as well as in the elution, substantially higher virus infectivity recovery would be obtained. As shown in Fig. 20, keeping the rest IMAC protocol the same as in Fig.19, incorporation of 20mM imidazole in the loading led to significantly improved infectivity recovery in the 140M imidazole elution fraction. Fig.20 also shows that the majority of protein and DNA impurities did not bind to IDA-Co^{2+} as expected and were removed in the flow through and wash fractions. Only less than 5% of the total protein or DNA impurities were released in the 140mM imidazole elution fractions. Fig. 20 demonstrates the effective purification of the tagged HSV-1 on IDA-Co^{2+} if using appropriate chromatographic procedure.

We also found that imidazole does not have to be present in the elution to achieve the high recovery. As shown in Fig.21, when 20mM imidazole was included in the loading and the subsequent wash step, high infectious virus recovery (58%) was obtained by eluting the column with a pH5.5 buffer (PBS, 0.5 M NaCl, pH5.5). This high recovery in Fig. 21, in comparison with the low recovery in Fig. 20 where imidazole was present in wash and elution but not in loading, suggests that imidazole has to be present in the loading virus suspension to impact significant protection on the viruses.

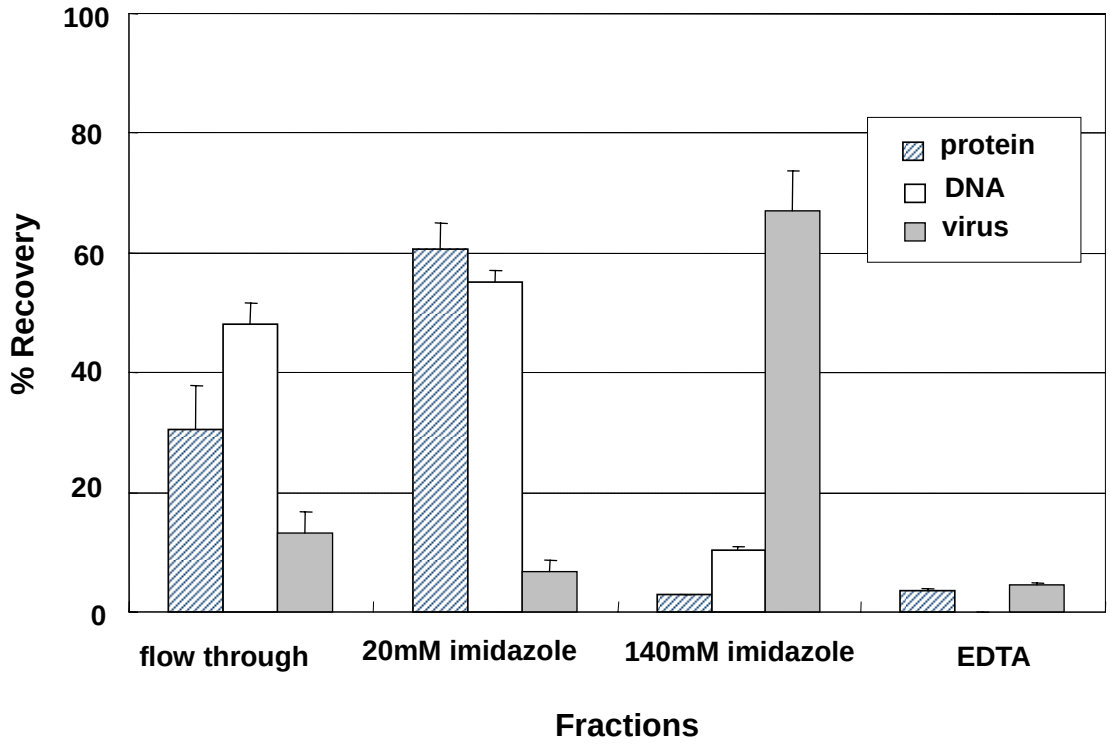

Figure 20. Inclusion of 20 mM imidazole in mobile phase protected KgBHAT from inactivation.

Two milliliters KgBHAT crude supernatant ($5.3*10^9$ pfu/ml) containing 20 mM imidazole was loaded on an IDA-Co^{2+} column. After loading, the column was eluted with 4ml of 20mM imidazole buffer (PBS-0.5 M NaCl, pH6.5), followed by 4ml of 140mM imidazole buffer (PBS-0.5M NaCl, pH6.5). Finally, the column was passed through with an EDTA containing buffer (PBS-0.5 M NaCl, 50 mM EDTA, pH6.5) to release the metal ions and remove any remaining viruses or impurities on the column. Flow rate was 1ml/min. The data represents the average of three independent experiments.

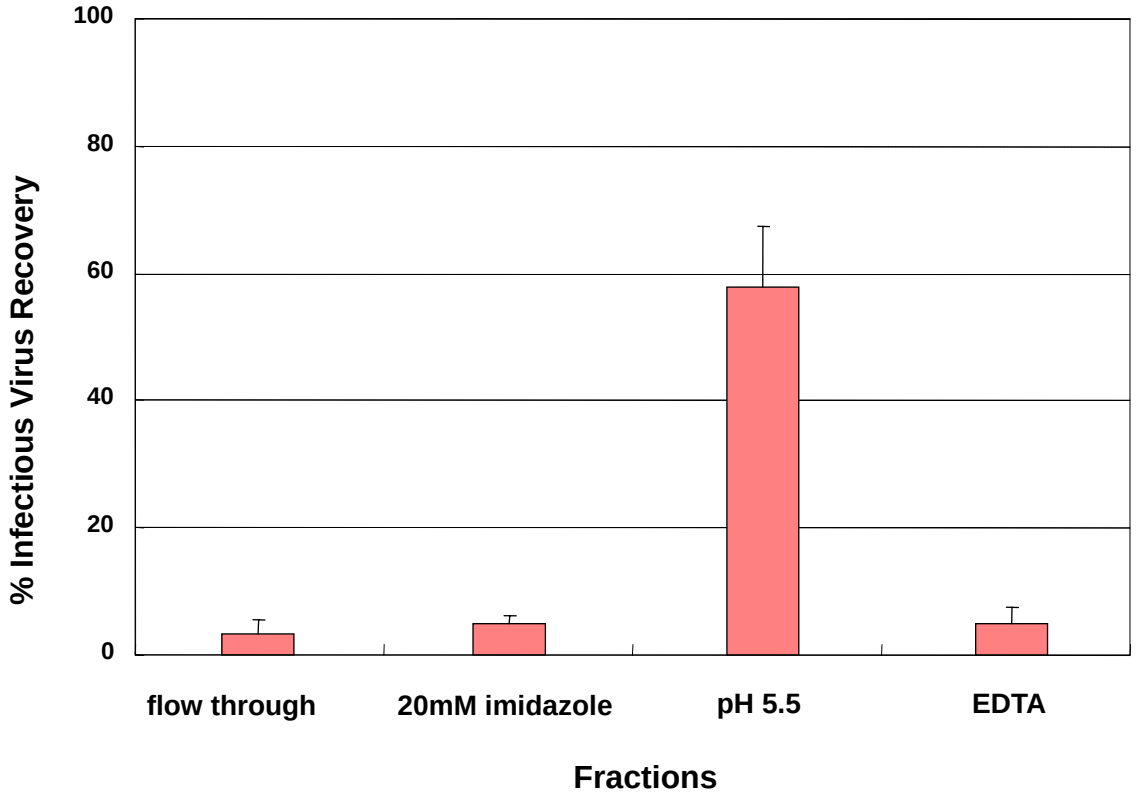

Figure 21. Inclusion of 20 mM imidazole in the loading virus suspension and the wash buffer resulted in high virus infectivity recovery.

2 ml KgBHAT crude supernatant ($5.3*10^9$ pfu/ml) containing 20 mM imidazole was loaded on an IDA-Co^{2+} column. After loading, the column was eluted with 4ml of 20mM imidazole buffer (PBS-0.5 M NaCl, pH6.5), followed by 4ml of pH5.5 buffer (PBS-0.5M NaCl). Finally, the column was passed through with an EDTA containing buffer (PBS-0.5 M NaCl, 50 mM EDTA, pH6.5) to release the metal ions and remove any remaining viruses or impurities on the column. Flow rate was 1ml/min. The data represents the average of three independent experiments.

4.2.5 ESR Measurements

IMAC experiments in the presence of ascorbate suggested that virus inactivation might be the result of free radicals generated in the column. To verify this hypothesis, ESR using DMPO as a spin trap was employed to directly detect oxygen free radicals.

As shown in Fig. 22A, a suspension of IDA-Co^{2+} beads in crude KgBHAT suspension generated a 1:2:2:1 quartet with splittings of $a_N=a_H=14.9$ G, where a_N and a_H denote hyperfine splittings of the nitroxyl nitrogen and α-hydrogen. Based on these splittings and 1:2:2:1 lineshape, this spectrum was assigned to DMPO/•OH [165], thus providing direct evidence of •OH generation from crude supernatant on IDA-Co^{2+}.

ESR signal of DMPO/•OH was significantly lower from the IDA-Co^{2+} beads suspended in the partially purified KgBHAT suspension, where most of the soluble impurities were removed by centrifugation (Fig. 22B). This explained the relative high infectious virus recovery (60%, Fig. 12) when this partially purified suspension was loaded on IDA-Co^{2+}.

When 20 mM ascorbate was incorporated in the crude supernatant before its mixing with IDA-Co^{2+} beads, ESR detected a doublet with hyperfine splitting $a_H=1.8$ G, a characteristic of ascorbate free radical (Fig. 22C) [166]. This spectrum indicated that the highly reactive •OH was scavenged by ascorbate to give rise to stable ascorbate free radicals. The stable ascorbate free radicals do not appear to cause significant KgBHAT inactivation (Fig. 17). when the IDA-Co^{2+} beads were suspended in the same crude supernatant containing 20mM imidazole, no free radical signal was readily detected (Fig. 22D). This spectrum indicated that imidazole prohibited hydroxyl radical generation from Co^{2+} complexes. The absence of detectible hydroxyl free radical in Fig. 22D explained the high infectious virus recovery in Fig. 20 and Fig. 21.

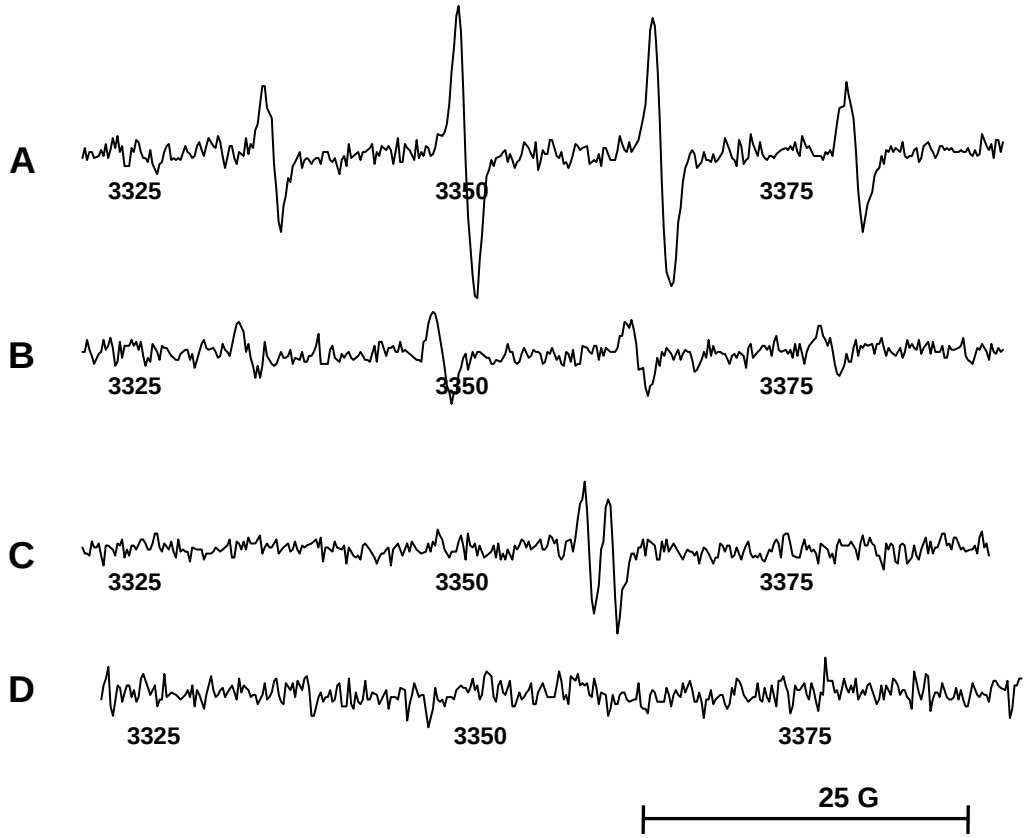

Figure 22. Detection of free radicals with ESR.

DMPO was added to the final concentration of 100 mM in (A) crude KgBHAT supernatant, (B) KgBHAT pellet suspension in buffer A, (C) crude supernatant containing 20 mM ascorbate, or (D) crude supernatant containing 20 mM imidazole for the use as spin-trap to detect free radicals. Freshly prepared IDA-Co^{2+} beads were mixed with the above samples in room temperature. Five minutes after mixing, 10 µl of the bead slurry was transferred into a capillary tube and subjected to ESR measurements.

4.3 DISCUSSION

Because dioxygen is a triplet molecule, its reaction with biomolecules is spin forbidden. Many transition metals (copper, iron, and cobalt in particular), which exist in several spin states, can relieve the spin restriction of dioxygen and enhance the rates of biomolecule oxidation [167]. There is a large body of literature documenting metal catalyzed oxidation (MCO) of biological molecules in solution. However, despite the great popularity of IMAC in protein purification, the MCO during an actual IMAC experiment has not been established.

Considering that IMAC has primarily been used for protein purification, two factors may have contributed to the lack of documentation of MCO in IMAC. First, biological activity loss may not be discernible for many proteins if the damage does not occur within a functional domain. Second, use of any purification step with significant activity loss usually will be abandoned and alternative strategies will be explored rather than dedicating significant resources for finding the fundamental mechanism of activity loss. In comparison to proteins, viruses rely on groups of functional domains from a variety of its surface proteins to bind cellular receptors and penetrate into cells during infection. Moreover, the viral genome should be free of DNA damage in order to faithfully encode the viral functions. Thus, it is likely that viruses are more vulnerable to inactivation than proteins, and could serve as better models for studying biological product inactivation during IMAC purification.

Here we report the inactivation of KgBHAT during the purification on an IDA-Co^{2+} column, particularly when the crude virus supernatant was used as starting material. ESR using DMPO as a spin trap detected a strong signal characteristic of DMPO/•OH in the inactivating condition. Removal of the soluble impurities by centrifugation significantly diminished •OH radical generation, leading to enhanced recovery of virus infectivity. Since

the viruses were stable in the crude supernatant, we concluded that the •OH radicals were generated from the interaction of the cobalt ions and soluble impurities on the IDA-Co^{2+} column.

The •OH radicals may have been produced from the uptake and activation of dissolved oxygen by chelated Co^{2+}. The ability of Co^{2+} complexes to bind and reduce dioxygen has long been exploited in the applications of dioxygen storage and oxidation catalysis [168-170]. Upon binding, dioxygen form a mononuclear superoxo or a dinucleat peroxo complex with cobalt ion, with a partial electron transfer from the metal center toward dioxygen [168, 170]. In certain circumstance where there are strong electron-donating ligands and/or solvents, irreversible reduction of dioxygen may occur. This reduction could result in the production of hydrogen peroxide [168]. More importantly, the hydrogen peroxide can react with the chelated Co^{2+} and generate highly reactive hydroxyl free radical through a Fenton reaction: Co^{2+} + $H_2O_2 \rightarrow Co^{3+}$ + •OH + $^{-}$OH [111, 112, 171]. The capability of Co^{2+} to bind and reduce molecular oxygen is highly influenced by the chelating ligands that coordinate with the cobalt [111, 112]. For example, oxygen binds to a Co^{2+}-(Gly-Gly) complex could result in the oxidation of Co^{2+} to Co^{3+} and the reduction of oxygen; however, a similar Co^{2+}-(Gly-Gly)-imidazole complex is more resistant to irreversible oxidation [172]. Furthermore, chelating ligands can modulate the oxidation potential of Co^{2+} to enhance or reduce its capability to generate •OH radicals from H_2O_2. For example, glutathione (GSH), anserine, and Gly-Gly-His were found to enhance the cobalt mediated •OH generation [112]. Whereas ADP, citrate, or EDTA can reduce it [111]. Results present in this study demonstrate that imidazole could reduce the •OH generation on the IDA-Co^{2+}, plausibly by diminishing the capability of Co^{2+} in catalyzing oxygen activation and hydroxyl radical generation. On the other hand, the crude virus supernatant contains a complex mixture of substances originated from lysed cells during virus replication, which

may include hydrogen peroxide, reducing agents, and cellular chelating agents. Upon contacting with chelated Co^{2+} on the IMAC column, these substances may create a favorable condition for dioxygen reduction and hydroxyl radical generation.

The •OH radical could cause protein damage such as fragmentation, carbonyl formation, and other single amino acid modification [113]. The reaction of •OH radical with DNA could result in strand scission, DNA-protein crosslinking, and base modification [116, 173, 174]. Our results (Table. 3) indicated that HSV-1 genome was damaged as the genomes from inactivated viruses failed to serve as functional templates for Q-PCR. The direct consequence of DNA damage was the loss of viral infectivity.

The hydroxyl radicals produced on IDA-Co^{2+} were efficiently scavenged by 20 mM ascorbate to generate ascorbate radicals (Fig. 22C). Since the ascorbate radical is much more stable than •OH radical [166], virus inactivation is prevented. Although a good free radical scavenger in high concentrations, ascorbate could also act as a pro-oxidant capable of promoting free radical generation in low concentrations, due to its reducing capability [106]. The presence of 1 mM ascorbate deteriorated virus inactivation in both crude virus supernatant (Fig. 15) and partially purified virus suspension (Fig. 16), with more pronounced effect in the later. This more pronounced effect of low concentration of ascorbate in the partially purified virus suspension implies that reducing agents from the cell lysate might be partially responsible for the catalysis of free radical generation in crude supernatant.

We also found that imidazole was able to protect KgBHAT from inactivation on IDA-Co^{2+} column. Similar to ascorbate, imidazole has to be present in the loading virus suspension during IMAC to impart effective protection. However, it appears that imidazole has a different protection mechanism than ascorbate. Rather than acting as a free radical scavenger that removes the generated hydroxyl radicals, imidazole prohibits free radical

formation in the first place (Fig. 22D), possibly by modifying the catalytic activity of Co^{2+} in oxidative free radical generation. The lack of free radical generation explained the high infectious virus recovery when 20 mM imidazole was included in the mobile phase during IMAC (Fig20, Fig.21). This result implied that the chelating ligand on IMAC support could be carefully designed and optimized so that the chelated transition metal ions will become inert or less active in promoting oxidative free radical generation.

In summary, we demonstrated hydroxyl free radical mediated HSV-1 inactivation on immobilized cobalt affinity chromatography where no exogenous hydrogen peroxide or reducing agents were intentionally introduced into the column. Moreover, we demonstrated that the inactivation can be reversed by inclusion of appropriate amounts of ascorbate or imidazole. The presence of 20 mM ascorbate or imidazole in the mobile phase was highly effective in preventing virus inactivation. The details of the mechanism responsible for free radical formation during IMAC may still need further clarification. However, it is of prime importance to note that free radical mediated damage might be prevalent in many IMAC purifications, particularly in those "one-step purifications" where crude harvest is used as starting material. Thus, attention must be given to free radical mediated damage when using IMAC for purification of biological products.

5.0 CONCLUSIONS

Recombinant HSV-1 vectors have demonstrated a great potential as delivery vehicles for gene therapy applications. As HSV-1 vectors are moving into clinical development, there is increasing demand for large quantities of highly purified HSV-1 vectors. Thus, efficient production and purification of HSV-1 vectors becomes paramount important. Here, we have demonstrated that HSV-1 vectors can be simply and effectively purified using immobilized metal affinity chromatography. Outcomes of this study can be summarized as following.

1. None of the transition metal ions investigated in this study (Cu^{2+}, Ni^{2+}, Zn^{2+}, and Co^{2+}) is able to provide a means of separation of untagged HSV-1 virus from protein and DNA contaminants. However, of interest is the finding that Co^{2+} column binds negligible amounts of protein, DNA, and virus, suggesting that this column could be useful for HSV-1 vector purification if the vector could be endowed with the ability to bind to immobilized cobalt.

2. We constructed an HSV-1 recombinant (KgBHAT) with a cobalt affinity tag (HAT) replacing the heparan sulfate binding domain of virion envelope glycoprotein B (gB). The productivity of KgBHAT on Vero cells is essentially identical to that of wild type HSV-1 (KOS), and the infectivity of KgBHAT is not severely impaired by the mutation.

3. We developed an immobilized cobalt affinity chromatography scheme for the tagged HSV-1 virus purification. By correct choice of IMAC parameters such as loading condition (pH, ascorbate concentration), flow rate, and chromatographic substrate, efficient purification of KgBHAT on immobilized cobalt affinity chromatography can be achieved with high virus infectivity yield.

4. We found that KgBHAT was inactivated on IDA-Co^{2+} when crude virus supernatant was used as loading material during IMAC (<5% infectivity recovery). Electron spinning resonance revealed that the virus inactivation is caused by hydroxyl free radicals that are generated from the interaction between cobalt ions and components in crude virus supernatant. It has been demonstrated that appropriate amount of ascorbate (20 mM), a free radical scavenger, or imidazole (20 mM) in the loading material is able to protect HSV-1 virus from inactivation, and leads to high virus infectivity recovery after IMAC purification. This finding is the first demonstration of oxygen free radical mediated biological inactivation in an actual IMAC purification and an effective method to prevent it.

Using the IMAC parameters optimized in the previous chapters, KgBHAT crude supernatant was purified on a 1-ml IDA-Co^{2+} column, with the results illustrated in Table 5. In this demonstration run, a blank IDA column was connected in the downstream of the IDA-Co^{2+} column to minimize metal leakage during purification. 4 ml of KgBHAT crude supernatant ($2.3*10^8$ pfu/ml) containing 20 mM ascorbate was loaded on the IDA-Co^{2+}. After washing with 4 ml of pH6.5 buffer (PBS, 0.5 M NaCl, pH6.5, 20mM ascorbate), the column was eluted with 4 ml of pH5.5 buffer (PBS, 0.5 M NaCl, pH5.5, 20mM ascorbate). The elution fraction was collected only after passing 2 ml of elution buffer, as little amount of recoverable viruses were found to be present in the first 2 ml of elution. As shown in Table 5, the final protein concentration in the purified virus stock was 4.4 μg/ml, a reduction of more than 97.8 % from the loaded virus stock. The final cellular DNA contaminant concentration was 2.9 ng/ml for a reduction of more than 97%. The overall virus infectivity recovery was 71.1% with about 1.4 fold concentration. In addition, the amount of defective virus particles in the purified virus stock was decreased as the ratio of virus genome number to infectious virus pfu decreased from 32 to 4.1 during the purification.

Table 5. Purification of KgBHAT on IDA-Co^{2+} column

	Before IMAC	After IMAC	% Recovery
Protein µg/ml	204.4	4.4	**2.2**
Cellular DNA ng/ml	96.7	2.9	**3.0**
Copies of viral genome	$7.4*10^9$	$1.4*10^9$	18.9
Virus infectivity pfu/ml	$2.3*10^8$	$3.3*10^8$	**71.1**
Viral genome / Infectious virus	32.0	4.1	/

BIBLIOGRAPHY

1. Anderson, W. F., Human gene therapy. *Nature* **1998,** 392, (6679 Suppl), 25-30.

2. Verma, I. M.; Somia, N., Gene therapy -- promises, problems and prospects. *Nature* **1997,** 389, (6648), 239-42.

3. Verma, I. M.; Weitzman, M. D., Gene therapy: twenty-first century medicine. *Annu Rev Biochem* **2005,** 74, 711-38.

4. Griesenbach, U.; Geddes, D. M.; Alton, E. W., Gene therapy for cystic fibrosis: an example for lung gene therapy. *Gene Ther* **2004,** 11 Suppl 1, S43-50.

5. Tate, S.; Elborn, S., Progress towards gene therapy for cystic fibrosis. *Expert Opin Drug Deliv* **2005,** 2, (2), 269-80.

6. Jones, J. M.; Koch, W. J., Gene therapy approaches to cardiovascular disease. *Methods Mol Med* **2005,** 112, 15-35.

7. Quarck, R.; Holvoet, P., Gene therapy approaches for cardiovascular diseases. *Curr Gene Ther* **2004,** 4, (2), 207-23.

8. Burton, E. A.; Bai, Q.; Goins, W. F.; Glorioso, J. C., Replication-defective genomic herpes simplex vectors: design and production. *Curr Opin Biotechnol* **2002,** 13, (5), 424-8.

9. Costantini, L. C.; Bakowska, J. C.; Breakefield, X. O.; Isacson, O., Gene therapy in the CNS. *Gene Ther* **2000,** 7, (2), 93-109.

10. Furlan, R.; Butti, E.; Pluchino, S.; Martino, G., Gene therapy for autoimmune diseases. *Curr Opin Mol Ther* **2004,** 6, (5), 525-36.

11. Lotze, M. T., Cancer Gene Therapy: The power of negative thinking. *Gene Ther* **2005**.

12. McNeish, I. A.; Bell, S. J.; Lemoine, N. R., Gene therapy progress and prospects: cancer gene therapy using tumour suppressor genes. *Gene Ther* **2004,** 11, (6), 497-503.

13. Kootstra, N. A.; Verma, I. M., Gene therapy with viral vectors. *Annu Rev Pharmacol Toxicol* **2003,** 43, 413-39.

14. Lundstrom, K., Latest development in viral vectors for gene therapy. *Trends Biotechnol* **2003,** 21, (3), 117-22.

15. Thomas, C. E.; Ehrhardt, A.; Kay, M. A., Progress and problems with the use of viral vectors for gene therapy. *Nat Rev Genet* **2003,** 4, (5), 346-58.

16. Nishikawa, M.; Huang, L., Nonviral vectors in the new millennium: delivery barriers in gene transfer. *Hum Gene Ther* **2001,** 12, (8), 861-70.

17. Glorioso, J. C., Perspectives on viral vector design and applications. *Adv Virus Res* **2000,** 55, 403-7.

18. Wolff, L.; Ruscetti, S., Malignant transformation of erythroid cells in vivo by introduction of a nonreplicating retrovirus vector. *Science* **1985,** 228, (4707), 1549-52.

19. Markowitz, D.; Goff, S.; Bank, A., Construction and use of a safe and efficient amphotropic packaging cell line. *Virology* **1988,** 167, (2), 400-6.

20. Markowitz, D.; Goff, S.; Bank, A., A safe packaging line for gene transfer: separating viral genes on two different plasmids. *J Virol* **1988,** 62, (4), 1120-4.

21. F Blanche, B. C., A Barbot, L Ferrero, T Guillemin, S Guyot, S Somarriba and D Bisch, An improved anion-exchange HPLC method for the detection and purification of adenoviral particles. *Gene Ther* **2000,** 7, (12), 1055-1062.

22. Lai, Z.; Han, I.; Park, M.; Brady, R. O., Design of an HIV-1 lentiviral-based gene-trap vector to detect developmentally regulated genes in mammalian cells. *Proc Natl Acad Sci U S A* **2002,** 99, (6), 3651-6.

23. Leander Johansen, J.; Dago, L.; Tornoe, J.; Rosenblad, C.; Kusk, P., A new versatile and compact lentiviral vector. *Mol Biotechnol* **2005,** 29, (1), 47-56.

24. Lusky, M.; Christ, M.; Rittner, K.; Dieterle, A.; Dreyer, D.; Mourot, B.; Schultz, H.; Stoeckel, F.; Pavirani, A.; Mehtali, M., In vitro and in vivo biology of recombinant adenovirus vectors with E1, E1/E2A, or E1/E4 deleted. *J Virol* **1998,** 72, (3), 2022-32.

25. O'Neal, W. K.; Zhou, H.; Morral, N.; Aguilar-Cordova, E.; Pestaner, J.; Langston, C.; Mull, B.; Wang, Y.; Beaudet, A. L.; Lee, B., Toxicological comparison of E2a-deleted and first-generation adenoviral vectors expressing alpha1-antitrypsin after systemic delivery. *Hum Gene Ther* **1998,** 9, (11), 1587-98.

26. Andrews, J. L.; Kadan, M. J.; Gorziglia, M. I.; Kaleko, M.; Connelly, S., Generation and characterization of E1/E2a/E3/E4-deficient adenoviral vectors encoding human factor VIII. *Mol Ther* **2001,** 3, (3), 329-36.

27. Morsy, M. A.; Caskey, C. T., Expanded-capacity adenoviral vectors--the helper-dependent vectors. *Mol Med Today* **1999,** 5, (1), 18-24.

28. Conlon, T. J.; Flotte, T. R., Recombinant adeno-associated virus vectors for gene therapy. *Expert Opin Biol Ther* **2004,** 4, (7), 1093-101.

29. Flotte, T. R., Gene therapy progress and prospects: recombinant adeno-associated virus (rAAV) vectors. *Gene Ther* **2004,** 11, (10), 805-10.

30. Smith-Arica, J. R.; Bartlett, J. S., Gene therapy: recombinant adeno-associated virus vectors. *Curr Cardiol Rep* **2001,** 3, (1), 43-9.

31. Miller, D. G.; Rutledge, E. A.; Russell, D. W., Chromosomal effects of adeno-associated virus vector integration. *Nat Genet* **2002,** 30, (2), 147-8.

32. Satoh, W.; Hirai, Y.; Tamayose, K.; Shimada, T., Site-specific integration of an adeno-associated virus vector plasmid mediated by regulated expression of rep based on Cre-loxP recombination. *J Virol* **2000,** 74, (22), 10631-8.

33. Conway, J. E.; Rhys, C. M.; Zolotukhin, I.; Zolotukhin, S.; Muzyczka, N.; Hayward, G. S.; Byrne, B. J., High-titer recombinant adeno-associated virus production utilizing a recombinant herpes simplex virus type I vector expressing AAV-2 Rep and Cap. *Gene Ther* **1999,** 6, (6), 986-93.

34. Roizman, B.; Knipe, D., Herpes simplex viruses and their replication. *Fields Viology* **2001**, 2399-2459.

35. Laquerre, S.; Argnani, R.; Anderson, D. B.; Zucchini, S.; Manservigi, R.; Glorioso, J. C., Heparan sulfate proteoglycan binding by herpes simplex virus type 1 glycoproteins B and C, which differ in their contributions to virus attachment, penetration, and cell-to-cell spread. *J Virol* **1998,** 72, (7), 6119-30.

36. Herold, B. C.; Gerber, S. I.; Polonsky, T.; Belval, B. J.; Shaklee, P. N.; Holme, K., Identification of structural features of heparin required for inhibition of herpes simplex virus type 1 binding. *Virology* **1995,** 206, (2), 1108-16.

37. Herold, B. C.; Visalli, R. J.; Susmarski, N.; Brandt, C. R.; Spear, P. G., Glycoprotein C-independent binding of herpes simplex virus to cells requires cell surface heparan sulphate and glycoprotein B. *J Gen Virol* **1994,** 75 (Pt 6), 1211-22.

38. Montgomery, R. I.; Warner, M. S.; Lum, B. J.; Spear, P. G., Herpes simplex virus-1 entry into cells mediated by a novel member of the TNF/NGF receptor family. *Cell* **1996,** 87, (3), 427-36.

39. Warner, M. S.; Geraghty, R. J.; Martinez, W. M.; Montgomery, R. I.; Whitbeck, J. C.; Xu, R.; Eisenberg, R. J.; Cohen, G. H.; Spear, P. G., A cell surface protein with herpesvirus entry activity (HveB) confers susceptibility to infection by mutants of herpes simplex virus type 1, herpes simplex virus type 2, and pseudorabies virus. *Virology* **1998,** 246, (1), 179-89.

40. Shukla, D.; Liu, J.; Blaiklock, P.; Shworak, N. W.; Bai, X.; Esko, J. D.; Cohen, G. H.; Eisenberg, R. J.; Rosenberg, R. D.; Spear, P. G., A novel role for 3-O-sulfated heparan sulfate in herpes simplex virus 1 entry. *Cell* **1999,** 99, (1), 13-22.

41. Fuller, A. O.; Lee, W. C., Herpes simplex virus type 1 entry through a cascade of virus-cell interactions requires different roles of gD and gH in penetration. *J Virol* **1992,** 66, (8), 5002-12.

42. Honess, R. W.; Roizman, B., Regulation of herpesvirus macromolecular synthesis. I. Cascade regulation of the synthesis of three groups of viral proteins. *J Virol* **1974,** 14, (1), 8-19.

43. Campbell, M. E.; Palfreyman, J. W.; Preston, C. M., Identification of herpes simplex virus DNA sequences which encode a trans-acting polypeptide responsible for stimulation of immediate early transcription. *J Mol Biol* **1984,** 180, (1), 1-19.

44. Preston, C. M.; Frame, M. C.; Campbell, M. E., A complex formed between cell components and an HSV structural polypeptide binds to a viral immediate early gene regulatory DNA sequence. *Cell* **1988,** 52, (3), 425-34.

45. Bearer, E. L.; Breakefield, X. O.; Schuback, D.; Reese, T. S.; LaVail, J. H., Retrograde axonal transport of herpes simplex virus: evidence for a single mechanism and a role for tegument. *Proc Natl Acad Sci U S A* **2000,** 97, (14), 8146-50.

46. Mellerick, D. M.; Fraser, N. W., Physical state of the latent herpes simplex virus genome in a mouse model system: evidence suggesting an episomal state. *Virology* **1987,** 158, (2), 265-75.

47. Spivack, J. G.; Fareed, M. U.; Valyi-Nagy, T.; Nash, T. C.; O'Keefe, J. S.; Gesser, R. M.; McKie, E. A.; MacLean, A. R.; Fraser, N. W.; Brown, S. M., Replication, establishment of latent infection, expression of the latency-associated transcripts and explant reactivation of herpes simplex virus type 1 gamma 34.5 mutants in a mouse eye model. *J Gen Virol* **1995,** 76 (Pt 2), 321-32.

48. Stevens, J. G.; Haarr, L.; Porter, D. D.; Cook, M. L.; Wagner, E. K., Prominence of the herpes simplex virus latency-associated transcript in trigeminal ganglia from seropositive humans. *J Infect Dis* **1988,** 158, (1), 117-23.

49. Miranda-Saksena, M.; Armati, P.; Boadle, R. A.; Holland, D. J.; Cunningham, A. L., Anterograde transport of herpes simplex virus type 1 in cultured, dissociated human and rat dorsal root ganglion neurons. *J Virol* **2000,** 74, (4), 1827-39.

50. Braz, J.; Beaufour, C.; Coutaux, A.; Epstein, A. L.; Cesselin, F.; Hamon, M.; Pohl, M., Therapeutic efficacy in experimental polyarthritis of viral-driven enkephalin overproduction in sensory neurons. *J Neurosci* **2001,** 21, (20), 7881-8.

51. Spaete, R. R.; Frenkel, N., The herpes simplex virus amplicon: a new eucaryotic defective-virus cloning-amplifying vector. *Cell* **1982,** 30, (1), 295-304.

52. Fraefel, C.; Jacoby, D. R.; Breakefield, X. O., Herpes simplex virus type 1-based amplicon vector systems. *Adv Virus Res* **2000,** 55, 425-51.

53. Suter, M.; Lew, A. M.; Grob, P.; Adema, G. J.; Ackermann, M.; Shortman, K.; Fraefel, C., BAC-VAC, a novel generation of (DNA) vaccines: A bacterial artificial chromosome (BAC) containing a replication-competent, packaging-defective virus genome induces protective immunity against herpes simplex virus 1. *Proc Natl Acad Sci U S A* **1999,** 96, (22), 12697-702.

54. Horsburgh, B. C.; Hubinette, M. M.; Qiang, D.; MacDonald, M. L.; Tufaro, F., Allele replacement: an application that permits rapid manipulation of herpes simplex virus type 1 genomes. *Gene Ther* **1999,** 6, (5), 922-30.

55. Boviatsis, E. J.; Scharf, J. M.; Chase, M.; Harrington, K.; Kowall, N. W.; Breakefield, X. O.; Chiocca, E. A., Antitumor activity and reporter gene transfer into rat brain neoplasms inoculated with herpes simplex virus vectors defective in thymidine kinase or ribonucleotide reductase. *Gene Ther* **1994,** 1, (5), 323-31.

56. Nakano, K.; Todo, T.; Chijiiwa, K.; Tanaka, M., Therapeutic efficacy of G207, a conditionally replicating herpes simplex virus type 1 mutant, for gallbladder carcinoma in immunocompetent hamsters. *Mol Ther* **2001,** 3, (4), 431-7.

57. Markert, J. M.; Medlock, M. D.; Rabkin, S. D.; Gillespie, G. Y.; Todo, T.; Hunter, W. D.; Palmer, C. A.; Feigenbaum, F.; Tornatore, C.; Tufaro, F.; Martuza, R. L., Conditionally replicating herpes simplex virus mutant, G207 for the treatment of malignant glioma: results of a phase I trial. *Gene Ther* **2000,** 7, (10), 867-74.

58. Rampling, R.; Cruickshank, G.; Papanastassiou, V.; Nicoll, J.; Hadley, D.; Brennan, D.; Petty, R.; MacLean, A.; Harland, J.; McKie, E.; Mabbs, R.; Brown, M., Toxicity evaluation of replication-competent herpes simplex virus (ICP 34.5 null mutant 1716) in patients with recurrent malignant glioma. *Gene Ther* **2000,** 7, (10), 859-66.

59. DeLuca, N. A.; McCarthy, A. M.; Schaffer, P. A., Isolation and characterization of deletion mutants of herpes simplex virus type 1 in the gene encoding immediate-early regulatory protein ICP4. *J Virol* **1985,** 56, (2), 558-70.

60. McCarthy, A. M.; McMahan, L.; Schaffer, P. A., Herpes simplex virus type 1 ICP27 deletion mutants exhibit altered patterns of transcription and are DNA deficient. *J Virol* **1989,** 63, (1), 18-27.

61. Krisky, D. M.; Marconi, P. C.; Oligino, T. J.; Rouse, R. J.; Fink, D. J.; Cohen, J. B.; Watkins, S. C.; Glorioso, J. C., Development of herpes simplex virus replication-defective multigene vectors for combination gene therapy applications. *Gene Ther* **1998,** 5, (11), 1517-30.

62. Krisky, D. M.; Wolfe, D.; Goins, W. F.; Marconi, P. C.; Ramakrishnan, R.; Mata, M.; Rouse, R. J.; Fink, D. J.; Glorioso, J. C., Deletion of multiple immediate-early genes from herpes simplex virus reduces cytotoxicity and permits long-term gene expression in neurons. *Gene Ther* **1998,** 5, (12), 1593-603.

63. Samaniego, L. A.; Neiderhiser, L.; DeLuca, N. A., Persistence and expression of the herpes simplex virus genome in the absence of immediate-early proteins. *J Virol* **1998,** 72, (4), 3307-20.

64. Glorioso, J. C.; Fink, D. J., Use of HSV vectors to modify the nervous system. *Curr Opin Drug Discov Devel* **2002,** 5, (2), 289-95.

65. Glorioso, J. C.; Mata, M.; Fink, D. J., Therapeutic gene transfer to the nervous system using viral vectors. *J Neurovirol* **2003,** 9, (2), 165-72.

66. Burton, E. A.; Bai, Q.; Goins, W. F.; Glorioso, J. C., Targeting gene expression using HSV vectors. *Adv Drug Deliv Rev* **2001,** 53, (2), 155-70.

67. Burton, E. A.; Fink, D. J.; Glorioso, J. C., Replication-defective genomic HSV gene therapy vectors: design, production and CNS applications. *Curr Opin Mol Ther.* **2005,** 7, (4), 326-36.

68. Wechuck, J. B., Production and purification of HSV-1 vectors and its use for gene thansfer to human CD34+ cells. *university of pittsburgh PhD thesis* **2002**.

69. Kuiper, M.; Sanches, R. M.; Walford, J. A.; Slater, N. K., Purification of a functional gene therapy vector derived from Moloney murine leukaemia virus using membrane filtration and ceramic hydroxyapatite chromatography. *Biotechnol Bioeng* **2002,** 80, (4), 445-53.

70. Geraerts, M.; Michiels, M.; Baekelandt, V.; Debyser, Z.; Gijsbers, R., Upscaling of lentiviral vector production by tangential flow filtration. *J Gene Med* **2005,** 7, (10), 1299-310.

71. Auricchio, A.; Hildinger, M.; O'Connor, E.; Gao, G. P.; Wilson, J. M., Isolation of highly infectious and pure adeno-associated virus type 2 vectors with a single-step gravity-flow column. *Hum Gene Ther* **2001,** 12, (1), 71-6.

72. Zolotukhin, S.; Potter, M.; Zolotukhin, I.; Sakai, Y.; Loiler, S.; Fraites, T. J., Jr.; Chiodo, V. A.; Phillipsberg, T.; Muzyczka, N.; Hauswirth, W. W.; Flotte, T. R.; Byrne, B. J.; Snyder, R. O., Production and purification of serotype 1, 2, and 5 recombinant adeno-associated viral vectors. *Methods* **2002,** 28, (2), 158-67.

73. Kaludov, N.; Handelman, B.; Chiorini, J. A., Scalable purification of adeno-associated virus type 2, 4, or 5 using ion-exchange chromatography. *Hum Gene Ther* **2002,** 13, (10), 1235-43.

74. Davidoff, A. M.; Ng, C. Y.; Sleep, S.; Gray, J.; Azam, S.; Zhao, Y.; McIntosh, J. H.; Karimipoor, M.; Nathwani, A. C., Purification of recombinant adeno-associated virus type 8 vectors by ion exchange chromatography generates clinical grade vector stock. *J Virol Methods* **2004,** 121, (2), 209-15.

75. Huyghe, B. G.; Liu, X.; Sutjipto, S.; Sugarman, B. J.; Horn, M. T.; Shepard, H. M.; Scandella, C. J.; Shabram, P., Purification of a type 5 recombinant adenovirus encoding human p53 by column chromatography. *Hum Gene Ther* **1995,** 6, (11), 1403-16.

76. Kamen, A.; Henry, O., Development and optimization of an adenovirus production process. *J Gene Med* **2004,** 6 Suppl 1, S184-92.

77. Guo, H. L.; Wolfe, D.; Epperly, M. W.; Huang, S.; Liu, K.; Glorioso, J. C.; Greenberger, J.; Blumberg, D., Gene transfer of human manganese superoxide dismutase protects small intestinal villi from radiation injury. *J Gastrointest Surg* **2003,** 7, (2), 229-35; discussion 235-6.

78. Zolotukhin S; Byrne BJ; Mason E; Zolotukhin I; Potter M; Chesnut K; Summerford C; Samulski RJ; N., M., Recombinant adeno-associated virus purification using novel methods improves infectious titer and yield. *Gene Ther* **1999,** 6, (6), 973-85.

79. O'Keeffe, R. S.; Johnston, M. D.; Slater, N. K., The affinity adsorptive recovery of an infectious herpes simplex virus vaccine. *Biotechnol Bioeng* **1999,** 62, (5), 537-45.

80. Segura, M. M.; Kamen, A.; Trudel, P.; Garnier, A., A novel purification strategy for retrovirus gene therapy vectors using heparin affinity chromatography. *Biotechnol Bioeng* **2005,** 90, (4), 391-404.

81. Auricchio, A.; O'Connor, E.; Hildinger, M.; Wilson, J. M., A single-step affinity column for purification of serotype-5 based adeno-associated viral vectors. *Mol Ther* **2001,** 4, (4), 372-4.

82. Walters RW; Yi SM; Keshavjee S; Brown KE; Welsh MJ; Chiorini JA; J., Z., Binding of adeno-associated virus type 5 to 2,3-linked sialic acid is required for gene transfer. *J Biol Chem.* **2001,** 276, (23), 20610-6.

83. Porath, J., Immobilized metal ion affinity chromatography. *Protein Expr Purif* **1992,** 3, (4), 263-81.

84. Yip, T. T.; Hutchens, T. W., Immobilized metal-ion affinity chromatography. *Methods Mol Biol* **2004,** 244, 179-90.

85. Porath, J.; Carlsson, J.; Olsson, I.; Belfrage, G., Metal chelate affinity chromatography, a new approach to protein fractionation. *Nature* **1975,** 258, (5536), 598-9.

86. Lopatin, S. A.; Varlamov, V. P., [A new trend toward using metal chelates in affinity chromatography of proteins (review)]. *Prikl Biokhim Mikrobiol* **1995,** 31, (3), 259-66.

87. Zachariou, M., Immobilized metal ion affinity chromatography of proteins. *Methods Mol Biol* **2004,** 251, 89-102.

88. Crowe, J.; Dobeli, H.; Gentz, R.; Hochuli, E.; Stuber, D.; Henco, K., 6xHis-Ni-NTA chromatography as a superior technique in recombinant protein expression/purification. *Methods Mol Biol* **1994,** 31, 371-87.

89. Hochuli, E.; Dobeli, H.; Schacher, A., New metal chelate adsorbent selective for proteins and peptides containing neighbouring histidine residues. *J Chromatogr* **1987,** 411, 177-84.

90. Chaga, G.; Bochkariov, D. E.; Jokhadze, G. G.; Hopp, J.; Nelson, P., Natural poly-histidine affinity tag for purification of recombinant proteins on cobalt(II)-carboxymethylaspartate crosslinked agarose. *J Chromatogr A* **1999,** 864, (2), 247-56.

91. Pasquinelli, R. S.; Shepherd, R. E.; Koepsel, R. R.; Zhao, A.; Ataai, M. M., Design of affinity tags for one-step protein purification from immobilized zinc columns. *Biotechnol Prog* **2000,** 16, (1), 86-91.

92. Patwardhan, A. V.; Goud, G. N.; Koepsel, R. R.; Ataai, M. M., Selection of optimum affinity tags from a phage-displayed peptide library. Application to immobilized copper(II) affinity chromatography. *J Chromatogr A* **1997,** 787, (1-2), 91-100.

93. Pasquinelli, R. S.; Koepsel, R. R.; Wu, N.; Ataai, M. M., Vector engineering anomalies: impact on fusion protein purification performance. *Protein Expr Purif* **1999,** 17, (3), 449-55.

94. Zhang, H. G.; Xie, J.; Dmitriev, I.; Kashentseva, E.; Curiel, D. T.; Hsu, H. C.; Mountz, J. D., Addition of six-His-tagged peptide to the C terminus of adeno-associated virus VP3 does not affect viral tropism or production. *J Virol* **2002,** 76, (23), 12023-31.

95. Ye, K.; Jin, S.; Ataai, M. M.; Schultz, J. S.; Ibeh, J., Tagging retrovirus vectors with a metal binding peptide and one-step purification by immobilized metal affinity chromatography. *J Virol* **2004,** 78, (18), 9820-7.

96. Bergamini, C. M.; Gambetti, S.; Dondi, A.; Cervellati, C., Oxygen, reactive oxygen species and tissue damage. *Curr Pharm Des* **2004,** 10, (14), 1611-26.

97. Hensley, K.; Robinson, K. A.; Gabbita, S. P.; Salsman, S.; Floyd, R. A., Reactive oxygen species, cell signaling, and cell injury. *Free Radic Biol Med* **2000,** 28, (10), 1456-62.

98. Sies, H.; de Groot, H., Role of reactive oxygen species in cell toxicity. *Toxicol Lett* **1992,** 64-65 Spec No, 547-51.

99. Toyokuni, S., Reactive oxygen species-induced molecular damage and its application in pathology. *Pathol Int* **1999,** 49, (2), 91-102.

100. Inoue, M.; Sato, E. F.; Nishikawa, M.; Park, A. M.; Kira, Y.; Imada, I.; Utsumi, K., Mitochondrial generation of reactive oxygen species and its role in aerobic life. *Curr Med Chem* **2003,** 10, (23), 2495-505.

101. Winterbourn, C. C., Toxicity of iron and hydrogen peroxide: the Fenton reaction. *Toxicol Lett* **1995,** 82-83, 969-74.

102. Bergstrand, H., The generation of reactive oxygen-derived species by phagocytes. *Agents Actions Suppl* **1990,** 30, 199-211.

103. Aust, S. D.; Morehouse, L. A.; Thomas, C. E., Role of metals in oxygen radical reactions. *Journal of Free Radicals in Biology & Medicine* **1985,** 1, (1), 3-25.

104. Stohs, S. J.; Bagchi, D., Oxidative mechanisms in the toxicity of metal ions. *Free Radic Biol Med* **1995,** 18, (2), 321-36.

105. Halliwell, B.; Gutteridge, J. M., Biologically relevant metal ion-dependent hydroxyl radical generation. An update. *FEBS Letters* **1992,** 307, (1), 108-12.

106. Buettner, G. R.; Jurkiewicz, B. A., Catalytic Metals, Ascorbate and Free Radicals: Combinations to Avoid. *RADIATION RESEARCH* **1996,** 145, 532-541.

107. Cowan, J. A., Inorganic biochemistry : an introduction **1997**.

108. Madurawe, R.; Lin, Z.; Dryden, P.; Lumpkin, J. A., Stability of Lactate Dehydrogenase in Metal-Catalyzed Oxidation Solutions Containing Chelated Metals. *Biotechnol Prog* **1997**, 179-184.

109. Torreilles, J.; Guerin, M. C., Nickel (II) as a temporary catalyst for hydroxyl radical generation. *FEBS Lett* **1990,** 272, (1-2), 58-60.

110.Torreilles, J.; Guerin, M. C.; Slaoui-Hasnaoui, A., Nickel (II) complexes of histidyl-peptides as Fenton-reaction catalysts. *Free Radic Res Commun* **1990,** 11, (1-3), 159-66.

111.Hanna, P. M.; Kadiiska, M. B.; Mason, R. P., Oxygen-derived free radical and active oxygen complex formation from cobalt(II) chelates in vitro. *Chem Res Toxicol* **1992,** 5, (1), 109-15.

112.Mao, Y.; Liu, K. J.; Jiang, J. J.; Shi, X., Generation of reactive oxygen species by Co(II) from H2O2 in the presence of chelators in relation to DNA damage and 2'-deoxyguanosine hydroxylation. *J Toxicol Environ Health* **1996,** 47, (1), 61-75.

113.Dean, R. T.; Fu, S.; Stocker, R.; Davies, M. J., Biochemistry and pathology of radical-mediated protein oxidation. *Biochemical Journal* **1997,** 324, (Pt 1), 1-18.

114.Stadtman, E. R., Oxidation of free amino acids and amino acid residues in proteins by radiolysis and by metal-catalyzed reactions. *Annu Rev Biochem* **1993,** 62, 797-821.

115.Termini, J., Hydroperoxide-induced DNA damage and mutations. *Mutation Research* **2000,** 450, (1-2), 107-24.

116.Valko, M.; Izakovic, M.; Mazur, M.; Rhodes, C. J.; Telser, J., Role of oxygen radicals in DNA damage and cancer incidence. *Mol Cell Biochem* **2004,** 266, (1-2), 37-56.

117.McCall, J. M.; Braughler, J. M.; Hall, E. D., Lipid peroxidation and the role of oxygen radicals in CNS injury. *Acta Anaesthesiologica Belgica* **1987,** 38, (4), 373-9.

118.Rikans, L. E.; Hornbrook, K. R., Lipid peroxidation, antioxidant protection and aging. *Biochimica et Biophysica Acta* **1997,** 1362, (2-3), 116-27.

119.Greenwald, R. A., Oxygen radicals, inflammation, and arthritis: pathophysiological considerations and implications for treatment. *Seminars in Arthritis & Rheumatism* **1991,** 20, (4), 219-40.

120. Sayre, L. M.; Perry, G.; Smith, M. A., Redox metals and neurodegenerative disease. *Current Opinion in Chemical Biology* **1999,** 3, (2), 220-5.

121. Khossravi, M., Mechanism of metal-catalyzed oxidation: physical instability of a protein pharmaceutical. *Ph.D. dissertation, The University of Kansas* **1999**.

122. Bush, K. D.; Lumpkin, J. A., Structural damage to lactate dehydrogenase during copper iminodiacetic acid metal affinity chromatography. *Biotechnol Prog* **1998,** 14, (6), 943-50.

123. Wiseman, H.; Halliwell, B., Damage to DNA by reactive oxygen and nitrogen species: role in inflammatory disease and progression to cancer. *Biochem J* **1996,** 313 (Pt 1), 17-29.

124. Weitzman, S. A.; Turk, P. W.; Milkowski, D. H.; Kozlowski, K., Free radical adducts induce alterations in DNA cytosine methylation. *Proc Natl Acad Sci U S A* **1994,** 91, (4), 1261-4.

125. Turrens, J. F.; Boveris, A., Generation of superoxide anion by the NADH dehydrogenase of bovine heart mitochondria. *Biochem J* **1980,** 191, (2), 421-7.

126. Chen, X.; Li, J.; Mata, M.; Goss, J.; Wolfe, D.; Glorioso, J. C.; Fink, D. J., Herpes simplex virus type 1 ICP0 protein does not accumulate in the nucleus of primary neurons in culture. *J Virol* **2000,** 74, (21), 10132-41.

127. Samaniego, L. A.; Wu, N.; DeLuca, N. A., The herpes simplex virus immediate-early protein ICP0 affects transcription from the viral genome and infected-cell survival in the absence of ICP4 and ICP27. *J Virol* **1997,** 71, (6), 4614-25.

128. Marconi, P.; Krisky, D.; Oligino, T.; Poliani, P. L.; Ramakrishnan, R.; Goins, W. F.; Fink, D. J.; Glorioso, J. C., Replication-defective herpes simplex virus vectors for gene transfer in vivo. *Proc Natl Acad Sci U S A* **1996,** 93, (21), 11319-20.

129. Cai, W. Z.; Person, S.; Warner, S. C.; Zhou, J. H.; DeLuca, N. A., Linker-insertion nonsense and restriction-site deletion mutations of the gB glycoprotein gene of herpes simplex virus type 1. *J Virol* **1987,** 61, (3), 714-21.

130. Goins, W. F.; Krisky, D. M.; Wolfe, D. P.; Fink, D. J.; Glorioso, J. C., Development of replication-defective herpes simplex virus vectors. *Methods Mol Med* **2002,** 69, 481-507.

131. Goins, W. F.; Lee, K. A.; Cavalcoli, J. D.; O'Malley, M. E.; DeKosky, S. T.; Fink, D. J.; Glorioso, J. C., Herpes simplex virus type 1 vector-mediated expression of nerve growth factor protects dorsal root ganglion neurons from peroxide toxicity. *J Virol* **1999,** 73, (1), 519-32.

132. Goins, W. F.; Sternberg, L. R.; Croen, K. D.; Krause, P. R.; Hendricks, R. L.; Fink, D. J.; Straus, S. E.; Levine, M.; Glorioso, J. C., A novel latency-active promoter is contained within the herpes simplex virus type 1 UL flanking repeats. *J Virol* **1994,** 68, (4), 2239-52.

133. Wu, N.; Watkins, S. C.; Schaffer, P. A.; DeLuca, N. A., Prolonged gene expression and cell survival after infection by a herpes simplex virus mutant defective in the immediate-early genes encoding ICP4, ICP27, and ICP22. *J Virol* **1996,** 70, (9), 6358-69.

134. Goss, J. R.; Goins, W. F.; Lacomis, D.; Mata, M.; Glorioso, J. C.; Fink, D. J., Herpes simplex-mediated gene transfer of nerve growth factor protects against peripheral neuropathy in streptozotocin-induced diabetes in the mouse. *Diabetes* **2002,** 51, (7), 2227-32.

135. Goss, J. R.; Harley, C. F.; Mata, M.; O'Malley, M. E.; Goins, W. F.; Hu, X.; Glorioso, J. C.; Fink, D. J., Herpes vector-mediated expression of proenkephalin reduces bone cancer pain. *Ann Neurol* **2002,** 52, (5), 662-5.

136. Hao, S.; Mata, M.; Goins, W.; Glorioso, J. C.; Fink, D. J., Transgene-mediated enkephalin release enhances the effect of morphine and evades tolerance to produce a sustained antiallodynic effect in neuropathic pain. *Pain* **2003,** 102, (1-2), 135-42.

137. Jones, T. L.; Sweitzer, S. M.; Wilson, S. P.; Yeomans, D. C., Afferent fiber-selective shift in opiate potency following targeted opioid receptor knockdown. *Pain* **2003,** 106, (3), 365-71.

138. Chattopadhyay, M.; Goss, J.; Lacomis, D.; Goins, W. C.; Glorioso, J. C.; Mata, M.; Fink, D. J., Protective effect of HSV-mediated gene transfer of nerve growth factor in pyridoxine neuropathy demonstrates functional activity of trkA receptors in large sensory neurons of adult animals. *Eur J Neurosci* **2003,** 17, (4), 732-40.

139. Chattopadhyay, M.; Wolfe, D.; Huang, S.; Goss, J.; Glorioso, J. C.; Mata, M.; Fink, D. J., In vivo gene therapy for pyridoxine-induced neuropathy by herpes simplex virus-mediated gene transfer of neurotrophin-3. *Ann Neurol* **2002,** 51, (1), 19-27.

140. Bennett, J. J.; Delman, K. A.; Burt, B. M.; Mariotti, A.; Malhotra, S.; Zager, J.; Petrowsky, H.; Mastorides, S.; Federoff, H.; Fong, Y., Comparison of safety, delivery, and efficacy of two oncolytic herpes viruses (G207 and NV1020) for peritoneal cancer. *Cancer Gene Ther* **2002,** 9, (11), 935-45.

141. Cozzi, P. J.; Burke, P. B.; Bhargav, A.; Heston, W. D.; Huryk, B.; Scardino, P. T.; Fong, Y., Oncolytic viral gene therapy for prostate cancer using two attenuated, replication-competent, genetically engineered herpes simplex viruses. *Prostate* **2002,** 53, (2), 95-100.

142. Marconi, P.; Tamura, M.; Moriuchi, S.; Krisky, D. M.; Niranjan, A.; Goins, W. F.; Cohen, J. B.; Glorioso, J. C., Connexin 43-enhanced suicide gene therapy using herpesviral vectors. *Mol Ther* **2000,** 1, (1), 71-81.

143. Moriuchi, S.; Wolfe, D.; Tamura, M.; Yoshimine, T.; Miura, F.; Cohen, J. B.; Glorioso, J. C., Double suicide gene therapy using a replication defective herpes simplex virus vector reveals reciprocal interference in a malignant glioma model. *Gene Ther* **2002,** 9, (9), 584-91.

144. Ozuer, A.; Wechuck, J. B.; Goins, W. F.; Wolfe, D.; Glorioso, J. C.; Ataai, M. M., Effect of genetic background and culture conditions on the production of herpesvirus-based gene therapy vectors. *Biotechnol Bioeng* **2002,** 77, (6), 685-92.

145. Ozuer, A.; Wechuck, J. B.; Russell, B.; Wolfe, D.; Goins, W. F.; Glorioso, J. C.; Ataai, M. M., Evaluation of infection parameters in the production of replication-defective HSV-1 viral vectors. *Biotechnol Prog* **2002,** 18, (3), 476-82.

146. Wechuck, J. B.; Goins, W. F.; Glorioso, J. C.; Ataai, M. M., Effect of protease inhibitors on yield of HSV-1-based viral vectors. *Biotechnol Prog* **2000,** 16, (3), 493-6.

147. Wechuck, J. B.; Ozuer, A.; Goins, W. F.; Wolfe, D.; Oligino, T.; Glorioso, J. C.; Ataai, M. M., Effect of temperature, medium composition, and cell passage on the production of herpes-based viral vectors. *Biotechnol Bioeng* **2002,** 79, (1), 112-119.

148. Lotfian, P.; Levy, M. S.; Coffin, R. S.; Fearn, T.; Ayazi-Shamlou, P., Impact of process conditions on the centrifugal recovery of a disabled herpes simplex virus. *Biotechnol Prog* **2003,** 19, (1), 209-15.

149. Sathananthan, B.; Rodahl, E.; Flatmark, T.; Langeland, N.; Haarr, L., Purification of herpes simplex virus type 1 by density gradient centrifugation and estimation of the sedimentation coefficient of the virion. *Apmis* **1997,** 105, (3), 238-46.

150. Svennerholm, B.; Vahlne, A.; Jeansson, S.; Lunden, R.; Olofsson, S.; Svantesson, G.; Lycke, E., Separation of herpes simplex virus virions and nucleocapsids on Percoll gradients. *J Virol Methods* **1980,** 1, (6), 303-9.

151. Szilagyi, J. F.; Cunningham, C., Identification and characterization of a novel non-infectious herpes simplex virus-related particle. *J Gen Virol* **1991,** 72 (Pt 3), 661-8.

152. Vahlne, A. G.; Blomberg, J., Purification of herpes simplex virus. *J Gen Virol* **1974,** 22, (2), 297-302.

153. Braas, G.; Searle, P. F.; Slater, N. K.; Lyddiatt, A., Strategies for the isolation and purification of retroviral vectors for gene therapy. *Bioseparation* **1996,** 6, (4), 211-28.

154. Spear, P. G., Entry of alphaherpesviruses into cells. *Sem. Virol* **1993,** 4, 167-180.

155. Rajcani, J.; Vojvodova, A., The role of herpes simplex virus glycoproteins in the virus replication cycle. *Acta Virol* **1998,** 42, (2), 103-18.

156. Stannard, L. M.; Fuller, A. O.; Spear, P. G., Herpes simplex virus glycoproteins associated with different morphological entities projecting from the virion envelope. *J Gen Virol* **1987,** 68 (Pt 3), 715-25.

157. WuDunn, D.; Spear, P. G., Initial interaction of herpes simplex virus with cells is binding to heparan sulfate. *J Virol* **1989,** 63, (1), 52-8.

158. Butcher, M.; Raviprakash, K.; Ghosh, H. P., Acid pH-induced fusion of cells by herpes simplex virus glycoproteins gB an gD. *J Biol Chem* **1990,** 265, (10), 5862-8.

159. Navarro, D.; Paz, P.; Pereira, L., Domains of herpes simplex virus I glycoprotein B that function in virus penetration, cell-to-cell spread, and cell fusion. *Virology* **1992,** 186, (1), 99-112.

160. Norton, D. D.; Dwyer, D. S.; Muggeridge, M. I., Use of a neural network secondary structure prediction to define targets for mutagenesis of herpes simplex virus glycoprotein B. *Virus Res* **1998,** 55, (1), 37-48.

161. Sagripanti, J. L.; Routson, L. B.; Bonifacino, A. C.; Lytle, C. D., Mechanism of copper-mediated inactivation of herpes simplex virus. *Antimicrob Agents Chemother* **1997,** 41, (4), 812-7.

162. Hughes, M. N., *The Inorganic Chemistry of Biological Processes Second Edition* **1981**.

163. Goldstein, S.; Meyerstein, D.; Czapski, G., The Fenton reagents. *Free Radical Biology & Medicine* **1993,** 15, (4), 435-45.

164. Krishnamurthy, R.; Madurawe, R.; Bush, K. L., JA, Conditions Promoting Metal-Catalyzed Oxidations during Immobilized Cu-Iminodiacetic Acid Metal Affinity Chromatography. *Biotechnol Prog* **1995,** 11, 643-650.

165. Buettner, G., Spin trapping: ESR parameters of spin adducts. *Free Radic Biol Med* **1987,** 3, (4), 259-303.

166. Buettner, G. R.; Jurkiewicz, B. A., Ascorbate free radical as a marker of oxidative stress: an EPR study. *Free Radic Biol Med* **1993,** 14, (1), 49-55.

167. Hippeli, S.; Elstner, E. F., Transition metal ion-catalyzed oxygen activation during pathogenic processes. *FEBS Letters* **1999,** 443, (1), 1-7.

168. Cabani, S., Binding of molecular dioxygen to Co(I1) complexes in aqueous solutions. *Reactive & Functional Polymers* **1996,** 28, 167-182.

169. Tang, H.; Shen, C.; Lin, M.; Sen, A., Cobalt porphyrin-catalyzed alkane oxidations using dioxygen as oxidant *Inorganica Chimica Acta* **2000,** 300-302, 1109-1111

170. Niederhoffer, E.; Timmons, J.; Martell, A., Thermodynamics of oxygen binding in natural and synthetic dioxygen complexes. *Chem, Rev.* **1984,** 84, 137-203.

171. Eberhardt, M. K.; Santos, C.; Soto, M. A., Formation of hydroxyl radicals and Co3+ in the reaction of Co(2+)-EDTA with hydrogen peroxide. Catalytic effect of Fe3+. *Biochim Biophys Acta* **1993,** 1157, (1), 102-6.

172. Vogt, A., Studies on the cobalt (II)- dipeptide-imidazole system: a new oxygen carrier. *polyhedron* **1990,** 9, (21), 2567-2574.

173. Lloyd, D. R.; Phillips, D. H.; Carmichael, P. L., Generation of putative intrastrand cross-links and strand breaks in DNA by transition metal ion-mediated oxygen radical attack. *Chem Res Toxicol* **1997,** 10, (4), 393-400.

174. Schneider, J. E.; Browning, M. M.; Floydt, R. A., Ascorbate/Iron Mediation of Hydroxyl Free Radical Damage to PBR322 Plasmid DNA. *Free Radical Biology & Medicine.* **1988,** 5, 287-295.